



# **COST Action CM1104**

## **Reducible oxide chemistry, structure and functions**

[www.cost-redox.nano.cnr.it](http://www.cost-redox.nano.cnr.it)

### **3<sup>rd</sup> General Meeting**



**Aula Magna Enric Casassas, 0th floor**

**Faculty of Chemistry, Universitat de Barcelona  
Calle Martí i Franquès 1, 08028 Barcelona, Spain**

**Metro line L3, “Palau Reial” station**

**November 12-14, 2014**

Local Organiser:

Prof. Konstantin Neyman (ICREA / Universitat de Barcelona)

# Programme of Oral Presentations

(final version Nov 14, 2014)

Wednesday, November 12<sup>th</sup>, 2014

13:30-14:15 Registration

14:15-14:30 Opening: Dean of the Chemistry Faculty - Pere L. Cabot, Director of the Institut de Química Teòrica i Computacional (UB) - Francesc Illas, Local Organiser - Konstantin Neyman

## Session 1: Discussion leader Jörg Libuda

14:30-15:10 I1 Jordi Llorca (Barcelona, ES)

*Strategies for soot oxidation over nanoshaped CeO<sub>2</sub>*

15:10-15:30 O1 Juan Jose Delgado (Cadiz, ES) *Contribution of electron microscopy to the characterization of ceria based catalysts*

15:30-15:50 O2 Joanna Gryboś (Krakow, PL) *Size and shape of cobalt spinel nanocrystals revealed by HAADF-STEM and DFT first-principles calculation*

15:50-16:10 O3 Günther Rupprechter (Vienna, AT)

*Model studies of Ni(Pd)-ZrO<sub>2</sub>-Pt<sub>3</sub>(Pd)<sub>3</sub>Zr solid oxide fuel cell anodes*

16:10-16:40 Coffee break

## Session 2: Discussion leader Cristiana Di Valentin

16:40-17:00 O4 Ulrich Vogt (Dübendorf, CH)

*Solar thermochemical syngas production by a CeO<sub>2</sub> based redox cycle*

17:00-17:20 O5 Arturo Martínez-Arias (Madrid, ES)

*Electronic properties of dispersed copper oxide entities interacting with ceria: Near-ambient XPS analysis of the reduction under CO*

17:20-17:40 O6 Clemens Barth (Marseille, FR)

*Reduction and oxidation of a bulk-like ceria film*

17:40-18:00 O7 Oliver Diwald (Salzburg, AT)

*Size reduction effects in MgO cube dissolution*

18:00-20:30 Poster presentations & refreshments

vestibule of the New Physics Building, 1st floor

## Thursday, November 13<sup>th</sup>, 2014

### Session 3: Discussion leader Alex Shluger

- 9:00-9:20 O8 Geoff Thornton (London, UK)  
*Structure of the rutile TiO<sub>2</sub>(110) interface with water*
- 9:20-9:40 O9 Igor Beinik (Aarhus, DK)  
*Cu attracts subsurface defects and wets the ZnO(0001)-Zn surface*
- 9:40-10:00 O10 Bjørk Hammer (Aarhus, DK)  
*Interfacial structure for Au/TiO<sub>2</sub> revealed by genetic algorithm search*
- 10:00-10:20 O11 Monica Calatayud (Paris, FR) *WGS reaction on ceria-supported Pt catalysts: The role of oxygen vacancies*
- 10:20-10:30 Intermission
- 10:30-10:50 O12 Claudine Noguera (Paris, FR) *Stoichiometry engineering of (ternary) oxide ultra-thin films: Ba<sub>x</sub>Ti<sub>2</sub>O<sub>3</sub> on Au(111)*
- 10:50-11:10 O13 Gareth Parkinson (Vienna, AT) *Subsurface cation vacancy stabilization of the magnetite (001) surface*
- 11:10-12:20 Coffee and discussion time for cooperating research teams

### Session 4: Discussion leader Sergio Valeri

- 12:20-12:40 O14 Jan Ingo Flege (Bremen, DE)  
*Growth and structural properties of terbium oxide on Cu(111)*
- 12:40-13:00 O15 Paola Luches (Modena, IT)  
*Atomic scale insight into the CeO<sub>2</sub>/Pt interface*
- 13:00-13:20 O16 Paulina Indyka (Krakow, PL)  
*Cryptomelane nanorods: TEM/STEM/EELS*
- 13:20-15:00 Lunch break

### Session 5: Discussion leader Notker Rösch

- 15:00-15:40 I2 Jun Li (Beijing, P. R. China) *The enigmatic Single-Atom Catalyst (SAC): Bridging the heterogeneous and homogeneous regime*
- 15:40-16:00 O17 Albert Bruix (Barcelona, ES; Aarhus, DK)  
*Origin, stability, and effect of atomically dispersed Pt on nanostructured catalytic Pt-CeO<sub>2</sub> materials with maximum noble-metal efficiency*
- 16:00-16:20 O18 Vladimir Matolin (Prague, CZ)  
*High efficiency Pt<sup>2+</sup>-CeO<sub>x</sub> novel thin film catalyst as anode for PEMFC*
- 16:20-16:40 O19 Yaroslava Lykhach (Erlangen, DE)  
*Model studies on novel ceria-based fuel cell catalysts*
- 16:40-17:00 COST information - Michael Reichling (Action Chair)
- 17:30-19:30 Management Committee (MC) meeting (MC members only; Department of Physical Chemistry, 4<sup>th</sup> floor of the Chemistry building, room number 400)
- 20:40- **Conference dinner, Restaurant Abrassame**, [www.abrassame.com/en](http://www.abrassame.com/en)  
Dome of the Las Arenas shopping mall, Gran Via de les Corts Catalanes, 375-385, 08015 Barcelona, Metro L1, L3 *Plaça Espanya*, T. 934 255 491

Friday, November 14<sup>th</sup>

**Session 6: Discussion leader M. Veronica Ganduglia-Pirovano**

- 9:00- 9:20 O20 Yuri Mastrikov (Riga, LV)  
*DFT calculations on formation and migration of oxygen vacancies in  $La_{0.5}Sr_{0.5}Co_{0.75}Fe_{0.125}M_{0.125}O_{3-\delta}$  (M=Pd, Ni) perovskites*
- 9:20- 9:40 O21 Joachim Sauer (Berlin, DE) *C-H bond activation by transition metal oxides. Atomistic understanding of  $CeO_2$  as non-innocent support*
- 9:40-10:00 O22 Alexander Shluger (London, UK)  
*The interaction of hydrogen with amorphous silica network*
- 10:00-10:20 O23 Florent Boudoire (Dübendorf, CH) *Photonic light trapping in self-organized all-oxide microspheroids impacts photoelectrochemical water splitting*
- 10:20-10:30 Intermission
- 10:30-10:50 O24 Marketa Zukalova (Prague, CZ)  
*Electrochemical properties of sol-gel  $TiO_2$  blocking layers*
- 10:50-11:10 O25 Oreste Madia (Leuven, BE)  
 *$SiPb_0$  defects at interfaces of Si-passivated SiGe channels with  $HfO_2$*
- 11:10-11:30 O26 Esa Korhonen (Aalto, FI) *Characterization of  $In_2O_3$  and  $Ga_2O_3$  using positron annihilation spectroscopy*
- 11:30-12:00 Closure

# Poster Session

Wednesday, November 12<sup>th</sup>, 18:00-20:30  
Vestibule of the New Physics Building, 1st floor

- P1. **Juan de la Figuera** (Madrid, ES) *A real-time view of the (001) magnetite surface*
- P2. M. Monti,<sup>1</sup> I. Palacio,<sup>2</sup> K. F. McCarty,<sup>3</sup> J. F. Marco,<sup>1</sup> **Juan de la Figuera**<sup>1</sup>  
(Madrid, ES;<sup>1</sup> Saint Aubin, FR;<sup>2</sup> Livermore, CA<sup>3</sup>)  
*Stoichiometry and structure control of iron-oxide ultra-thin film*
- P3. **Alex Walton**, J. Fester, V. Lauritsen (Aarhus, DK)  
*Cobalt oxide nanoparticles on Au(111): Structure, composition and surface chemistry*
- P4. **Cristiana Di Valentin**, G. Pacchioni (Milan, IT)  
*TiO<sub>2-x</sub>, ZnO<sub>1-x</sub>, WO<sub>3-x</sub>: a perspective on reducible oxides from hybrid DFT*
- P5. **Hsin-Yi Tiffany Chen**, G. Pacchioni (Milan, IT) *Properties of two-dimensional insulators: a DFT study of Co adsorption on NaCl and MgO ultrathin films*
- P6. **Krzysztof Kośmider**, M. V. Ganduglia-Pirovano, R. Pérez (Madrid, ES)  
*AFM imaging of the Au/CeO<sub>2</sub>(111) system: DFT study*
- P7. P. G. Lustemberg,<sup>1</sup> **Adrian Bonivardi**,<sup>2</sup> M. V. Bosco,<sup>2</sup> H. F. Busnengo,<sup>1</sup> M. V. Ganduglia-Pirovano<sup>3</sup> (Santa Fe, AR;<sup>1,2</sup> Madrid, ES<sup>3</sup>)  
*Study of formate species in the CH<sub>3</sub>OH/CeO<sub>2</sub> reaction: combining IR spectroscopy and statistical thermodynamics techniques*
- P8. **László Deák**, I. Szentí, R. Gubó, L. Óvári, A. Berkó, Z. Kónya (Szeged, HU)  
*The effect of atomically thin TiO<sub>x</sub> structures on the morphology and reactivity of nano-sized Rh films*
- P9. **Martin Setvin**, C. Franchini, X. Hao, B. Daniel, M. Schmid, G. Kresse, U. Diebold (Vienna, AT) *Excess electrons in TiO<sub>2</sub> – delocalized solutions in anatase vs. localized polarons in rutile*
- P10. **Martin Setvin**,<sup>1</sup> V. Mansfeldova,<sup>2</sup> M. Schmid,<sup>1</sup> L. Kavan,<sup>2</sup> U. Diebold<sup>1</sup> (Vienna, AT;<sup>1</sup> Prague, CZ<sup>2</sup>)  
*TiO<sub>2</sub> anatase(101) – single crystal growth and surface preparation in UHV*
- P11. N. Doudin, S. Pomp, F. P. Netzer, **Svetlozar Surnev** (Graz, AT)  
*Reaction of (WO<sub>3</sub>)<sub>3</sub> clusters with NiO(100) layers on a Ni(110) surface: Formation of epitaxial ternary oxide NiWO<sub>4</sub>(100) films*
- P12. **Christoph Rameshan**, K. Anic, A. Bukhtiyarov, G. Rupprechter (Vienna, AT)  
*Cobalt oxide model catalyst as alternative to noble metal catalysts*
- P13. M. Y. Mihaylov, E. Z. Ivanova, H. A. Aleksandrov, **Georgi N. Vayssilov**, K. I. Hadjiivanov (Sofia, BG)  
*Theoretical and experimental study of the interaction of NO with ceria*
- P14. **José C. Conesa** (Madrid, ES)  
*Hybrid DFT study of the Fe:NiOOH O<sub>2</sub> electroevolution catalyst*
- P15. **Matti Hellström**, D. Spångberg, Peter Broqvist, K. Hermansson (Uppsala, SE)  
*Cu/ZnO charge transfer depends on Cu size, Cu shape, and H<sub>2</sub>O pressure*
- P16. **Getachew Kebede**, D. Spångberg, P. Broqvist, P. M. Mitev, K. Hermansson (Uppsala, SE) *Comparison of vdW-functionals for improved description of water-ionic surface interactions – NaCl(100) and MgO(100) as prototype substrates*

- P17. **Dou Du**, K. Hermansson, P. Broqvist (Uppsala, SE)  
*Supercharged oxygen storage in nanoceria revisited using hybrid functionals*
- P18. **Seif Alwan**, K. Hermansson, P. Broqvist (Uppsala, SE)  
*Half hydroxylation of the ceria(111) surface at monolayer-water adsorption*
- P19. **Maxime Van den Bossche**, H. Grönbeck (Göteborg, SE)  
*A first-principles microkinetic model for CH<sub>4</sub> oxidation over PdO(101)*
- P20. **Adriana Trincherro**, A. Hellman, H. Grönbeck (Göteborg, SE)  
*Metal-oxide sites for facile methane dissociation*
- P21. **Christopher Heard**, S. Siahrostami, H. Grönbeck (Göteborg, SE)  
*Ethylene hydrogenation over transition metal surfaces: What governs the reactivity?*
- P22. **Ladislav Kavan**, S. Civiš, M. Ferus, B. Laskova, M. Zukalova (Prague, CZ)  
*Oxygen-isotopes labeled titanium dioxide*
- P23. F. Guller,<sup>1,2</sup> V. Vildosola,<sup>1,2</sup> **Ana María Llois**,<sup>1,2,3</sup> J. Goniakowski,<sup>4,5</sup> C. Noguera<sup>4,5</sup>  
(Buenos Aires, AR;<sup>1,2,3</sup> Paris, FR<sup>4,5</sup>)  
*Magnetic interactions, polarity effects and phase transitions in low dimensional covalent systems: Transition metal dichalcogenides nanoribbons*
- P24. **Gustavo E. Murgida**,<sup>1</sup> M. V. Ganduglia-Pirovano,<sup>2</sup> V. Ferrari,<sup>1</sup> A. M. Llois<sup>1</sup>  
(Buenos Aires, AR;<sup>1</sup> Madrid, ES<sup>2</sup>)  
*Ordering of oxygen vacancies and charge localization in reduced bulk ceria*
- P25. I. Urdayeta, E. Luppi, D. Finkelstein-Shapiro, A. Keller, V. Mujica, **Monica Calatayud** (Paris, FR;<sup>1</sup> Phoenix, US<sup>2</sup>)  
*SERS effect of dopamine adsorbed on TiO<sub>2</sub> nanoparticles*
- P26. A. Tribalis, **Soghomon Boghosian** (Patras, GR) *Aspects of morphology, molecular structure, O-lattice order and defect induced vibrational properties of CeO<sub>2</sub>/ZrO<sub>2</sub> based materials probed by in situ Raman spectroscopy*
- P27. **Ilja Makkonen**, F. Tuomisto (Espoo, FI)  
*Polaronic trapping of positrons and holes on acceptor sites in ZnO and GaN*
- P28. **Michele Melchionna**, A. Beltram, M. Prato, P. Fornasiero (Trieste, IT)  
*MWCNT@Pd/TiO<sub>2</sub> hybrids as efficient catalysts for ethanol and glycerol photoreforming*
- P29. A. Rednyk,<sup>1</sup> **Anna Ostroverkh**,<sup>2</sup> V. Johánek,<sup>1</sup> V. Matolín,<sup>1</sup> P. Kůš<sup>1</sup> (Prague, CZ;<sup>1</sup> Kiev, UA<sup>2</sup>) *Methanol partial oxidation over PtO<sub>x</sub>, Pt/CeO<sub>2</sub>, and CeO<sub>2</sub>/Pt catalysts*
- P30. **Vera Prozheeva**,<sup>1</sup> E. Korhonen,<sup>1</sup> F. Tuomisto,<sup>1</sup> O. Bierwagen,<sup>2,5</sup> J. S. Speck,<sup>2</sup> M. E. White,<sup>2</sup> Z. Galazka,<sup>3</sup> H. Liu,<sup>4</sup> N. Izyumskaya,<sup>4</sup> V. Avrutin,<sup>4</sup> Ü. Özgür,<sup>4</sup> H. Morkoç<sup>4</sup>  
(Aalto, FI;<sup>1</sup> Santa Barbara, California, USA;<sup>2</sup> Berlin, DE;<sup>3</sup> Richmond, Virginia, USA;<sup>4</sup> Berlin, DE<sup>5</sup>)  
*Cation vacancies and electrical compensation in Sb-doped thin-film SnO<sub>2</sub> and ZnO*
- P31. **Annapaola Migani** (Bellaterra, ES) *Comparing the quasiparticle level alignment for the TiO<sub>2</sub>(110) – H<sub>2</sub>O and TiO<sub>2</sub>(110) – CH<sub>3</sub>OH photocatalytic interfaces*
- P32. **Željko Šljivančanin** (Belgrade, RS)  
*Diffusion of gold clusters trapped at F-centers of MgO(100) and CaO(100) surfaces*
- P33. C. M. Yim,<sup>1</sup> M. B. Watkins,<sup>2</sup> **Chi Lun Pang**,<sup>1</sup> M. J. Wolf,<sup>2,3</sup> K. Hermansson,<sup>3</sup> A. L. Shluger,<sup>2</sup> G. Thornton<sup>1</sup> (London, UK;<sup>1,2</sup> Uppsala, SE<sup>3</sup>)  
*Engineering polarons at a metal oxide surface*
- P34. B.-J. Shaw, **David C. Grinter**, C. L. Pang, G. Thornton (London, UK) *A model catalyst system for the water-gas shift reaction*

- P35. R. Bliem, O. Gamba, Z. Novotny, M. Schmid, U. Diebold, **Gareth S. Parkinson** (Vienna, AT) *Characterizing metal adsorption at the  $Fe_3O_4(001)$  surface*
- P36. J. Kullgren,<sup>1</sup> **Matthew J. Wolf**,<sup>1,2</sup> C. W. M. Castleton,<sup>3</sup> P. Mitev,<sup>1</sup> W. Briels,<sup>4</sup> K. Hermansson<sup>1</sup> (Uppsala, SE;<sup>1</sup> London, UK;<sup>2</sup> Nottingham, UK;<sup>3</sup> Enschede, NL<sup>4</sup>) *Oxygen vacancies vs. fluorine impurities at  $CeO_2(111)$ : A case of mistaken identity?*
- P37. A. Iglesias-Juez,<sup>1</sup> F. Viñes,<sup>2</sup> **Oriol Lamiel-García**,<sup>2</sup> M. Fernandez-García,<sup>1</sup> F. Illas<sup>2</sup> (Madrid, ES;<sup>1</sup> Barcelona, ES<sup>2</sup>)  
*Surface contact engineering in photoactive ZnO nanostructures*
- P38. **Alberto Figueroba**, K. M. Neyman (Barcelona, ES) *Atomically dispersed M species (M = Pd, Ni, Cu) in ceria nanoparticles: Stability and red-ox processes*
- P39. **Mario Chiesa**,<sup>1</sup> M. C. Paganini,<sup>1</sup> S. Livraghi,<sup>1</sup> E. Giamello,<sup>1</sup> Z. Sojka<sup>2</sup> (Torino, IT;<sup>1</sup> Krakow, PL<sup>2</sup>) *Charge Trapping in  $TiO_2$  polymorphs as studied by means of EPR and HR-TEM techniques*
- P40. **Suzana Petrović**, B. Salatić, D. Milovanović, B. Jelenković (Belgrade, RS)  
*Synthesis and characterization of NiO:Au nanoparticles by laser ablation of Ni bulk in Au colloidal solution*
- P41. **Brana Jelenković**,<sup>1</sup> A. Kovačević,<sup>1</sup> B. Salatić,<sup>1</sup> S. Petrović,<sup>2</sup> D. Pantelić,<sup>1</sup> M. Trtica<sup>2</sup> (Belgrade, RS<sup>1,2</sup>) (Belgrade, RS) *Synthesis of ultra-thin bimetallic AlFe-oxide layer on 3x(Al/Fe)/Si multilayer structure by laser processing*
- P42. C. M. Olmos,<sup>1</sup> A. Villa,<sup>2</sup> L. E. Chinchilla,<sup>1</sup> J. J. Delgado,<sup>1</sup> A. B. Hungría,<sup>1</sup> J. J. Calvino,<sup>1</sup> L. Prati,<sup>2</sup> **Xiaowei Chen**<sup>1</sup> (Puerto Real, ES;<sup>1</sup> Milan, IT<sup>2</sup>)  
*Influence of post-treatment of bimetallic Au-Pd catalysts supported on ceria-zirconia for selective oxidation of benzyl alcohol*
- P43. **Hristiyan A. Aleksandrov**,<sup>1,2</sup> K. M. Neyman,<sup>2,3</sup> G. N. Vayssilov<sup>1</sup> (Sofia, BG;<sup>1</sup> Barcelona, ES<sup>2,3</sup>) *Theoretical study of the CO interactions with mononuclear platinum species supported on nanoparticulate ceria*
- P44. T. S. Nguyen, G. Postole, F. Morfin, **Laurent Piccolo** (Villeurbanne, FR)  
*Solution combustion synthesis of noble metal-loaded ceria catalysts and application to hydrogen production and purification for fuel cells*
- P45. O. Brummel,<sup>1</sup> R. Fiala,<sup>2</sup> M. Vorokhta,<sup>2</sup> I. Khalakhan,<sup>2</sup> V. Matolín,<sup>2</sup> **Jörg Libuda**<sup>1</sup> (Erlangen, DE;<sup>1</sup> Prague, CZ<sup>2</sup>) *Electrochemical in-situ IR spectroscopy on Pt electrodes: Single crystals, metallic thin-films, Pt nanoparticles, and Pt-doped  $CeO_2$*
- P46. **Iskra Koleva**,<sup>1</sup> H. A. Aleksandrov,<sup>1</sup> G. N. Vayssilov,<sup>1</sup> J. A. van Bokhoven<sup>2,3</sup> (Sofia, BG;<sup>1</sup> Zürich, SW<sup>2,3</sup>) *Relative stability of  $CeO_2$  species on the surfaces and the cavities of  $\gamma-Al_2O_3$ : A periodic DFT study*
- P47. F. Puleo,<sup>1</sup> G. Pantaleo,<sup>1</sup> V. La Parola,<sup>1</sup> X. Collard,<sup>2</sup> C. Aprile,<sup>2</sup> A. Martinez-Arias,<sup>3</sup> **Leonarda F. Liotta**<sup>1</sup> (Palermo, IT;<sup>1</sup> Namur, BL;<sup>2</sup> Madrid, ES<sup>3</sup>)  
*Bi- and trimetallic Ni-based catalysts for methane dry reforming: TEM and DRIFTS investigations of the metals effect*
- P48. **T. Tabakova**,<sup>1</sup> L. Ilieva,<sup>1</sup> I. Ivanov,<sup>1</sup> P. Petrova,<sup>1</sup> R. Zanella,<sup>2</sup> Z. Kaszukur,<sup>3</sup> J. W. Sobczak,<sup>3</sup> W. Lisowski,<sup>3</sup> L. F. Liotta,<sup>4</sup> A. M. Venezia<sup>4</sup> (Sofia, BG;<sup>1</sup> México D.F., MX;<sup>2</sup> Warsaw, PL;<sup>3</sup> Palermo, IT<sup>4</sup>) *Structure-WGS activity relationship study of gold catalysts supported on  $Y_2O_3$ -doped ceria*
- P49. **Mihaela Florea**,<sup>1</sup> G. Postole,<sup>2</sup> C. G. Rotaru,<sup>1</sup> F. Matei,<sup>2</sup> P. Gelin<sup>2</sup> (Bucharest, RO;<sup>1</sup> Villeurbanne, FR<sup>2</sup>) *Characterization of ceria for SOFC anodes applications*

- P50. F. Ribeiro, **Matteo Farnesi Camellone**, S. Fabris (Trieste, IT)  
*Thermodynamics and spectroscopy of Pt species at ceria surfaces*
- P51. **L. Ilieva**,<sup>1</sup> P. Petrova,<sup>1</sup> T. Tabakova,<sup>1</sup> G. Pantaleo,<sup>2</sup> L. F. Liotta,<sup>2</sup> R. Zanella,<sup>3</sup> Z. Kaszkar,<sup>4</sup> A. M. Venezia<sup>2</sup> (Sofia, BG;<sup>1</sup> Palermo, IT;<sup>2</sup> México D.F., MX;<sup>3</sup> Warsaw, PL<sup>4</sup>)  
*Gold catalysts on Y doped-ceria for CO-free hydrogen production via PROX*
- P52. **Shaoli Guo**,<sup>1,2</sup> F. Puleo,<sup>1</sup> A. Longo,<sup>1,3</sup> V. La Parola,<sup>1</sup> G. Pantaleo,<sup>1</sup> **Leonarda F. Liotta**<sup>1</sup> (Palermo, IT;<sup>1</sup> Xi'an, P.R. China;<sup>2</sup> Grenoble, FR<sup>3</sup>)  
*One pot synthesis of  $La_{0.6}Sr_{0.4}Co_{1-x}Fe_{x-0.03}M_{0.03}O_{3-\delta}$  ( $x=0.2/0.8$ ;  $M=Pd/Ni$ ) perovskites with tailored oxygen vacancies: structure-properties relationship*
- P53. **Tomas Duchoň**,<sup>1</sup> M. Aulická,<sup>1</sup> E. F. Schwier,<sup>2</sup> Y. Xu,<sup>3</sup> J. Jiang,<sup>2</sup> H. Iwasawa,<sup>2</sup> K. Veltruská,<sup>1</sup> V. Matolín,<sup>1</sup> K. Shimada,<sup>2</sup> H. Namatame,<sup>2</sup> M. Taniguchi<sup>2,4</sup> (Prague, CZ;<sup>1</sup> Hiroshima, JP;<sup>2,4</sup> Baton Rouge, USA<sup>3</sup>)  
*Covalency in ceria: A res-ARPES and DFT study*
- P54. **Yaroslava Lykhach**,<sup>1</sup> A. Neitzel,<sup>1</sup> O. Brummel,<sup>1</sup> N. Tsud,<sup>2</sup> T. Skála,<sup>2</sup> V. Stetsovych,<sup>2</sup> K. Ševčíková,<sup>2</sup> M. Vorokhta,<sup>2</sup> D. Mazur,<sup>2</sup> K. C. Prince,<sup>3</sup> J. Mysliveček,<sup>2</sup> V. Matolín,<sup>2</sup> J. Libuda<sup>1,4</sup> (Erlangen, GE;<sup>1,4</sup> Prague, CZ;<sup>2</sup> Basovizza-Trieste, IT<sup>3</sup>)  
*Hydrogen activation on ceria-based fuel cell catalysts*
- P55. **Gilles R. Bourret**,<sup>1,2,4</sup> T. Ozel,<sup>3,4</sup> M. Blaber,<sup>2,4</sup> K. A. Brown,<sup>3,4</sup> A. L. Schmucker,<sup>2,4</sup> M. Rycenga,<sup>2,4</sup> C. Shade,<sup>2,4</sup> G. C. Schatz,<sup>2,3,4</sup> Chad A. Mirkin<sup>2,3,4</sup> (Salzburg, AT;<sup>1</sup> Evanston, USA<sup>2,3,4</sup>)  
*Templated Synthesis of One-Dimensional Nanostructures for Plasmonic Applications*
- P56. A. R. Gheisi,<sup>1</sup> C. Neygandhi,<sup>1</sup> A. K. Sternig,<sup>1</sup> E. Carrasco,<sup>2</sup> H. Marbach,<sup>2</sup> D. Thomele,<sup>3</sup> **Oliver Diwald**<sup>3</sup> (Erlangen, GE;<sup>1,2</sup> Salzburg, AT<sup>3</sup>) *O<sub>2</sub> Adsorption dependent Photoluminescence Emission from Metal Oxide Nanoparticles*
- P57. **Xiao Hu**, C. Wu, M. S. J. Marshall, M. R. Castell (Oxford, UK)  
*Surface structures of ultrathin TiO<sub>x</sub> and NbO<sub>x</sub> films on Au (111)*
- P58. M. S. J. Marshall,<sup>1</sup> **Yakun Gao**,<sup>1</sup> A. E. Becerra-Toledo,<sup>2</sup> L. D. Marks,<sup>2</sup> M. R. Castell<sup>1</sup> (Oxford, UK;<sup>1</sup> Evanston, USA<sup>2</sup>)  
*TiO<sub>x</sub>-based linear nanostructures on the SrTiO<sub>3</sub> (001) surface*
- P59. A. Feliczak-Guzik, L. Szczesniak, **Izabela Nowak** (Poznan, PL) *Application of mesoporous materials containing ruthenium for hydrogenation of citral*
- P60. A. Wawrzyńczak, M. Górzyńska, **Izabela Nowak** (Poznan, PL)  
*Ordered mesoporous silicas with SBA-16-like structure modified with aminosilanes*
- P61. **L. Alejandro Miccio**,<sup>1</sup> M. Abadía,<sup>2</sup> R. González-Moreno,<sup>3</sup> C. Rogero,<sup>4</sup> F. Schiller,<sup>4</sup> **J. Enrique Ortega**<sup>1,2,4</sup> (San Sebastian,<sup>1-4</sup> ES) *Structure and electronic states of Au nanodots grown on a curved TiO<sub>2</sub>(110) rutile single crystal*
- P62. **Kyoung Chul Ko**,<sup>1,2</sup> O. Lamiel-García,<sup>1</sup> J. Y. Lee,<sup>2</sup> F. Illas<sup>1</sup> (Barcelona, ES;<sup>1</sup> Suwon, KR<sup>2</sup>) *Exploring TiO<sub>2</sub> polymorphs with a modified hybrid functional*
- P63. **Hildur Guðmundsdóttir**, H. Jónsson (Reykjavik, IS)  
*Self-interaction corrected density functional calculations of localized electron hole at Al dopant in SiO<sub>2</sub>*

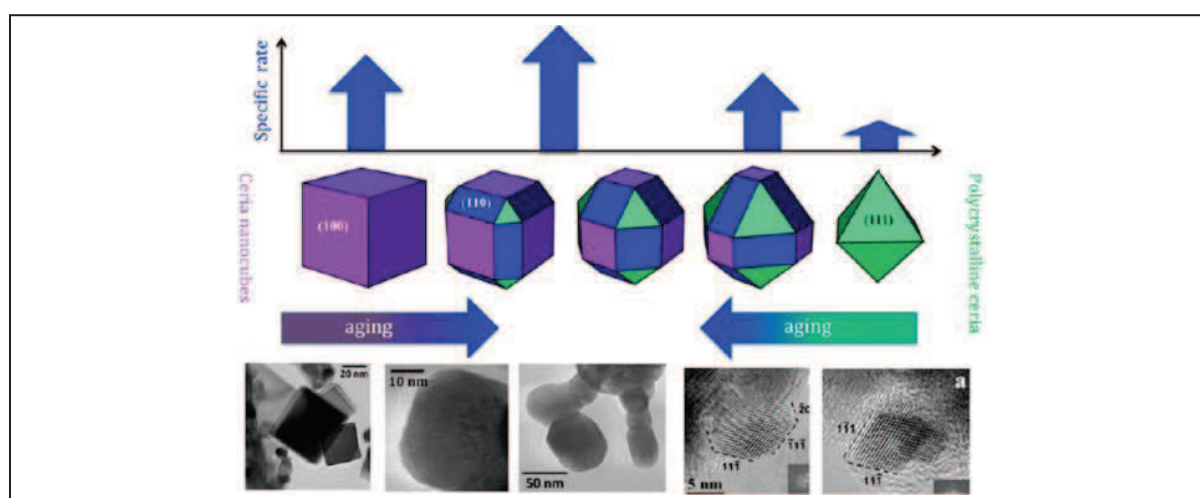
# INVITED LECTURES

## Strategies for soot oxidation over nanoshaped CeO<sub>2</sub>

**Jordi Llorca**

Institute of Energy Technologies, Universitat Politècnica de Catalunya, Barcelona, Spain  
jordi.llorca@upc.edu

Ceria is a key component of catalyst formulations for several applications in the environment and energy sector, and these applications benefit from ceria redox properties, which are in turn associated with the arrangement of its surfaces and the shape and dimensions of its crystals. Nanoshaped ceria commonly exhibits higher catalytic activity than conventional polycrystalline ceria. This is correlated to the exposure of reactive crystal planes in CeO<sub>2</sub> nanoparticles: {001} and {110} planes are more active than conventional ceria with preferred exposure of {111} planes. The facet-dependent activity in ceria has been reported in the CO oxidation, CO<sub>2</sub> reforming of methane, methanol and ethanol reforming, and low temperature water-gas shift. The higher activity of specific ceria surfaces has also been recognized in ceria films grown with different orientations. The majority of these results, which rely on the redox properties of ceria and its ability to release/capture oxygen, are supported by theoretical evidence that correlate higher activity to the lower stability of {100} and {110}-type surfaces compared with {111} and to their lower energy of oxygen vacancies formation. The ability of ceria to promote oxygen storage/redox behavior is also at the basis of its application as a catalyst for combustion of soot particulate under conditions typical of diesel car exhaust [1-3]. We have prepared a series of nanoshaped ceria with cubic and rod shapes and compared their activity in soot oxidation (both specific rate and overall activity) with the activity of irregularly shaped polycrystalline ceria. By comparing samples within the same surface area range, higher activity and conversion is observed over nanocubes and nanorods as compared with polycrystalline ceria octahedral particles. Thermal aging at  $T > 773$  K markedly affects the crystal shape by truncation of the edges and corners, generating surfaces with higher index plane exposure, resulting in an increase in the specific activity. Interestingly, it is shown that starting either from nanocubes or from polycrystalline ceria, similar morphologies and shapes are obtained after aging [1]. These results open up new possibilities in the design of highly active ceria-based catalysts with controlled morphologies.



- [1] E. Aneggi, D. Wiater, C. Leitenburg, J. Llorca, A. Trovarelli, ACS Catal. **4**, 172 (2014)
- [2] E. Aneggi, N.J. Divins, C. Leitenburg, J. Llorca, A. Trovarelli, J. Catal. **312**, 191 (2014)
- [3] E. Aneggi, C. Leitenburg, J. Llorca, A. Trovarelli, Catal. Today **197**, 119 (2012)



# ORAL CONTRIBUTIONS

# Contribution of Electron Microscopy to the characterization of ceria based catalysts

J.J. Delgado<sup>1</sup>, T. Montini<sup>2</sup>, S. Collins<sup>3</sup>, X. Chen<sup>1</sup>, A. Bonivardi<sup>3</sup>, H. Pan<sup>1</sup>, J.J. Calvino<sup>1</sup>, E. del Río<sup>1</sup>, M. López-Haro<sup>1</sup>, I. Romero<sup>2</sup> and P. Fornasiero<sup>2</sup>

<sup>1</sup> Inorganic Chemistry Department. University of Cadiz

<sup>2</sup> Department of Chemical and Pharmaceutical Sciences. University of Trieste

<sup>3</sup> Instituto de Desarrollo Tecnológico para la Industria Química (INTEC). Santa Fe

e-mail: juanjose.delgado@uca.es

It is unquestionable that one of the most important challenges of our society is the development of new energy strategies to tackle global warming and exhaustion of fossil fuels. In this context, catalysis has been proven as a critical enabling science for developing the use of alternative feedstocks, such as biomass or hydrogen, and increasing energy production efficiency [1].

Real catalysts commonly are complex multicomponent systems whose characterization usually demands an insight at the atomic level, and they are continuously posing new challenges and calling for further improvements in Electron Microscopy techniques. On the other hand, real catalysts contain morphological, structural and compositional heterogeneities and it is also obvious the need of developing new methodologies, based in statistical studies, that will give us a real picture of our catalyst. This point is really crucial for the rationalization of structure-activity relationships and understanding the deactivation processes.

The major goal of this contribution will be to review the possibilities of (Scanning) Transmission Electron Microscopy to reveal the ultimate details of the structure of nanostructured catalysts and how this information allow us gaining some understanding of how they work as catalysts. Data obtained between the labs at University of Cadiz and University of Trieste will be shown. We will specially focus on the use of an environmental reaction cell specific for an anaerobic-transfer TEM holder is an alternative approach that allows carrying out the pre-treatment of the sample under more realistic conditions and subsequently transferring it to the TEM, under conditions which prevent any ulterior sample modification. Although the dynamic aspects of the gas-solid interactions are lost in this alternative approach, the characterization of those structural and compositional features which are induced by realistic thermo-chemical treatments, which could be lost by interaction with air components but which are not reversed by evacuation or cooling, can be investigated.

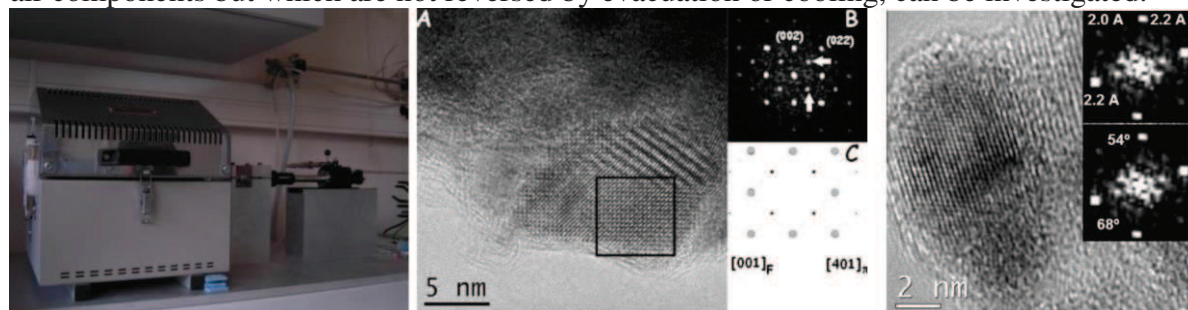


**Figure 1.** Anaerobic transfer holder and reaction cell (left) and High-resolution micrographs of a Rh/CeO<sub>2</sub> sample after pre-treatment under H<sub>2</sub>-Ar (central) and one Pd-Ga nanoparticle using the anaerobic transfer approach. Digital diffraction patterns showing the presence of a ceria reduced  $\pi$  like structure is also included(central) and Pd<sub>2</sub>Ga<sub>5</sub> [2].

[1] G.M. Whitesides and G.W. Crabtree, *Science*, 315 (2007), 796.

[2] S. Collins et al, *Journal of Catalysis* 292 (2012), 90.

# Size and shape of cobalt spinel nanocrystals revealed by HAADF-STEM and DFT first-principles calculation

Joanna Grybos<sup>1</sup>, Jan Kaczmarczyk<sup>1</sup>, Filip Zasada<sup>1</sup>, Juri Barthel<sup>2</sup>, Juan Jose Delgado Jean<sup>3</sup> and Zbigniew Sojka<sup>1</sup>

<sup>1</sup> Faculty of Chemistry, Jagiellonian University, Ingardena 3, Krakow

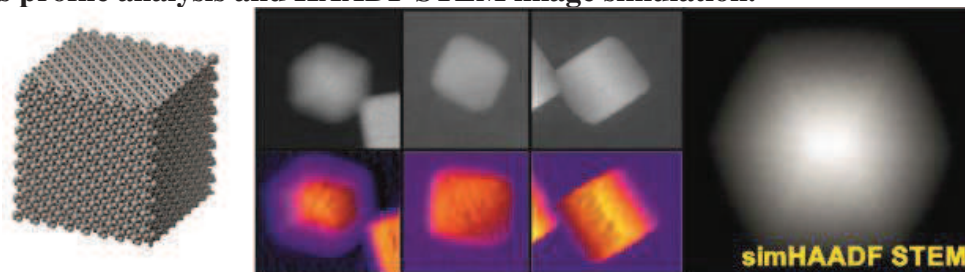
<sup>2</sup> Ernst Ruska-Centre, Forschungszentrum Jülich GmbH, D-52425 Jülich, Germany.

<sup>3</sup>Inorganic Chemistry Department, University of Cadiz

grybosjo@chemia.uj.edu.pl

Being widely used in heterogeneous catalysis, oxide nanocrystals are characterized by clear-cut structure and substantial surface area. This makes them excellent model systems for experimental and theoretical investigations into the surface related properties at atomic scale. New catalytic materials of enhanced activity and selectivity can be designed by exploiting the phenomenon that faceted polyhedral crystals expose well-defined crystallographic planes, depending on the synthesis method. In such an approach, facets exposing crystallographic planes of high activity or with a higher density of active sites could be intentionally promoted. It has been shown that HAADF/ADF imaging allows for a quantification of the number and location of all atoms in a 3D arbitrary shaped nanocrystal without the need for calibration standards [2]. We propose a simplified approach to determine the 3-dimensional shape of nanocrystals, which involves combined use of HAADF STEM imaging and DFT ab-initio calculations together with 3D morphology determination using Wulff construction. The validity of our approach is tested with  $\text{Co}_3\text{O}_4$  nanoparticles with a controlled cubic morphology. Samples were obtained by microwave assisted hydrothermal synthesis. The experimental part of the shape analysis is based on the acquisition of HAADF STEM images with an intentionally increased electron probe size. The high-angle elastic scattering signal is registered as a fraction of the incident probe current by a respectively calibrated detector. Numerical calculations of HAADF STEM images under such a condition show a linear dependency of the recorded signal on the specimen thickness for randomly oriented nanocrystals and for probe diameters larger than the crystal unit cell. By inversion of the relation between local object thickness and HAADF signal, thickness profiles are extracted from calibrated HAADF STEM images of  $\text{Co}_3\text{O}_4$  nanocrystals. The 3D shape of nanocrystals is deduced from the thickness profiles in comparison to energetically favourable morphologies as suggested by DFT calculations. Such theoretical structure models have been calculated using DFT/PW91 level of theory within the VASP code [3]. The geometry of the exposed (100) surface was constructed by cleaving the solid in the normal (100) direction (Fig.1). It is planned to apply this approach for a shape analysis of nano-oxide catalytic materials with lower crystal symmetry, such as t- and m- $\text{ZrO}_2$ .

**Fig1. Structure and HAADF STEM images of  $\text{Co}_3\text{O}_4$  nanocrystals together with thickness profile analysis and HAADF STEM image simulation.**



[1] J. M. LeBeau, S. D. Findlay, L. J. Allen, S. Stemmer: Nano Lett **10** (2010), p. 4405-4408.

[2] J. Hafner: J. Compt. Chem. **29** (2008), p. 2046.

The project was financed by the Polish National Science Center awarded by decision number DEC-2011/03/B/ST5/01564

## Model studies of Ni(Pd)-ZrO<sub>2</sub>-Pt<sub>3</sub>(Pd<sub>3</sub>)Zr solid oxide fuel cell anodes

Hao Li <sup>1</sup>, Jake (Joong-Il) Choi <sup>2</sup>, Wernfried Mayr-Schmölzer <sup>2,3</sup>, Christian Weilach <sup>1</sup>, Christoph Rameshan <sup>1</sup>, Florian Mittendorfer <sup>2,3</sup>, Josef Redinger <sup>2,3</sup>, Michael Schmid <sup>2</sup> and Günther Rupprechter <sup>1</sup>

<sup>1</sup> Institute of Materials Chemistry, Vienna University of Technology, 1060 Vienna, Austria

<sup>2</sup> Institute of Applied Physics, Vienna University of Technology, 1040 Vienna, Austria

<sup>3</sup> Center for Computational Materials Science, Vienna Univ. of Techn., 1040 Vienna, Austria  
(corresponding author: G. Rupprechter, e-mail: grupp@imc.tuwien.ac.at)

Solid Oxide Fuel Cells (SOFCs) are promising devices for effective energy generation. Nevertheless, improvements of their performance rely on a fundamental understanding of their components, such as the anode, the electrolyte and the cathode. The FWF SFB FOXSI, which is hosted at TU Wien, aims at elucidating the involved processes on a molecular level. In order to model SOFC anodes well-ordered ultrathin films of ZrO<sub>2</sub> were grown in ultrahigh vacuum (UHV) by oxidation and annealing of Pt<sub>3</sub>Zr or Pd<sub>3</sub>Zr single crystals [1]. Ni or Pd was then deposited by physical vapor deposition. Ni particles supported by ZrO<sub>2</sub> are also widely used in the field of heterogeneous catalysis, such as for reforming reactions.

The chemical composition of the ZrO<sub>2</sub> model system was examined by high resolution X-ray Photoelectron Spectroscopy (XPS), the structure was characterized by Scanning Tunneling Microscopy (STM). Water and CO were used to probe the chemical properties of the ZrO<sub>2</sub>-film and the metal nanoparticles, studied at near ambient pressure by AP-XPS and polarization modulation infrared reflection-adsorption spectroscopy (PM-IRAS).

A previously described route was followed to obtain a well-ordered and ultra-thin trilayer ZrO<sub>2</sub> film [1]: A cleaned Pt<sub>3</sub>Zr (0001) alloy substrate was oxidized at 673 K, followed by post-annealing at 1023 K. Apart from a signal characteristic of metallic zirconium resulting from the substrate (Zr<sub>m,s</sub>), (synchrotron) XPS showed two distinctive oxidic species (Zr<sub>1,o</sub> and Zr<sub>2,o</sub>). Depth profiling indicated that Zr<sub>2,o</sub> extended to deeper layers than Zr<sub>1,o</sub>. After post-annealing of the oxide at 923 K, STM detected many small clusters with a height of about 1 nm. Increasing the annealing temperature to 1023 K led to the disappearance of most of the small clusters, accompanied by a significant decrease of the intensity of Zr<sub>2,o</sub> in XPS. Thus, Zr<sub>1,o</sub> and Zr<sub>2,o</sub> were assigned to Zr oxide species within the trilayer zirconia film and a Zr oxide species in the zirconia clusters, respectively. Density Functional Theory (DFT) calculations corroborated and explained these assignments. Thermal Desorption Spectroscopy (TDS) using CO as probe molecule was then utilized to demonstrate that the entire substrate was covered by the zirconia thin film.

The interaction of ZrO<sub>2</sub> with water was examined by synchrotron XPS (Lund). Surface defects, likely oxygen vacancies, created by soft sputtering, induced water dissociation, which was also enhanced at higher water pressures (low mbar range).

Ni and Pd nanoparticles grown on ZrO<sub>2</sub> were characterized via CO adsorption, monitored by TDS, XPS and PM-IRAS. At 200 K CO adsorbed on Ni particles in on-top adsorption geometry but at increasing temperature CO dissociation was observed that led to catalyst deactivation. Corresponding experiments with Pd-ZrO<sub>2</sub> did not show CO dissociation but likely encapsulation of the Pd nanoparticles.

Support by the Austrian Science Fund (FWF SFB-F45 FOXSI; projects 01/02/05/11) is gratefully acknowledged.

[1] M. Antlanger, et al., Phys. Rev. B., **86**, 03451, (2012).

## Solar Thermochemical Syngas Production by a CeO<sub>2</sub> based Redox Cycle

Alexander Bonk<sup>1,2</sup>, Ulrich F. Vogt<sup>1,2</sup>, Aldo Steinfeld<sup>3</sup>, Andreas Züttel<sup>1</sup>

<sup>1</sup> Empa, Laboratory for Hydrogen & Energy, CH-8600 Dübendorf

<sup>2</sup> University of Freiburg, Crystallography, D-79098 Freiburg i. Brsg.

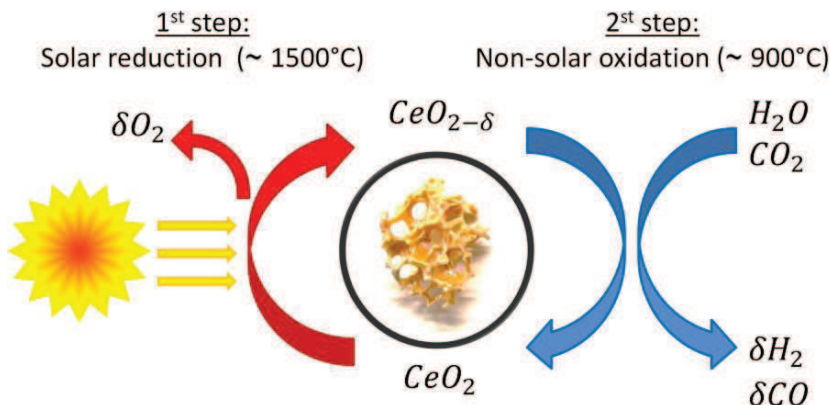
<sup>3</sup> Department of Mechanical and Process Engineering, ETH Zurich, CH-8092 Zurich

ulrich.vogt@empa.ch

H<sub>2</sub>O and CO<sub>2</sub> can be reduced to H<sub>2</sub> and CO by a CeO<sub>2</sub> based solar thermochemical RedOx cycle.<sup>1</sup> Due to its excellent high temperature-, thermodynamic-, and kinetic properties, cerium dioxide is a very promising metal oxides for this application. In a 2-step solar thermochemical cycle, above 1400°C and under vacuum, Ceria releases oxygen from its lattice by forming oxygen vacancies (CeO<sub>2-δ</sub>). In a following up step, the oxygen vacancies react with H<sub>2</sub>O and CO<sub>2</sub> to form H<sub>2</sub> and CO below 1000°C.<sup>2</sup> Stoichiometric CeO<sub>2</sub> is regained by closing the RedOx cycle.

Doped CeO<sub>2</sub> based reticulated porous ceramics (RPC) has demonstrated high conversion efficiencies for this Solar to Fuel conversion process. The control of thermodynamics, kinetics and the transport of concentrated solar energy to the reactant is essential for designing highly efficient ceria based structures.<sup>3</sup>

Doping of CeO<sub>2</sub> with isovalent cations was proposed to have remarkable impact on ceria RedOx properties. For this purpose, doped M<sub>x</sub>Ce<sub>1-x</sub>O<sub>2-d</sub> (M = Hf, Zr, Pr, Ti; 0 < x < 0.2) were investigated concerning RedOx characteristics, CeO<sub>2</sub> phase conversions, microstructural evolution as well as sintering properties.



The Solar Thermochemical Cycle with CeO<sub>2</sub> Ceramic foams

[1] A. Steinfeld *et al.*, *Solar Energy*, **2005**, 78 (5), 603-615

[2] P. Furler *et al.*, *Energy & Fuels*, **2012**, 26, 7051-7059

[3] P. Furler *et al.*, *Phys. Chem. Chem. Phys.*, **2014**, 16, 10503-10511

# Electronic properties of dispersed copper oxide entities interacting with ceria: near-ambient XPS analysis of the reduction under CO

Manuel Monte<sup>1</sup>, Dominique Costa,<sup>2</sup> José C. Conesa<sup>1</sup>, Guillermo Munuera<sup>3</sup>, Arturo Martínez-Arias<sup>1</sup>

<sup>1</sup> Instituto de Catálisis y Petroleoquímica, CSIC, Marie Curie 2, 28049 Madrid, Spain. E-mail: amartinez@icp.csic.es

<sup>2</sup> IFP, 1 & 4 Avenue de Bois-Preau, 92852 Reuil-Malmaison Cedex, France.

<sup>3</sup> Departamento de Química Inorgánica. Universidad de Sevilla, 41092 Spain.

Catalysts combining copper and cerium oxides are an economically interesting alternative to noble metal catalysts for various processes involved during production-purification of hydrogen generated from hydrocarbons or biomass feedstocks. In particular, they show promising characteristics for processes involving CO oxidation like the water-gas shift reaction (WGS) or preferential oxidation of CO (CO-PROX). Their catalytic properties for such processes depend strongly on the characteristics of the interface formed between the two oxide components [1,2]. However, direct information on interfacial properties as well as about those of well dispersed copper oxide nanoparticles interacting with CeO<sub>2</sub> in powder catalysts is not generally available due to the important difficulties for the characterization of such nanosized generally amorphous entities. The present contribution explores these issues by means of near-ambient XPS spectroscopy complemented with theoretical DFT analysis. Two samples of copper oxide dispersed on two different ceria supports (in the form of nanospheres –NS- and nanocubes –NC-, respectively), which allow comparison between well differentiated situations in terms of degree of dispersion and interfacial morphology, are employed for this purpose. Direct evidence of reduced interfacial copper entities, considered as active sites for CO oxidation in this type of catalysts [1,2], as well as significant details of the electronic properties of the dispersed partially reduced copper oxide entities are provided by detailed analysis of the results obtained.

Details of the preparation and multitechnique (XRD, HREM, Raman, XPS, EPR, H<sub>2</sub>-TPR, S<sub>BET</sub>) characterization of the two catalysts can be found elsewhere [3]. The catalysts subjected to treatment under diluted CO up to 300 °C are examined by XPS in gas environment (100 Pa) obtained at ISSS station of the BESSY II synchrotron in Berlin. Figure 1 provides an example of the results obtained. New XPS Cu 2p (at 930.1 eV) and Auger L<sub>3</sub>M<sub>45</sub>M<sub>45</sub> signals (at ca. 913 eV) specific of interfacial Cu<sup>+</sup> entities are identified on the basis of theoretical analysis and consideration of respective amount and characteristics of the interfacial sites present in each sample [3]. The evolution of the chemical

state of the various copper species as a function of the reduction temperature under CO will be shown while information from other spectral regions, providing interesting hints on the characteristics of the carbonyl species formed under CO, will be also presented.

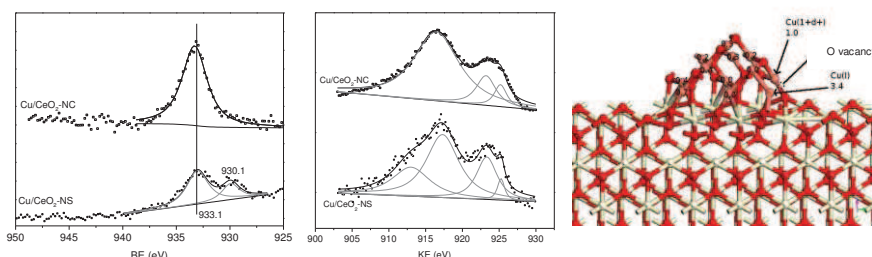


**Figure 1.** XPS Cu 2p<sub>3/2</sub> (left) and Auger L<sub>3</sub>M<sub>45</sub>M<sub>45</sub> (centre) spectra for the indicated samples under CO at 150 °C. Example of a model employed for the theoretical study with (111) exposed face of CeO<sub>2</sub> indicating the calculated core level shifts with respect to pure CuO

- [1] X. Wang et al. *J. Phys. Chem. B* **110**, 428 (2006).  
[2] D. Gamarra et al. *J. Am. Chem. Soc.* **129**, 12064 (2007).  
[3] D. Gamarra et al. *Appl. Catal. B* **130-131**, 224 (2013).

## Reduction and oxidation of a bulk-like ceria film

R. Olbrich<sup>1</sup>, C. Laffon<sup>3</sup>, M. H. Zoellner<sup>2</sup>, G. Niu<sup>2</sup>, T. Schroeder<sup>2</sup>, Ph. Parent<sup>3</sup>, C. Barth<sup>3</sup> and M. Reichling<sup>1</sup>

<sup>1</sup>Fachbereich Physik, Universität Osnabrück, Barbarastr. 7, 49076 Osnabrück, Germany

<sup>2</sup>IHP, Im Technologiepark 25, 15236 Frankfurt (Oder), Germany

<sup>3</sup>CINaM, CNRS / Aix Marseille Université, 13288 Marseille Cedex 09, France

email: [barth@cinam.univ-mrs.fr](mailto:barth@cinam.univ-mrs.fr)

We characterise high-quality ceria thick (150 nm to 250 nm) films grown with a hexagonal Pr<sub>2</sub>O<sub>3</sub>(0001) buffer layer on Si(111) substrates by molecular beam epitaxy [1]. The as-prepared film exhibits a surface morphology dominated by pyramidal structures resulting from kinetically limited growth modes (Figure, frame 1). By annealing the surface under ultra-high vacuum (UHV) conditions, we create a high-temperature morphology characterised by large terraces separated by steps with triple-layer height (Figure, frame 2) [2]. However, during this procedure, the film is significantly reduced.

We discuss the process of reduction and explore to what extent the film can be re-oxidized. We use non-contact atomic force microscopy (NC-AFM) to analyse the film topography and morphology as a function of annealing temperature and oxidation/reduction state. To determine the (near-)surface stoichiometry, photo-electron spectroscopy (XPS) is applied.

First, we show that the high-temperature morphology can also be obtained by annealing in air (Figure, frame 2), however, in comparison to UHV annealed samples, a contamination, mostly by surface hydroxyls and carbon (as verified by XPS) results in a surface roughness that is considerably higher than that for the vacuum annealed surface. Annealing in oxygen at a pressure of  $5 \times 10^{-6}$  mbar at temperatures of 850 K in UHV removes the contamination (Figure, frame 3), and yields a much more well-defined surface, however, with a nanoscale granular structure. We show that cycles of annealing in UHV and oxygen result in a reproducible partial reduction and oxidation evidenced by the changing surface morphology and stoichiometry.

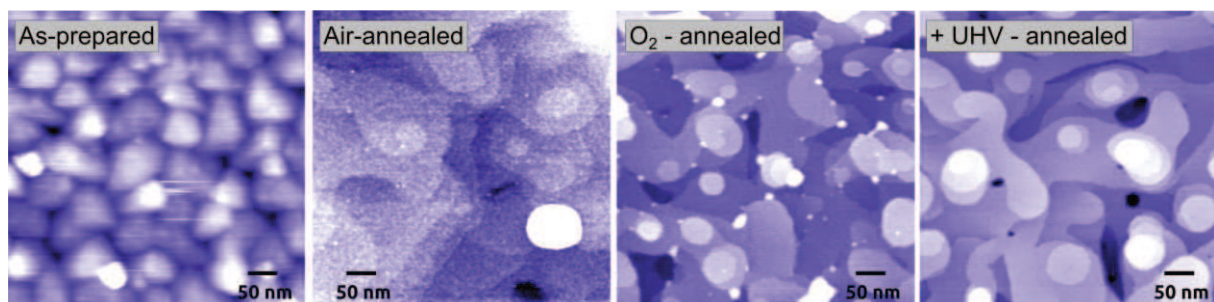


**Figure** Topography images of 180 nm thick ceria films obtained by NC-AFM in UHV. *As-prepared* - the surface after the preparation by molecular beam epitaxy. *Air-annealed* - the surface is flattened after an annealing in air during 15 h at 1100 K. The granular structure on the terraces is due to surface hydroxyls and carbon containing species. *O<sub>2</sub>-annealing* - the surface is cleaned from the contaminants. *+UHV annealing* After an additional reduction by UHV annealing, the surface is almost atomically flat.

[1] M. H. Zoellner, J. Dabrowski, P. Zaumseil, A. Giussani, M. A. Schubert, G. Lupina, H. Wilkens, J. Wollschläger, M. Reichling, M. Bäumer and T. Schroeder, *Phys. Rev. B* **85**, 035302, (2012).

[2] R. Olbrich, H. H. Pieper, R. Oelke, H. Wilkens, J. Wollschläger, M. H. Zoellner, T. Schroeder and M. Reichling, *Appl. Phys. Lett.* **104**, 081910, (2014).

## Size Reduction Effects in MgO Cube Dissolution

Stefan O. Baumann<sup>1</sup>, Johannes Schneider<sup>2</sup>, Andreas Sternig<sup>1</sup>, Daniel Thomele<sup>2</sup>, Slavica Stankic<sup>3</sup>, Thomas Berger<sup>2</sup>, Henrik Grönbeck<sup>4</sup>, **Oliver Diwald**<sup>1,2,\*</sup>

<sup>1</sup> Institute of Particle Technology, Universität Erlangen-Nürnberg, Erlangen (Germany)

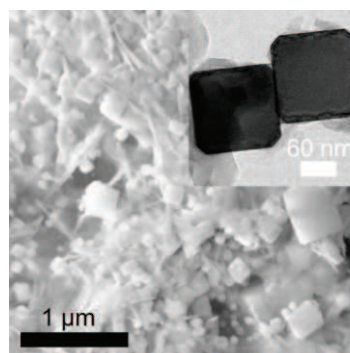
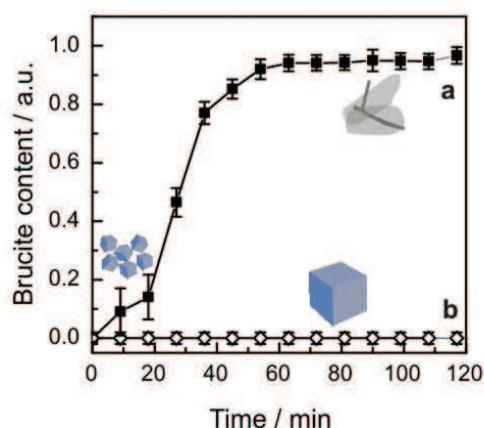
<sup>2</sup> Department of Materials Science and Physics, University of Salzburg, Salzburg (Austria)

<sup>3</sup> CNRS, Institut des Nanosciences de Paris, Paris (France)

<sup>4</sup> Department of Applied Physics, Chalmers University of Technology, Göteborg, (Sweden)

oliver.diwald@sbg.ac.at

Stability parameters and dissolution behavior in aqueous systems is critical to assess functionality and fate of engineered nanomaterials under environmental conditions. Using electron microscopy and X-ray diffraction we investigated the stability of cubic MgO particles which were synthesized by different combustion techniques. In H<sub>2</sub>O MgO dissolution proceeding via water dissociation at the oxide surface, disintegration of Mg<sup>2+</sup>-O<sup>2-</sup> surface elements and their subsequent solvation ultimately leads to precipitation of Mg(OH)<sub>2</sub> nanosheets. MgO nanocubes with a size distribution below 10 nm quantitatively dissolve within few minutes at a pH ≥ 10 and convert into Mg(OH)<sub>2</sub> nanosheets. This effect is different from MgO cubes originating from magnesium combustion in air. With a size distribution in the range 20 nm ≤ d ≤ 1000 nm they exhibit substantially delayed dissolution in water. On these particles water induced etching generates (110) faces which – above a critical face area – dissolve at a rate equal to that of (100) planes.[2] The delayed solubility of microcrystalline MgO is attributed to self-inhibition effects occurring at the (100) and (110) microplanes.[3] The present work underlines the importance of morphology evolution and surface faceting of particles during the dissolution of engineered nanomaterials.



Time-dependent XRD pattern evolution of MgO nanocube (a) and MgO cubes (b) in contact with liquid water. The EM images in the right panel show MgO cubes after 2 hours in water.

- [1] A. Gheisi, A. Sternig, M. Rangus, G. Redhammer, M. Hartmann and O. Diwald, *Crystal Growth & Design*, DOI: 10.1021/cg500538d (2014).
- [2] P. Geysmans, F. Finocchi, J. Goniakowski, R. Hacquart and J. Jupille, *Physical Chemistry Chemical Physics*, **11**, 2228–2233 (2009)
- [3] F. Ringleb, M. Sterrer and H.-J. Freund, *Appl. Catal. A-General*, **474**, 186–193 (2014)

## Structure of the rutile TiO<sub>2</sub>(110) interface with water

H. Hussain<sup>1,2</sup>, T. Woolcot<sup>1</sup>, X. Torrelles<sup>3</sup>, D. Grinter<sup>1</sup>, C.Y. Yim<sup>1</sup>, C.L. Pang<sup>1</sup>, R. Lindsay<sup>4</sup>, O. Bikondoa<sup>2</sup>, J. Zegenhagen<sup>2</sup>, **G. Thornton**<sup>1</sup>

*1. London Centre for Nanotechnology*

*University College London*

*2. ESRF, Grenoble*

*3. CSIC, Barcelona*

*4. School of Materials, University of Manchester*

Much attention has been focused on the surface science of titanium dioxide due to its numerous scientific and industrial to its applications in photocatalysis, electrochemistry, active coatings, gas sensors. Among these studies, many have focused on the interaction of water with rutile and anatase (110) surfaces, due to the fundamental role of water in many of the present and potential applications of TiO<sub>2</sub>. The vast majority of experimental and theoretical understanding of the adsorption behaviour of water on TiO<sub>2</sub>(110) concerns gas phase adsorption in ultra-high vacuum environments ( $<1 \times 10^{-10}$  mbar). Here we present work that has characterised the atomic scale structure and composition of the liquid water interface using surface X-ray diffraction. For rutile (110), a 2x1 an ordered interface of terminal hydroxyls is formed, with water in the second layer.

## Cu attracts subsurface defects and wets the ZnO(0001)-Zn surface

Igor Beinik<sup>1\*</sup>, Matti Hellström<sup>2</sup>, Peter Broqvist<sup>2</sup>, Jeppe V. Lauritsen<sup>1</sup>

<sup>1</sup>Interdisciplinary Nanoscience Center (iNANO), Aarhus University, Denmark

<sup>2</sup>Department of Chemistry – Ångström Laboratory, Uppsala University, Sweden

\*[beinik@inano.au.dk](mailto:beinik@inano.au.dk)

Cu/ZnO-based catalysts are used for the synthesis of methanol and the water-gas shift reaction on an industrial scale [1]. In spite of their widespread use, a number of questions regarding the nature of the active sites, deactivation mechanisms and the role of Cu-Zn alloying in these catalysts remain unresolved. Furthermore, recent studies also showed evidence of noticeable dynamic changes in the structure and shape of the Cu nanoparticles (NPs) supported on ZnO as a function of reaction conditions [2]. These changes have been discussed in terms of a surface defect mediated wetting/dewetting process and pointed out the important role of beneficial metal-support interactions for high catalytic activity of the Cu/ZnO system [2]. In view of the fact that the most active catalysts have primarily polar ZnO faces exposed [3] it is of great interest to investigate the interaction of Cu with the polar ZnO faces.

In the present investigation we have studied thermally-induced Cu-ZnO interactions using a model Cu/ZnO system prepared by depositing 0.2 ML of Cu on a UHV-treated ZnO(0001)-Zn polar surface. The model system was subjected to cyclic thermal annealing up to 650 K and characterized in-situ by a combination of Scanning Tunneling Microscopy (STM), X-ray Photoelectron Spectroscopy (XPS) and Thermal Desorption Spectroscopy (TDS). To better understand the experimental observations, the model system has also been examined in detail using density functional theory (DFT) calculations.

Both the STM and XPS data indicated that Cu diffuses into the bulk ZnO starting from as low as 380 K concurring with the process of NPs coarsening via Ostwald ripening. In contrast, high-temperature annealing (above 450 K) in UHV results in a complete wetting of ZnO(0001) by Cu. The experiments suggest that the presence of Cu on the surface leads to charge transfer from shallow ionized donors (most probably substitutional hydrogen trapped on oxygen vacancies, H<sub>O</sub>) to Cu. Upon annealing, these subsurface defects drift towards the surface. DFT calculations confirmed that the drift of charged subsurface defects such as H<sub>O</sub> towards the surface is favorable in presence of Cu adatoms. Furthermore, the calculations revealed that the presence of H<sub>O</sub> in the subsurface region results in increased Cu adhesion. As the concentration of such defects in the subsurface region increases upon annealing, this effect may account for the experimentally observed wetting of ZnO(0001) by Cu at high temperatures.

### References

- [1] M. Behrens, F. Studt, I. Kasatkin, S. Kuhl, M. Havecker, F. Abild-Pedersen, S. Zander, F. Girgsdies, P. Kurr, B.L. Kniep, M. Tovar, R.W. Fischer, J.K. Nørskov, and R. Schlögl, *Science* **336**, 893 (2012).
- [2] P.C.K. Vesborg, I. Chorkendorff, I. Knudsen, O. Balmes, J. Nerlov, A.M. Molenbroek, B.S. Clausen, and S. Helveg, *Journal of Catalysis* **262**, 65 (2009).
- [3] S.V. Didziulis, K.D. Butcher, S.L. Cohen, and E.I. Solomon, *J. Am. Chem. Soc.* **111**, 7110 (1989).

## Interfacial structure for Au/TiO<sub>2</sub> revealed by genetic algorithm search

Bjørk Hammer, Aarhus University

Using a newly developed and implemented genetic algorithm for structure optimization[1], we investigate the structure and chemical composition of Au nano-particles supported on rutile TiO<sub>2</sub>(110) surfaces. Introducing oxygen to the Au nano-particles, the genetic algorithm search reveals that oxygen can be incorporated most favorably at the interface between the Au and the support[2]. Saturation of these interfacial sites with oxygen represents a requirement for the successful closing of a catalytic cycle on the particles – in other words, thermodynamically all the oxygen reacting at such nano-particles will be trapped at the interface (if the kinetics permits) until all these sites are populated. Oxygen atoms at the perimeter of the Au-TiO<sub>2</sub> interface may subsequently be active in CO oxidation reactions[3].

[1] A genetic algorithm for first principles global structure optimization of supported nano structures, L. B. Vilhelmsen and B. Hammer, *J. Chem. Phys* **141**, 044711 (2014).

[2] Interfacial oxygen under TiO<sub>2</sub>-supported Au clusters revealed by a genetic algorithm search, L. B. Vilhelmsen and B. Hammer, *J. Chem. Phys* **139**, 204701 (2013).

[3] Identification of the catalytic site at the interface perimeter of Au clusters on rutile TiO<sub>2</sub>(110), L. B. Vilhelmsen and B. Hammer, *ACS Catalysis* **4**, 1626 (2014).

## WGS reaction on ceria-supported Pt catalysts: The role of oxygen vacancies

J. Vecchietti<sup>1</sup>, A. Bonivardi<sup>1</sup>, W. Xu<sup>2</sup>, D. Stacchiola<sup>2</sup>, J. J. Delgado<sup>3</sup>, M. Calatayud<sup>4</sup>, S. Collins<sup>2</sup>

<sup>1</sup> Universidad Nacional del Litoral and CONICET, Santa Fe, Argentina.

<sup>2</sup> Department of Chemistry, Brookhaven National Laboratory, USA

<sup>3</sup> Universidad de Cadiz, Cadiz, Spain

<sup>4</sup> Université Pierre et Marie Curie and CNRS, IUF, Paris, France

calatayu@lct.jussieu.fr

The precise mechanism of the water gas shift WGS reaction is a matter of intense debate, but the dissociation of water is generally considered a key step in the reaction. In this work, we report a study of the relationship between the catalytic activity and the reducibility of the support (oxygen vacancies) to activate water on well characterized platinum catalysts supported on pure and gallium-doped ceria [1-4]. Pt/CeO<sub>2</sub> and Pt/CeGaO<sub>x</sub> catalysts investigated here presented a remarkable reducibility, enhanced by the incorporation of Ga<sup>3+</sup> cations [1,3] and a very stable metal dispersion. An inverse correlation was found between the catalytic activity to WGS and the amount of oxygen vacancies [4]. In situ time resolved X-ray diffraction, mass spectrometry and diffuse reflectance infrared spectroscopy (DRIFT) showed that the replenishment of oxygen vacancies by water is always fast either in Pt/CeO<sub>2</sub> or Pt/CeGaO<sub>x</sub>. DFT calculation provides molecular insights to understand the pathway of water reaction with vacancies at the of metal–oxide interface sites. Concentration-modulation spectroscopy (c-MES) in DRIFT mode under WGS reaction conditions allows the selective detection of key reaction intermediates. Altogether, the experimental and DFT results clearly suggest that although the oxygen vacancies can react with water, it is not the rate-determining step in the WGS reaction mechanism on these catalysts. The c-MES results suggest that monodentate formate (m-HCOO) and carboxylate (CO<sub>2</sub><sup>δ-</sup>) are reaction intermediates, which clearly indicate the prevalence of an associative mechanism activated at the oxide-metal interface of the catalyst.

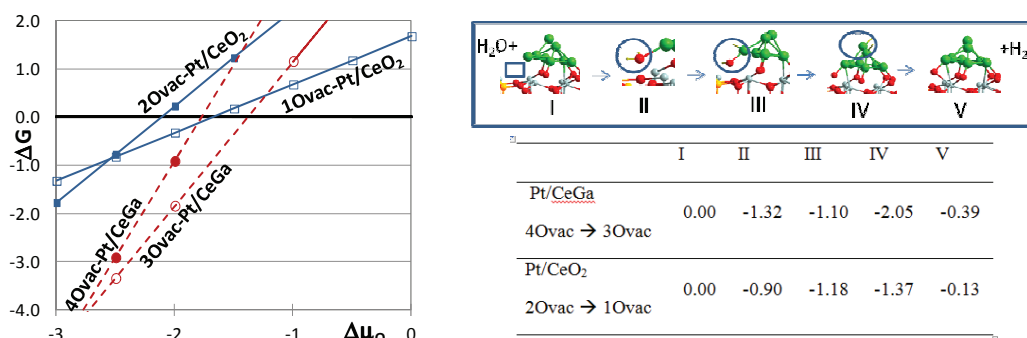


**Figure:** Left,  $\Delta G$  as a function of the chemical potential of oxygen  $\Delta\mu_{\text{O}}$ , in eV. Right: schematic mechanism for the water filling mechanism as calculated with DFT methods. The relative energy for each intermediate is reported in eV.

[1] G. Finos, S. Collins, G. Blanco, E. del Rio, J.M. Cies, S. Bernal, A. Bonivardi. Catal. Today **180**, 9, (2012).

[2] P. Quaino, F. Tielens, C. Minot, M. Calatayud et al., Chem. Phys. Lett. **519-520**, 69, (2012).

[3] J. Vecchietti, S. Collins, D. Stacchiola, M. Calatayud, J. J. Delgado, A. Bonivardi, et al. J. Phys. Chem. C **117**, 8822, (2013).

[4] J. Vecchietti, A. Bonivardi, W. Xu, D. Stacchiola, J. J. Delgado, M. Calatayud, S. Collins ACS Catalysis **4**, (2014) 2088

## Stoichiometry engineering of (ternary) oxide ultra-thin films: $\text{Ba}_x\text{Ti}_2\text{O}_3$ on Au(111)

C. Wu, M.R. Castell, J. Goniakowski<sup>1</sup>, C. Noguera<sup>1</sup>

Department of Materials, University of Oxford, UK

<sup>1</sup>INSP, CNRS, 4 Place Jussieu, 75252 Paris, Cedex05, France.

claudine.noguera@insp.jussieu.fr

Spontaneous two-dimensional ordering of adatoms on metal-supported thin oxide films is of potential applicative interest due to their singular magnetic, electronic and optical properties. It is also relevant to heterogeneous catalysis where design and control at the atomic level is the ultimate goal. Most of the attention to date has been directed at the interaction between the adatoms and the support, however the interactions between the adatoms is also a critical factor that can control the atomic ordering. While transition and noble metal adatoms were often in focus of catalysis-related studies, adsorption of simple metals may display novel and qualitative different features. Indeed, such atoms may be directly incorporated into the supported oxide film, forming ternary phases with crystalline structures and stoichiometries which would not exist in the bulk. These so-called “surface oxide” phases are expected to display new functionalities, as well as flexible electronic and structural properties as a function of preparation conditions, in particular the metal coverage

In this joint experimental and theoretical work [1], we focus on a model ternary oxide system  $\text{Ba}_x\text{Ti}_2\text{O}_3$  obtained by the deposition of Ba adatoms on an epitaxial  $(2 \times 2)$   $\text{Ti}_2\text{O}_3$  honeycomb ultra-thin films grown on Au(111) [2]. Starting from isolated atoms adsorbed in the hollow sites of the  $\text{Ti}_2\text{O}_3$  honeycomb lattice, two ordered phases were found in STM experiments at  $1/3$  and  $2/3$  Ba coverage, separated by a disordered phase displaying labyrinth patterns. Such coverage-dependent phase sequence has been further reproduced in Monte Carlo simulation on a 2D lattice gas model with parameters of the pairwise Ba-Ba interactions deduced from DFT calculations on a series of model  $\text{Ba}_x\text{Ti}_2\text{O}_3/\text{Au}(111)$  configurations. The particular ordering pattern of Ba adatoms has been directly linked to the repulsive character of first, second, and third neighbour Ba-Ba interactions ( $J_1$ ,  $J_2$ ,  $J_3$ ), induced by the spontaneous positive charging of Ba in contact with the  $\text{Ti}_2\text{O}_3/\text{Au}(111)$  support.

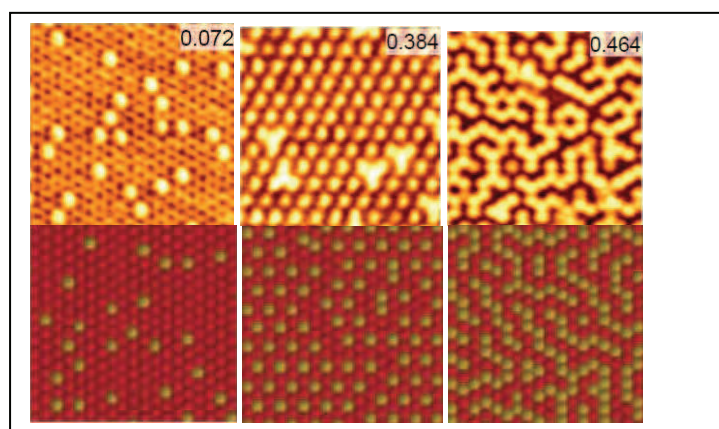


*Figure 1: Top panels: STM images at Ba coverages  $c=0.072$ ,  $0.384$  and  $0.464$ . Bottom panels: Corresponding Monte Carlo snapshots obtained for  $k_B T/J_1=0.1$ ;  $J_2/J_1=0.25$ ;  $J_3/J_2=0.666$ . Only hollow sites are imaged, which appear red when empty and yellow when occupied by a Ba atom.*

[1] C. Wu, M.R. Castell, J. Goniakowski, C. Noguera, in preparation

[2] C. Wu, M.S.J. Marshall, M. R. Castell, *J. Phys. Chem. C* **115**, 8643, (2011).

## Subsurface Cation Vacancy Stabilization of the Magnetite (001) Surface

R. Bliem,<sup>1</sup> E. McDermott,<sup>2</sup> P. Ferstl,<sup>3</sup> M. Setvin,<sup>1</sup> O. Gamba,<sup>1</sup> M. A. Schneider,<sup>3</sup> M. Schmid,<sup>1</sup> U. Diebold,<sup>1</sup> P. Blaha,<sup>2</sup> L. Hammer,<sup>3</sup> **G.S. Parkinson**<sup>1</sup>

<sup>1</sup> Institute of Applied Physics, Vienna University of Technology, 1040 Vienna, Austria

<sup>2</sup> Institute of Materials Chemistry, Vienna University of Technology, 1060 Vienna, Austria

<sup>3</sup> Chair of Solid State Physics, University of Erlangen-Nürnberg, Erlangen, Germany.

Parkinson@iap.tuwien.ac.at

The Fe<sub>3</sub>O<sub>4</sub>(001) surface exhibits a ( $\sqrt{2}\times\sqrt{2}$ )R45° reconstruction characterized by the observation of undulating rows of Fe atoms in scanning tunnelling microscopy images. The existing model for the surface is a “polar” bulk truncation stabilized by subtle lattice distortions that couple to subsurface charge ordering [1]. In this presentation it will be shown that the current model fails to explain the adsorption behaviour of molecules and metal adatoms. We have solved the structure using a combination of quantitative STM, DFT based theoretical calculations and a quantitative LEED intensity analysis ( $R_p \sim 0.13$ , 40 beams, total database 11000 eV). The true structure, based on an ordered array of subsurface Fe vacancies and interstitials, explains all existing experimental observations for this surface to date, including the extraordinary thermal stability of metal adatoms (700 K) [3-5]. This hitherto unobserved stabilization mechanism is in line with the iron oxides' tendency to redistribute cations in the lattice in response to oxidizing or reducing environments, and can also be seen as a surface only Fe<sub>11</sub>O<sub>16</sub> phase. Since many other metal oxides also achieve stoichiometric variation through reorganization of the cation sublattice, cation vacancy reconstructions may be commonplace.

- [1] R. Bliem...G.S. Parkinson, *submitted* (2014).
- [2] R. Pentcheva et al., *Physical Review Letters* **94**, 126101 (2005).
- [3] G. S. Parkinson *et al.*, *Nature Materials* **12**, 724 (2013).
- [4] R. Bliem ... G.S. Parkinson, *ACS Nano* **8**, 7531 (2014).
- [5] Z. Novotný...G.S.Parkinson, *Physical Review Letters* **108**, 216103 (2012).

## Growth and structural properties of terbium oxide on Cu(111)

Jan Höcker, William Cartas<sup>1</sup>, Andreas Schaefer<sup>2</sup>, Marcus Bäumer<sup>2</sup>, Jason Weaver<sup>1</sup>, Jens Falta, **Jan Ingo Flege**

Institute of Solid State Physics, University of Bremen, Bremen, Germany

<sup>1</sup>Department of Chemical Engineering, University of Florida, Gainesville, United States

<sup>2</sup>Institute of Applied and Physical Chemistry, University of Bremen, Bremen, Germany  
flege@ifp.uni-bremen.de

The binary rare-earth oxides (REOs) are widely known for their peculiar structural, electronic, and chemical properties [1]. While cerium oxide has attracted the most attention and its properties are increasingly well documented [2], surface science model studies of terbium oxide thin films and nanostructures are almost completely lacking [3]. Here, we present the first structural investigation of terbium oxide growth on a Cu(111) surface. Using low-energy electron microscopy (LEEM), we follow the growth of terbium oxide in real-time during reactive deposition of metallic Tb in an oxygen background. Using low-energy electron diffraction patterns acquired from sample regions down to 250 nm, three different oxide constituents are identified, whose relative surface coverages are shown to depend on the growth conditions. Specifically, room temperature deposition followed by thermal annealing induces the formation of dendritic structures with TbO<sub>x</sub>(111) separated by copper oxide (Figure 1(a)). Conversely, for reactive deposition at elevated temperature both the terbia(111) and terbia(112) oxide phases are observed. Clearly, the island shapes directly reflect the crystallographic symmetry of the oxide face (Figure 1(b)): The (112) majority phase gives rise to the nucleation and growth of rectangular oxide stripes while the (111) minority phase forms triangular islands. Furthermore, annealing studies show that the relative abundance of the different terbia faces can be controlled by post-annealing the as-deposited film.

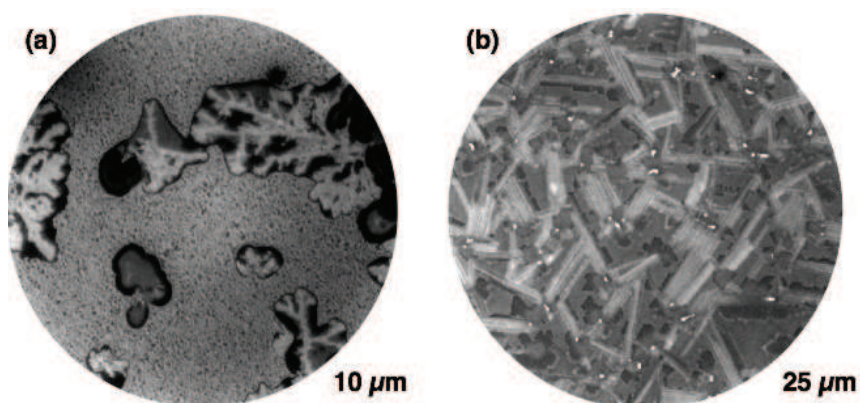


**Figure 1:** LEEM bright-field images of terbium oxide epitaxial growth on Cu(111) by (a) room temperature deposition and annealing and (b) reactive epitaxy at elevated temperature.

[1] G.-Y. Adachi and N. Imanaka, *Chem. Rev.* **98**, 1479 (1998).

[2] A. Trovarelli and P. Fornasiero, *Catalysis by Ceria and Related Materials*, 2<sup>nd</sup> ed. (2013).

[3] W. Cartas *et al.*, *J. Phys. Chem. C* **118**, 20916 (2014).

## Atomic scale insight into the CeO<sub>2</sub>/Pt interface

P. Luches<sup>1</sup>, L. Giordano<sup>2</sup>, S. Prada<sup>2</sup>, V. Grillo<sup>1,3</sup>, M. Campanini<sup>3</sup>, C. Magen<sup>4</sup>, F. Pagliuca<sup>1,5</sup>, G. C. Gazzadi<sup>1</sup>, G. Pacchioni<sup>2</sup>, S. Valeri<sup>1,5</sup>

<sup>1</sup> CNR – Istituto Nanoscienze, Modena, Italy

<sup>2</sup> Dipartimento di Scienza dei Materiali, Università di Milano-Bicocca, Milano, Italy

<sup>3</sup> CNR – Istituto Materiali per Elettronica e Magnetismo, Parma, Italy

<sup>4</sup> LMA-INA, ARAID and Dept. Fisica de Materia Condensada, University of Zaragoza, Spain

<sup>5</sup> Dipartimento FIM, Università di Modena e Reggio Emilia, Modena, Italy

e-mail: paola.luches@unimore.it

Catalysts made of cerium oxide combined with metals have been shown to be surprisingly active in a number of different reactions. A relevant role for the activity of the catalysts has been ascribed to atomic sites at the interface between cerium oxide and the metal, and systems in which the extent of the interface is maximized have been shown to have unprecedented activity [1]. Studies of model systems, such as cerium oxide epitaxial single crystalline films on metal surfaces, can be of help in simplifying part of the complexity of real catalysts and may help to identify important intrinsic properties of the combined material.

With this work we provide an atomic scale insight into the CeO<sub>2</sub>/Pt interface by the use of transmission electron microscopy combined with DFT +U calculations.

A cross sectional lamella has been prepared by focused ion beam out of a CeO<sub>2</sub> epitaxial thin film on a Pt(111) single crystal, grown by reactive deposition with the procedures exposed in [2]. TEM measurements have revealed that the coincidence cell between cerium oxide and Pt lattices at the interface varies locally from 4:5 to 3:4. Moreover the presence of dislocations both at the interface and within the cerium oxide film along with twinning of the CeO<sub>2</sub> has been evidenced. Aberration corrected STEM images with different detection geometries have been compared with theoretical models in order to determine in detail the relative arrangement of atoms at the CeO<sub>2</sub>/Pt interface. The occurrence of a charge transfer and the formation of different oxide phases at the interface between the two materials have also been investigated.

[1] M. Cargnello, J. J. Delgado Jaén, J. C. Hernández Garrido, K. Bakhmutsky, T. Montini, J. J. Calvino Gámez, R. J. Gorte, P. Fornasiero, *Science* **337**, 713 (2012).

[2] P. Luches, F. Pagliuca, S. Valeri, *J. Phys. Chem. C* **115**, 10718 (2011).

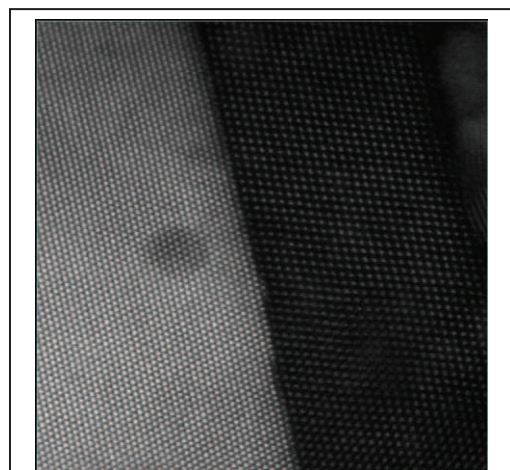


**Fig.1:** TEM image of the interface between a CeO<sub>2</sub> film and Pt(111).

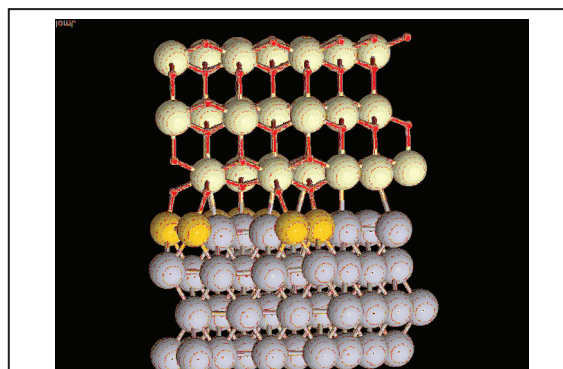


**Fig.2:** Model of the adsorption geometry of a CeO<sub>2</sub> film on Pt(111) with O interface atoms on top of Pt atoms, predicted to be the most stable by DFT calculations. The yellow atoms are the Pt atoms with the shortest Pt-O bonds.

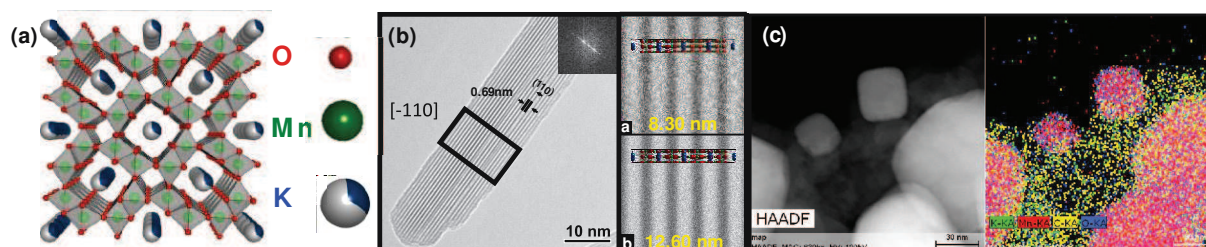
## Cryptomelane nanorods: TEM/STEM/EELS

Paulina Indyka<sup>1</sup>, Joanna Gryboś<sup>1</sup>, Piotr Legutko<sup>1</sup>, Paweł Stelmachowski<sup>1</sup>, Andrzej Kotarba<sup>1</sup>, Zbigniew Sojka<sup>1</sup>

Faculty of Chemistry, Jagiellonian University, Ingardena 3, 30-060 Krakow, Poland  
paulina.indyka@uj.edu.pl,

Tunnel-based frameworks based on manganese oxides are used as catalytic materials in various oxidation processes. Among critical factors determining the performance of such materials, the interlayer structure that could facilitate ion insertion and extraction is vital for their catalytic activity. In the particular case of the cryptomelane - a tunneled potassium manganese oxide  $\text{KMn}_8\text{O}_{16}$  (Fig.1a) - the one-dimensional architecture of nanorods may contribute to facilitate potassium ion diffusion and spreading on the activated reactant, which is beneficial for soot combustion. A cryptomelane potassium manganese oxide  $\text{KMn}_8\text{O}_{16}$  was synthesized through a hydrothermal process. TEM studies revealed nanorod morphology of the as-synthesized cryptomelane of the crystallite size in the range 20-500 nm. Selected area electron diffraction (SAED) pattern taken from a large group of the nanorods consists of sharp rings that can be indexed in accordance with the  $\text{KMn}_8\text{O}_{16}$  tetragonal structure. The high resolution TEM image shown in Fig.1b, reveals lattice fringes with the interplanar spacing of 0.69 nm, which correspond well to the (110) plane of the cryptomelane manganese oxide. An in-depth analysis and image simulations (Fig.1b) showed also that bright contrast in the HR TEM images comes from the K and O ions, whereas darker contrast is associated with the planes containing the Mn and O ions. The EDS, EELS and EFTEM techniques were employed to determine elemental distribution of all elements within the cryptomelane nanorods. The EELS spectroscopic data were acquired using spectrum imaging technique. Comparison of the EELS spectra obtained at different areas in the bulk and at the surface of the cryptomelane nanorods, revealed significant variations of the chemical composition, uneven repartition of potassium and variations of manganese valence state. The results obtained using several S/TEM techniques provided a nanoscale picture of the structural and spectroscopic changes of cryptomelane with respect to its catalytic performance. These studies, complemented by species resolved thermal desorption and work function measurements, allow for detailed understanding of potassium ion interlayer and surface diffusion in the cryptomelane tunnel structure in relation to its redox properties.

**Fig1. Structure and catalytic properties of cryptomelane determined within the scope of soot combustion process analysis. (a) cryptomelane tunnel structure model, (b) HRTEM image with clearly visible lattice fringes coupled with simulated image, (c) STEM (HAADF) image together with EDX chemical composition map.**



### Acknowledgements

The project was financed by the Polish National Science Center awarded by decision number DEC-2011/01/B/ST4/00574

# Origin, Stability, and Effect of Atomically Dispersed Pt on Nanostructured Catalytic Pt-CeO<sub>2</sub> Materials with Maximum Noble-Metal Efficiency

Albert Bruix,<sup>1,2</sup> Alberto Figueroba,<sup>2</sup> Yaroslava Lykhach,<sup>3</sup> Iva Matolínová,<sup>4</sup> Armin Neitzel,<sup>3</sup> Tomáš Skála,<sup>4</sup> Nataliya Tsud,<sup>4</sup> Mykhailo Vorokhta,<sup>4</sup> Vitalii Stetsovych,<sup>4</sup> Klára Ševčíková,<sup>4</sup> Josef Mysliveček,<sup>4</sup> Kevin C. Prince,<sup>5</sup> Francesc Illas,<sup>2</sup> Vladimír Matolín,<sup>3</sup> Jörg Libuda,<sup>3</sup> Konstantin M. Neyman<sup>2,6</sup>

<sup>1</sup>Interdisciplinary Nanoscience Center (iNANO), Aarhus University, Denmark

<sup>2</sup>Departament de Química Física and IQTC, Universitat de Barcelona, Barcelona, Spain

<sup>3</sup>LFPC II, Friedrich-Alexander-Universität Erlangen-Nürnberg, Germany

<sup>4</sup>Dept. of Surface and Plasma Science, Charles University, Prague, Czech Republic

<sup>5</sup>Elettra-Sincrotrone Trieste SCpA and IOM, Basovizza-Trieste, Italy

<sup>6</sup>Institució Catalana de Recerca i Estudis Avançats (ICREA), Barcelona, Spain

abruix@phys.au.dk

The high price of Pt often hinders large-scale applications of catalysts containing this precious metal. However, the noble-metal efficiency, i.e. the activity per Pt atom used, can be improved by dispersing Pt in the form of atoms at the outermost surface layer of a material. Nevertheless, atomically dispersed Pt is likely to diffuse and agglomerate in catalytic operating conditions, leading to the undesired loss of per atom efficiency.

By means of DFT calculations, we have identified binding sites for Pt on {100} facets of nanostructured CeO<sub>2</sub> leading to disperse Pt<sup>2+</sup> species that are stable enough to resist bulk diffusion and sintering processes. The predicted behaviour of these systems is in good agreement with XPS measurements on model Pt-CeO<sub>2</sub> catalysts, where the presence of the different Pt species (cationic and metallic) as well as the extraordinary stability of Pt<sup>2+</sup> is also detected. Furthermore, such Pt<sup>2+</sup> species and their anchoring sites are also found in real Pt-CeO<sub>2</sub> nanocomposites featuring high Pt efficiency in fuel cell catalysis.[1] Very recently, we have also studied the interplay between different Pt species and reductive environments and the effect of Pt<sup>2+</sup> in the hydrogenation process. Namely, we have investigated the hydrogenation and vacancy formation processes leading to the either Pt<sup>4+</sup>, Pt<sup>2+</sup>, or metallic Pt, and also considered different possible mechanisms which may give rise to the high efficiency of Pt<sup>2+</sup>-CeO<sub>2</sub> in fuel cell catalysis.



[1] Bruix, A., Lykhach, Y., Matolínová, I., Neitzel, A., Skála, T., Tsud, N., Vorokhta, M., Stetsovych, V., Ševčíková, K., Mysliveček, J., Fiala, R., Václavů, M., Prince, K. C., Bruyère, S., Potin, V., Illas, F., Matolín, V., Libuda, J. and Neyman, K. M., *Angew. Chem. Int. Ed.*, (2014) DOI: 10.1002/anie.201402342.

## Model Studies on Novel Ceria-Based Fuel Cell Catalysts

**Yaroslava Lykhach**,<sup>1</sup> Albert Bruix,<sup>2</sup> Armin Neitzel,<sup>1</sup> Olaf Brummel,<sup>1</sup> Nataliya Tsud,<sup>3</sup> Tomáš Skála,<sup>3</sup> Vitalii Stetsovych,<sup>3</sup> Klára Ševčíková,<sup>3</sup> Mykhailo Vorokhta,<sup>3</sup> Daniel Mazur,<sup>3</sup> Kevin C. Prince,<sup>4</sup> Josef Mysliveček,<sup>3</sup> Francesc Illas,<sup>2</sup> Konstantin M. Neyman,<sup>2,5</sup> Vladimír Matolín,<sup>3</sup> Jörg Libuda<sup>1,6</sup>

<sup>1</sup>Lehrstuhl für Physikalische Chemie II, FAU Erlangen-Nürnberg, Erlangen, Germany

<sup>2</sup>Departament de Química Física and IQTC, Universitat de Barcelona, Barcelona, Spain

<sup>3</sup>Department of Surface and Plasma Science, Charles University, Prague, Czech Republic

<sup>4</sup>Elettra-Sincrotrone Trieste SCpA and IOM, Basovizza-Trieste, Italy

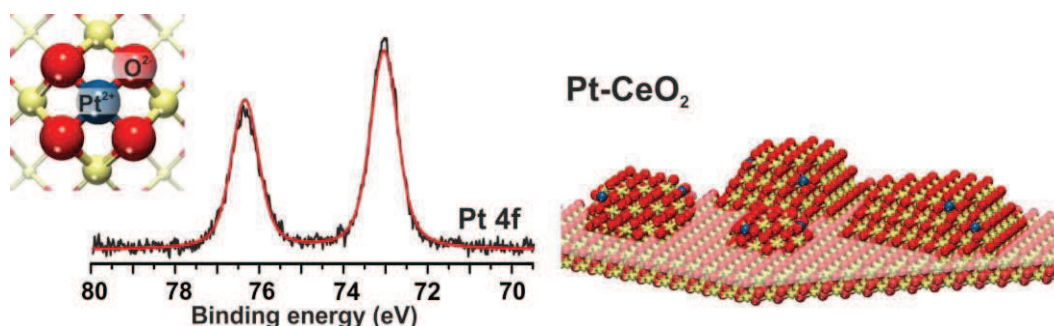
<sup>5</sup>Institució Catalana de Recerca i Estudis Avançats (ICREA), Barcelona, Spain

<sup>6</sup>Erlangen Catalysis Resource Center, FAU Erlangen-Nürnberg, Erlangen, Germany

yaroslava.lykhach@fau.de

The high costs of noble metals for catalytic materials are the main factor limiting large-scale application of fuel cell technology. Principle strategies to resolve this challenge involve either the replacement of the noble metal or a more efficient use of the precious material. The latter is achieved by maintaining a very high dispersion during operation. Recently, a significant progress along this line was made by using nanostructured cerium oxide as a support for atomically dispersed Pt [1]. We found that Pt<sup>2+</sup> can be anchored at (100) nanofacets, which are abundant at the surface of nanostructured cerium oxide. The outstandingly high adsorption energy of Pt<sup>2+</sup> ions at these surface sites result from a specific coordination, with Pt in the center of a perfect square formed by four surface oxygen ions, i.e. a square oxygen pocket. The thermal stability of the nanostructured Pt-CeO<sub>2</sub> depends strongly on the Pt concentration. Using CO molecules as a probe we identified the changes in the composition and morphology of Pt-CeO<sub>2</sub> mixed oxide films caused by annealing in ultrahigh vacuum [2]. We find excellent stability of Pt<sup>2+</sup> in the CeO<sub>2</sub> film at low Pt content. At higher Pt concentration, a large fraction of the Pt<sup>2+</sup> is converted into metallic Pt particles above 300 K.

We have investigated the reactivity of Pt-CeO<sub>2</sub> mixed oxides towards H<sub>2</sub> and CH<sub>3</sub>OH as a function of Pt loading and Pt oxidation state under both ultrahigh vacuum and electrochemical conditions. Several samples were prepared that contained exclusively Ce<sup>4+</sup>, Pt<sup>2+</sup>/Ce<sup>4+</sup>, and Pt<sup>2+</sup>/Ce<sup>4+</sup> in combination with Pt<sup>0</sup> in the form of small particles. The role of Pt<sup>0</sup> in the activation of molecular hydrogen will be discussed in detail.



[1] A. Bruix, Y. Lykhach, I. Matolínová, A. Neitzel, T. Skála, N. Tsud, M. Vorokhta, V. Stetsovych, K. Ševčíková, J. Mysliveček, R. Fiala, M. Václavů, K.C. Prince, S. Bruyere, V. Potin, F. Illas, V. Matolín, J. Libuda, K.M. Neyman, *Angew. Chem. Int. Ed.* 53 (2014) 10525.

[2] A. Neitzel, Y. Lykhach, T. Skála, N. Tsud, M. Vorokhta, D. Mazur, K.C. Prince, V. Matolín, J. Libuda, *Phys. Chem. Chem. Phys.*, submitted (2014).

## High efficiency Pt<sup>2+</sup>-CeO<sub>x</sub> novel thin film catalyst as anode for PEMFC

R. Fiala<sup>1</sup>, M. Vaclavu<sup>1</sup>, I. Khalakhan<sup>1</sup>, M. Vorokhta<sup>1</sup>, J. Lavkova<sup>1</sup>, I. Matolinova<sup>1</sup>, F. Faisal<sup>2</sup>, O. Brummel<sup>2</sup>, J. Libuda<sup>2</sup>, **V. Matolin<sup>1</sup>**

<sup>1</sup>Department of Surface and Plasma Science, Charles University, Prague, Czech Republic

<sup>2</sup>Lehrstuhl für Physikalische Chemie II, FAU Erlangen-Nürnberg, Erlangen, Germany

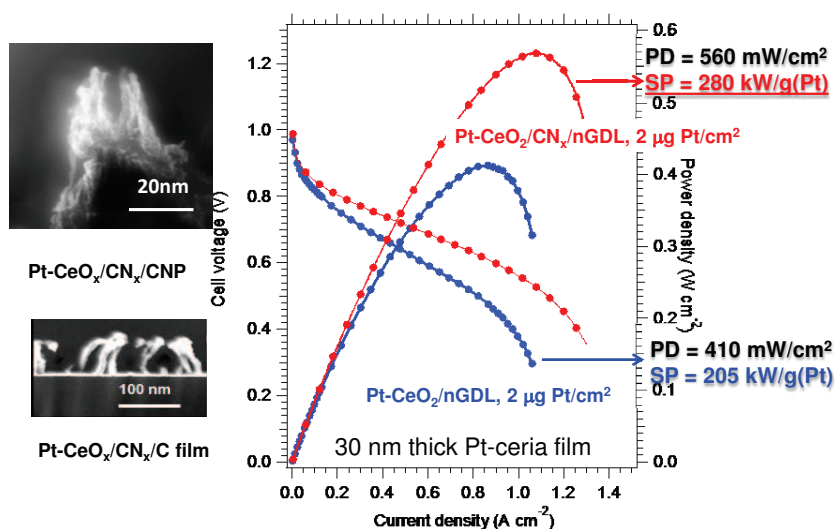
Platinum is the mostly used element in catalysts for fuel cell technology, but its high price limits large-scale applications. Platinum doped cerium oxide represents an alternative solution due to very low loading, typically few micrograms per 1 cm<sup>2</sup>, at the proton exchange membrane fuel cell (PEMFC) anode. High efficiency is achieved by using plasma enhanced magnetron sputtering deposition of cerium oxide and Pt of 10 nm thick nanoporous films on large surface carbon nanoparticle substrates coated by CN<sub>x</sub> thin films.

Thin film techniques permits to grow the catalyst film characterised by highly dispersed platinum, mostly in ionic Pt<sup>2+</sup> state. Such dispersed Pt species show high activity and stability. These new materials may help to substantially reduce the demand for expensive noble-metals in catalytic applications.

We measured Pt-CeO<sub>x</sub> thin film anode catalyst activity in a hydrogen PEMFC and compared it with performance of a standard reference cell. Photoelectron spectroscopy was used to investigate chemical composition of Pt-CeO<sub>x</sub> induced by the catalyst interaction with hydrogen.

Nanostructured character of the catalyst was confirmed by electron microscopy.

### PEMFC test of Pt<sup>2+</sup>-CeO<sub>x</sub>/nanoGDL /CN<sub>x</sub> anode



# DFT calculations on formation and migration of oxygen vacancies in $\text{La}_{0.5}\text{Sr}_{0.5}\text{Co}_{0.75}\text{Fe}_{0.125}\text{M}_{0.125}\text{O}_{3-\delta}$ (M=Pd, Ni) perovskites

Yu. A. Mastrikov<sup>1</sup>, S. Guo<sup>2,3</sup>, F. Puleo<sup>2</sup>, L.F. Liotta<sup>2</sup> and E. A. Kotomin<sup>1</sup>

<sup>1</sup> Department of Theoretical Physics and Computer Modelling of Materials, Institute of Solid State Physics, University of Latvia, Kengaraga 8, LV-1063, Riga, Latvia

<sup>2</sup> Istituto per lo Studio di Materiali Nanostrutturati (ISMN)-CNR, Via Ugo La Malfa 153, 90146 Palermo, Italy

<sup>3</sup> Northwestern Polytechnical University, Xi'an 710072 PR China.

**e-mail:** [yuri.mastrikov@cfi.lu.lv](mailto:yuri.mastrikov@cfi.lu.lv); [guoshaoli@mail.nwpu.edu.cn](mailto:guoshaoli@mail.nwpu.edu.cn);

$\text{ABO}_3$  perovskites are widely used as cathodes in intermediate temperature solid oxide fuel cells (IT-SOFCs).  $\text{ABO}_3$  compositions containing more than two types of metal ions at the *B*-site are more active for oxygen reduction reaction (ORR) than those with only one type of metal ion [1]. Therefore, plenty of researches have been focused on cathode property improvement of *B*-site substitution in  $\text{La}_{1-x}\text{Sr}_x\text{Co}_{1-y}\text{Fe}_y\text{O}_{3-\delta}$  (LSCF), that are currently employed in IT-SOFCs [2]. It is well accepted that experimental studies are unavoidable limited in getting specific mechanism of multi-steps ORR. Theoretical tools such as first principles DFT calculations are often used as complementary approach [3].

In our preliminary investigations, Pd and Ni substituted LSCF prepared by sol-gel citric method have shown enhanced cathode performances than pure LSCF, as it was confirmed by XPS, TGA, TPR, EXAFS and AC impedance spectroscopy. In order to well understand the effect of metal substitution on fundamental cathode property, DFT calculations have been carried out. Specific attention was paid to the effect of metal substitution on the oxygen vacancies formation energy and charge redistribution. Computational experiments were performed on LSCF, LSCF-Pd and LSCF-Ni by the DFT-based computer code VASP5.3 [4]. For calculations we used distorted perovskite 2x2x2 supercell and full geometry optimization was performed for each compound. Obtained energies clearly show that vacancies can be easier created in the vicinity of Pd and Ni. Doping by Pd reduces the Co- $V_o$ -Co formation energy in the whole supercell by  $\sim 1.2\text{eV}$ . Ni, in its turn, reduces the Co- $V_o$ -Co formation energy two times stronger ( $0.25\text{eV}$ ), and unlike Pd also reduces the Co- $V_o$ -Fe formation energy by  $0.13\text{ eV}$ . The charge redistribution in the Co- $V_o$ -Pd is well localized, whereas for Co- $V_o$ - Ni delocalized.

The preliminary calculations clearly evidence a decrement of oxygen vacancy formation energy for Pd and Ni doped compounds, confirming experimental results. Strong delocalization of electron charge redistribution observed for Co- $V_o$ -Ni needs to be carefully investigated. Applied method could be used for the future calculations on the compounds with smaller concentration of dopants.

## Acknowledgements

Authors thank

COST Action CM 1104, STSM (COST-STSM-ECOST-STSM-CM1104-010414-042095),

ESF project Nr. 2013/0015/1DP/1.1.1.2.0/13/APIA/VIAA/010,

CHINA SCHOLARSHIP COUNCIL for supporting S. Guo's scholarship.

## References

- [1] L. Tai et al, Solid State Ionics, **76**, 259 (1995)
- [2] S. Wang et al, Journal of Power Sources, **201**, 18 (2012)
- [3] Y. Mastrikov et al, Phys. Chem. Chem. Phys., **15**, 911 (2013)
- [4] G. Kresse and J. Furthmüller. Phys. Rev. B, **54**,11169, (1996)

## C-H bond activation by transition metal oxides. Atomistic understanding of CeO<sub>2</sub> as non-innocent support

Thomas Kropp, Joachim Paier, **Joachim Sauer**

Department of Chemistry, Humboldt University, Berlin, Germany

js@chemie.hu-berlin.de

The mechanism of the methanol oxidation is studied by density functional theory for the VO<sub>x</sub>/CeO<sub>2</sub>(111) system, and found to be different from that for VO<sub>x</sub>/SiO<sub>2</sub>. In agreement with experiment the VO<sub>x</sub>/CeO<sub>2</sub> system is found to be more active. There exist several pathways which involve different active sites on vanadia, on ceria and on the vanadia-ceria interphase bonds.

The results are used to simulate temperature programmed desorption peaks which agree with previous experiments on thin film VO<sub>x</sub>/CeO<sub>2</sub> catalysts [1].

[1] M.V. Ganduglia-Pirovano, C. Popa, J. Sauer, H.L. Abbott, A. Uhl, M. Baron, D. Stacchiola, O. Bondarchuk, S. Shaikhutdinov, H.-J. Freund, *J. Am. Chem. Soc.* **132**, 2345 (2010).

## The interaction of hydrogen with amorphous silica network

Al-Moatasem El-Sayed, Valery Afanas'ev<sup>1</sup>, and **Alexander Shluger**

Department of Physics and Astronomy, University College London, UK

<sup>1</sup>Department of Physics and Astronomy, Katholieke Universiteit Leuven, Belgium  
a.shluger@ucl.ac.uk

Hydrogen is ubiquitous in amorphous silica (a-SiO<sub>2</sub>), silica-based natural minerals, and synthesized materials used in a broad variety of devices and applications. It is known to strongly interact with network defects, such as oxygen vacancies and dangling Si and O bonds. At the same time it is assumed that both atomic and molecular hydrogen interacts only very weakly with defect-free a-SiO<sub>2</sub> network. Indeed, experiments demonstrate that atomic hydrogen becomes mobile at temperatures as low as 30 K and the barrier for H diffusion in silica glass samples is about 0.1 eV, whereas H<sub>2</sub> diffuses in synthetic vitreous silica in a virtually reversible manner and remains in molecular form at temperatures below 470 K. In other words, in the current paradigm the defect-free SiO<sub>2</sub> network is assumed to be an inert transport medium for hydrogen.

In this presentation we use the results of *ab initio* modelling to demonstrate that, contrary to common perceptions, atomic hydrogen can break Si–O bonds in a defect-free a-SiO<sub>2</sub> network, generating a three-coordinated Si defect centre facing a silanol Si–O–H group, which shall be referred to as a hydroxyl E' centre. The ReaxFF force-field was used to generate 116 periodic models of amorphous silica each containing 216 atoms. Density functional theory (DFT), implemented in the CP2K code was used to further optimize the geometries of amorphous structures and calculate the hydrogen defects in these models. The non-local functional PBE0/TC/LRC was used in all calculations. The hydrogen reactions are possible due to the disorder of amorphous structure and the hydroxyl E' centre is preferentially generated at bridging O sites associated with statistically long Si–O bonds. The calculated barriers to form this defect from an H atom in an interstitial position range between 0.5 and 1.3 eV. The hydroxyl E' centre can be passivated by further anneal in atomic or molecular hydrogen but there exists the possibility that it will be reactivated again in the excess of atomic hydrogen.

The hydroxyl E' centre is similar to the MgO<sub>step</sub>(H<sup>+</sup>)(e<sup>-</sup>)<sub>trapped</sub> centre at the MgO surface introduced in ref. [1] as an alternative to surface oxygen vacancies. Furthermore, as the extreme bondings in the oxide are expected to become more abundant under influence of strain, this discovery of unexpected reactivity of atomic hydrogen may have significant implications for our understanding of processes in nano-scaled silica as well as shed a new light on the behaviour of atomic hydrogen in other amorphous solids.

[1] D. Ricci, C. Di Valentin, G. Pacchioni, P. V. Sushko, A. L. Shluger, and E. Giamello, J. Am. Chem Soc. **125**, 738 (2003)

## Photonic light trapping in self-organized all-oxide microspheroids impacts photoelectrochemical water splitting

Florent Boudoire<sup>1,3</sup>, Rita Toth<sup>1</sup>, Jakob Heier<sup>2</sup>, Edwin Constable<sup>3</sup>, Artur Braun<sup>1</sup>

<sup>1</sup> Laboratory for High Performance Ceramics, EMPA, Duebendorf, Switzerland.

<sup>2</sup> Laboratory for Functional Polymers, EMPA, Duebendorf, Switzerland.

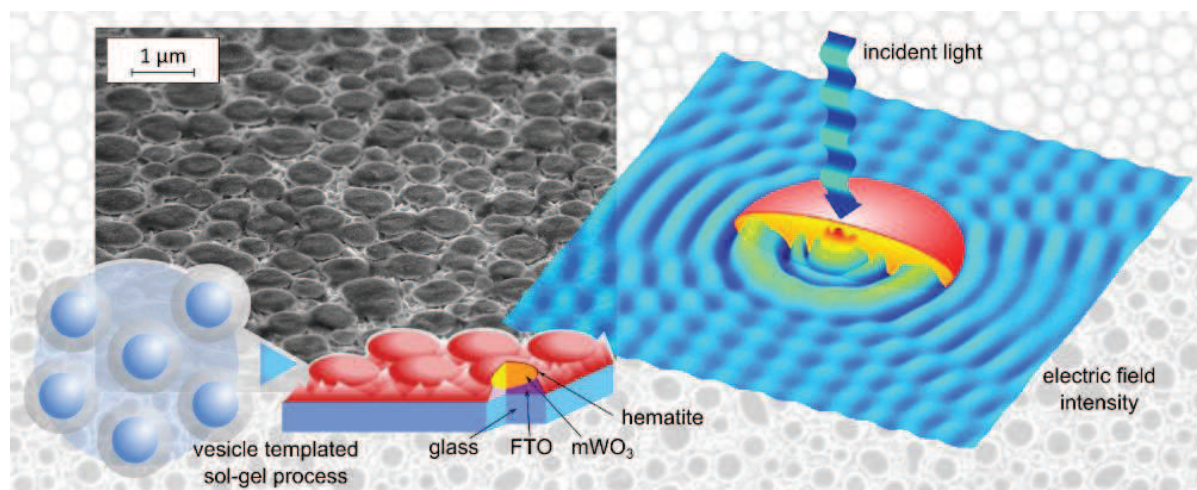
<sup>3</sup> Department of Chemistry, University of Basel, Basel, Switzerland.

florent.boudoire@empa.ch

Thin films involving an oxide heterojunction is a proven strategy for the catalysis of water splitting reactions using solar light. Hematite ( $\alpha\text{-Fe}_2\text{O}_3$ ) and tungsten oxide have suitable properties to achieve such heterojunctions. A major limitation of this strategy is the short charge carrier diffusion length in hematite. Ultra-thin films were implemented to address this low conductivity issue. Nevertheless, such ultrathin films do not absorb light efficiently. The present study explores light trapping strategies to increase the optical path length of photons in hematite.

Micelle suspensions were developed to obtain thin films composed of microspheroids array with a tungsten oxide core and a hematite nanometric overlay. This bottom-up approach allows a fine control of the spheroids dimensions at the micrometric to submicrometric scale. By tuning the spheroids dimensions, different photonic regimes were observed experimentally.

Using the Finite Difference Time Domain method, light propagation inside the microstructures was quantitatively simulated. The simulation results were coupled to an analysis of the photoelectrochemical response of the films. Experiments and simulation showed good agreement and bring important insights in the relationship between the light interaction with the microstructure and the photoanode performances [1].



- [1] F. Boudoire, R. Toth, J. Heier, A. Braun, E. C. Constable, *Energy Environ. Sci.*, **7**, 2680-2688

## Electrochemical properties of sol-gel TiO<sub>2</sub> blocking layers

Marketa Zukalova<sup>1</sup>, Ladislav Kavan<sup>1</sup>, Milan Bousa<sup>1</sup>, Zdenek Bastl<sup>1</sup> and David Havlicek<sup>2</sup>

<sup>1</sup>J. Heyrovský Institute of Physical Chemistry, AS CR, Dolejškova 3, CZ-182 23 Prague 8

<sup>2</sup>Dept. of Inorg Chem, Faculty of Science, Charles University, Albertov 2030, Prague 2, CR  
marketa.zukalova@jh-inst.cas.cz

Compact TiO<sub>2</sub> thin films are used as blocking layers in solid state dye sensitized solar cells (DSCs), and in the methylammonium-lead-iodide (perovskite) based solar cells. Here, the TiO<sub>2</sub> film serves as an electron collector and simultaneously as a buffer layer, preventing recombination of photoexcited electrons from the substrate, typically F-doped SnO<sub>2</sub> conducting glass (FTO) with the hole conductor[1]. The compact TiO<sub>2</sub> film is grown on top of FTO, usually by spray pyrolysis, DC-magnetron sputtering, electrochemical deposition, atomic layer deposition and spin coating. Recently, we developed facile sol-gel dip coating technique producing dense and extremely mechanically stable TiO<sub>2</sub> thin films on various substrates from precursor solutions containing poly(hexafluorobutylmethacrylate) or hexafluorobutyl methacrylate as the structure-directing agents[2]. The films are quasi-amorphous, but crystallize to TiO<sub>2</sub> (anatase) upon heat treatment at 500°C. Blocking properties of the films were tested by cyclic voltammetry using Fe(CN)<sub>6</sub><sup>3-/4-</sup> in aqueous electrolyte solution as the model redox probe[3]. The same test was repeated by spiro-OMeTAD in dichloromethane electrolyte solution. The as-grown films can exhibit an excellent rectifying interface with almost no pinholes, however, defects are created upon heat treatment at 500°C in air, when anatase crystallization occurs. The overall area of thermally induced pinholes is comparable to that in spray-pyrolyzed titania films. The flat-band potentials,  $\phi_{FB}$  of the as-grown films are upshifted by about 0.2–0.4 V against the values predicted for a perfect anatase single-crystal surface, but they still follow the Nernstian pH dependence. Proton insertion into titania takes place during electrochemical n-doping in aqueous acidic electrolyte solution at sufficiently negative potential[4]. The good-quality films are ideally compact, mimicking the properties of a macroscopic single crystal electrode. In contrast to porous polycrystalline electrodes, the doping of our dense films is permanent, i.e. it persists for at least weeks, if the electrode is stored in air at room temperature. Doping manifests itself by permanent color changes and characteristic morphological differences on the surface. The doped films still accommodate Li<sup>+</sup> by electrochemical insertion, but competition between Li<sup>+</sup> and H<sup>+</sup> ions in the lattice is detected by cyclic voltammograms.

Acknowledgement: This research was supported by the COST Action CM1104.

[1] Lee, M. M.; Teuscher, J.; Miyasaka, T.; Murakami, T. N.; Snaith, H. J. *Science*, 338, (2012), 643-647.

[2] Prochazka, J.; Kavan, L.; Zukalova, M.; Janda, P.; Jirkovsky, J.; Zivcova, Z. V.; Poruba, A.; Bedu, M.; Dobbelin, M.; Tena-Zaera, R. *Journal of Materials Research*, 28, (2013), 385-393.

[3] Kavan, L.; Zukalova, M.; Vik, O.; Havlicek, D. *ChemPhysChem*, 15, (2014), 1056-61.

[4] Zukalova, M. B., M.; Jirka, I.; Bastl, Z.; Kavan, L. *The Journal of Physical Chemistry*, (2014), submitted

## Si P<sub>b0</sub> defects at interfaces of Si-passivated SiGe channels with HfO<sub>2</sub>

O.Madia, J.Kepa, F.Cerbu, V.V. Afans'ev, M.Houssa, A.Stesmans  
KULeuven, University of Leuven, Celestijnenlaan200D, B-3001 Leuven, Belgium

Negative bias temperature instability (NBTI) has become a major reliability issue for aggressively-scaled (sub-1nm equivalent oxide thickness, EOT) metal-oxide-semiconductor transistors (MOSFETs), since it causes a shift in the threshold voltage and a degradation of the carrier's mobility. It is commonly accepted that NBTI originates from the metastable bulk oxide defects (the *recoverable* component) and the interfacial traps (the *permanent* component), both related to the intrinsic defects introduced upon thermal processing of the semiconductor/oxide entities. Recently [1], high-k metal-gate p-FETs with Si-capped SiGe channel have been shown to exhibit superior reliability as compared to the pure Si-channel devices. This finding may pave the way to solve the NBTI problem in deep-scaled p-FETs. However, the understanding of the physical mechanism behind this defect density reduction is still missing.

In this work we show that chemical reduction of the interfacial oxide, unavoidably formed between the semiconductor channel and the high-k insulator (HfO<sub>2</sub>) plays a critical role causing severe interface degradation in terms of generation of interfacial dangling bonds (DBs) defects. Nevertheless, by performing ESR analysis on Si-channel reference samples with HfO<sub>2</sub> as oxide insulator, we give evidences that the use of He gas during the high-temperature scavenging process allows one to reduce the aforementioned damage and retain the initially low defect density.

Next, by analyzing the Si-passivated SiGe-channel structures with different Ge concentrations, we found that the presence of Si DB defects –revealed also by previous studies– at the interface between the Si passivation layer and the oxide decreases as more Ge is introduced into the channel region. This observation supports the hypothesis concerning the reduction of the permanent component of NBTI due to enhanced segregation of Ge atoms at the Si/SiO<sub>x</sub> interface [1]. Furthermore, by changing the layers thicknesses in structures with comparable amount of Ge in the SiGe layer, the effect of strain on the density of Si dangling bond defects becomes visible. In particular, samples with a thick (3 nm) Si cap exhibit a low interfacial defect density regardless of the thickness of the SiGe layer underneath. Conversely, the samples with a thin (1 nm) Si cap show a higher defect density when the SiGe layer becomes thicker. Assuming a comparable amount of Ge atoms diffusing towards the top layers, we suggest that a thicker SiGe layer under a thinner Si cap would accommodate the increasing lattice mismatch by generating dislocations.

These results suggest the impact of two factors on the defect formation upon annealing of SiGe/Si/HfO<sub>2</sub> stacks: First, as hypothesized earlier [1], at high anneal temperature (1050 °C) Ge atoms are likely to diffuse from the SiGe layer through the Si cap towards the interface with the oxide. This reduces the availability of Si atoms at the interface and, as a result, makes the Si DB defect density lower. Second, as a consequence of the Ge out-diffusion, a local strain relaxation in the SiGe layer occurs [2]. This would subject the Si cap to a tensile strain which helps to further reduce the Si DB density [3].

- [1] J. Franco, B. Kaczer, M. Cho, G. Eneman, G. Groeseneken, and T. Grasser, "Improvements of NBTI reliability in SiGe p-FETs" *Reliab. Phys. Symp. IRPS 2010 IEEE Int.*, pp. 1082–1085, 2010.
- [2] Y.S. Lim, J.Y. Lee, H.S. Kim, D.W. Moon, "Strain-induced anisotropic Ge diffusion in SiGe/Si superlattices", *Appl. Phys. Lett.* **80**, 14 2002
- [3] A.Stesmans, P.Somers, V.V.Afanas'ev, C.Claeys, E.Simoen, "Inherent density of point defects in thermal tensile strained (100)Si/SiO<sub>2</sub> entities probed by electron spin resonance", *Appl. Phys. Lett.* **89**, 15 2006

## Characterization of $\text{In}_2\text{O}_3$ and $\text{Ga}_2\text{O}_3$ using positron annihilation spectroscopy

E. Korhonen<sup>1</sup>, F. Tuomisto<sup>1</sup>, O. Bierwagen<sup>2</sup>, J. S. Speck<sup>2</sup>, Z. Galazka<sup>2</sup>, D. Gogova<sup>2</sup>, G. Wagner<sup>2</sup>, M. Baldini<sup>2</sup>, R. Schewski<sup>2</sup> and M. Albrecht<sup>2</sup>

<sup>1</sup>Department of Applied Physics, Aalto University, 00076 Aalto, Finland

<sup>2</sup>Leibniz Institute for Crystal Growth, 12489 Berlin, Germany

esa.korhonen@aalto.fi

Indium oxide ( $\text{In}_2\text{O}_3$ ) and gallium oxide ( $\text{Ga}_2\text{O}_3$ ) are transparent semiconducting oxides (TSO), a material category that combines electrical conductivity with optical transparency. They are used for example in the fields of solid state gas sensors, transparent contacts and LCD-displays. So far, these materials have been mostly used in their polycrystalline state since in typical applications the requirements for material quality are low. These TSOs could be used as transparent semiconductor devices if the electric properties could be controlled similar to traditional semiconductor materials.

In their stoichiometric state both materials are insulating, however high conductivities are achieved by *n*-doping, often with Sn.  $\text{In}_2\text{O}_3$  is by far the more widely used material, as heavy Sn-doping turns it into highly conducting Indium-Tin-Oxide (ITO). Even in its as-grown state  $\text{In}_2\text{O}_3$  is *n*-conductive due to unintentional doping (UID). The source of this doping is not known but oxygen vacancies, cation interstitials and impurity atoms have been suggested as causes.  $\text{Ga}_2\text{O}_3$  is generally less used but has potential applications in UV devices due to its wide band gap.

In this study, we used positron annihilation Doppler broadening spectroscopy [1] to characterize the two materials, mostly in epitaxial thin-film form. Positron spectroscopy is sensitive to vacancy type defects, especially in their negatively charged state. Our goal is to check for interactions between the doping, annealings and cation-oxygen vacancy complexes. In  $\text{In}_2\text{O}_3$  the results show that annealing in oxygen reduces the number of oxygen vacancies in In-O vacancy complexes and that donors are compensated by something else than Indium vacancies. In  $\text{Ga}_2\text{O}_3$  we find a high concentration of vacancies, most likely  $V_{\text{Ga}}$ , as a possible source for *n*-compensation.

[1] F. Tuomisto and I. Makkonen, Rev. Mod. Phys., **85**, 1583, (2013).

# POSTER PRESENTATIONS

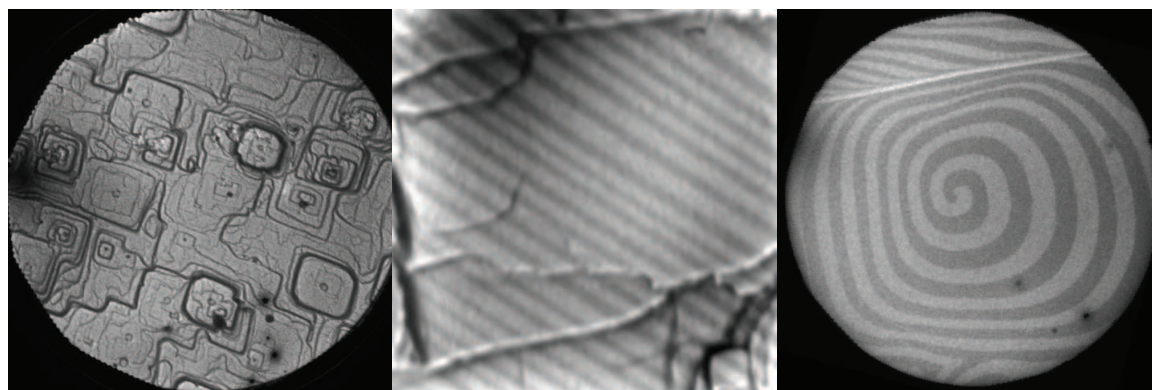
## A real-time view of the (001) magnetite surface

**J. de la Figuera**

Instituto de Química Física “Rocasolano”, CSIC, Madrid, 28006  
juan.delafiguera@iqfr.csic.es

Magnetite is the ultimate functional material: ferrimagnetic with a high Curie temperature, a half-metal conductor, multiferroic at low temperatures and with a metal-insulator transition known for the last century. It finds use in applications as diverse as catalysis, information storage and manipulation, or soil decontamination. Given the level of interest on this material, it is somewhat surprising that so many of its properties are still under discussion, from the origin of the metal-insulator transition to how it transforms into other oxides.

We have been studying the surface of magnetite with low energy electron microscopy, spin-polarized low-energy electron microscopy and photoemission electron microscopy both at the surface of bulk crystals [1-5], thin [6] and ultrathin films[7-8]. The techniques are based on imaging with low-energy electrons a surface in ultra-high vacuum conditions. The current generation of instruments allow for spatial resolutions of 10 nm for non-aberration corrected instruments, and down to 2 nm with aberration correction, together with time resolution of tenths of a second, while temperature is varied between 120 K and 1500 K. We will first present a brief introduction to those surface electron microscopies and how they can be applied to magnetite characterization and growth [7], showing then how dynamic measurements of the magnetite's surface allow both a direct observation of magnetite's Verwey metal-insulator transition [2], and to understand the oxidation of magnetite at elevated temperature, where magnetite transforms locally into hematite while the magnetite surface itself grows [4,5].



Left: LEEM image of magnetite, field of view 10  $\mu\text{m}$ . Center: Magnetite surface below the Verwey transition, image is 5  $\mu\text{m}$  wide. Right: Spiral mound imaged in dark field in LEEM, field of view 20  $\mu\text{m}$ .

- [1] J. de la Figuera et al, *Ultramicroscopy* 130, 77, (2013)
- [2] J. de la Figuera et al., *Phys. Rev. B* 88, 16410, (2013)
- [3] S. Nie et al., *Phys. Rev. B* 88, 235436, (2013)
- [4] S. Nie et al., *J. Amer. Chem. Soc.* 135, 10091, (2013)
- [5] K.F. McCarty et al., *J. Phys. Chem. C* (2014) doi:10.1021/jp5037603
- [6] M. Monti et al., *J. App. Phys.* 114 (2013) 223902
- [7] M. Monti et al., *Phys. Rev. B* 85 (2012) 020404(R)
- [8] M. Monti et al., *J. Phys. Chem. C* 116 (2012) 11539

# Stoichiometry and structure control of iron-oxide ultra-thin film

M. Monti<sup>1</sup>, I. Palacio<sup>2</sup>, K. F. McCarty<sup>3</sup>, J. F. Marco<sup>1</sup>, and J. de la Figuera<sup>1</sup>

<sup>1</sup>Instituto de Química Física Rocasolano IQFR-CSIC, Madrid, ES 28009

<sup>2</sup>Synchrotron SOLEIL, Saint Aubin, FR 91190

<sup>3</sup>Sandia National Laboratories, Livermore, CA 94550

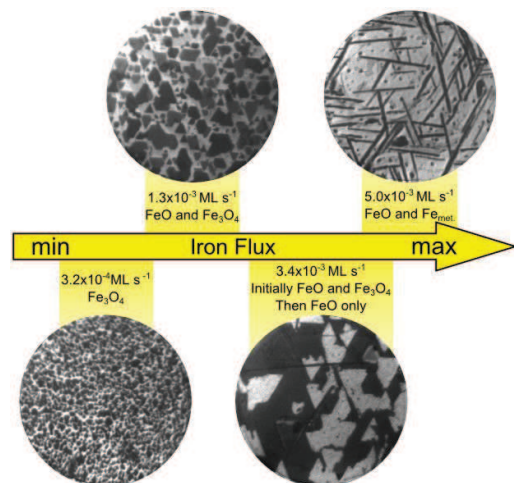
juan.delafiguera@iqfr.csic.es

Iron oxides are promising materials because their physical and chemical properties can be tailored by changing their stoichiometry and structure. Binary iron oxides vary their electrical properties from conductors, like magnetite, to insulators, like maghemite, and their magnetic properties range from ferrimagnets to antiferromagnets. For these reasons, understanding the role of the experimental parameters during their synthesis is a fundamental issue in iron oxides research, with implications in different fields as corrosion, medicine, catalysis and spintronics [2-4].

In the present work we aim at understanding the growth details of different iron oxide ultra-thin films by varying the experimental parameters. The iron oxide were grown on a Ru(0001) single crystal using oxygen-assisted molecular beam epitaxy. The nucleation and growth of the iron oxide films have been observed in real time by low-energy electron microscopy (LEEM), and the films have been characterized using selected-area low-energy electron diffraction (LEED).

First, the influence of the oxygen pressure on the growth mechanism will be presented. We propose that, during the initial stages, the film thickness is controlled by the concentration of oxygen absorbed on Ru(0001)[5]. Second, the influence of the iron dosing rate on the iron oxide ultra-thin film will be reported. We finally discuss the possibility to control the stoichiometry and structure of the ultra-thin film by choosing accurately the iron deposition rate.

- [1] R. Cornell and U. Schwertmann, *The Iron Oxides*; (1997)
- [2] M. Bibes and A. Barthelemy, *IEEE Trans. Electron. Devices* **54**, 1003, (2007)
- [3] W. Weiss and W. Ranke, *Prog. Surf. Sci.* **70**, 1, (2002)
- [4] M. Monti et al., *Phys. Rev. B* **85**, 020404 (R), (2012)
- [5] I. Palacio et al., *J. Phys.: Condens. Matter* **25**, 484001, (2013)

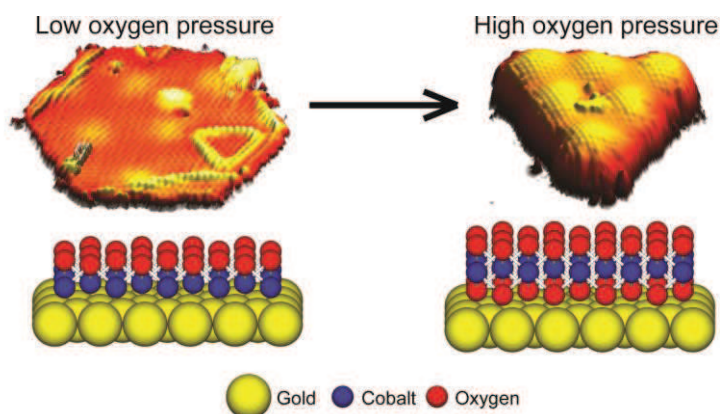


## Cobalt oxide nanoparticles on Au(111): Structure, composition and surface chemistry

Alex Walton, Jakob Fester and Jeppe. V. Lauritsen  
Interdisciplinary Nanoscience Centre (iNANO), Aarhus University  
Gustav Wieds Vej 14, 8000 Aarhus C, Aarhus, Denmark  
walton@inano.au.dk

Nanostructured cobalt oxide is a promising catalyst for the oxygen evolution reaction (OER) – half of the water splitting reaction. Its OER activity has been shown to improve dramatically when promoted with gold.<sup>1</sup> However, a detailed understanding of the structure and surface chemistry of this catalyst is lacking – as is an explanation for the promotional effect of gold. We used atom-resolved Scanning Tunneling Microscopy and X-Ray Photoelectron Spectroscopy to study a model system of cobalt oxide (CoO) nanoparticles synthesized on a single crystal gold substrate, Au(111). We find that the gold substrate stabilizes an extra layer of oxygen, creating a O-Co-O trilayer. We hypothesize that this weakly bound oxygen is highly active for oxidation catalysis and this may explain the promotional effect of gold. Furthermore we note that this trilayer structure is identical to a single layer of  $\beta$ -CoOOH, proposed to be the true active phase for the OER<sup>2,3</sup> – and therefore represents an exciting model system for the search for the active sites of this important catalytic material.

Finally, we present STM and XPS data on the interaction of Au supported  $\text{CoO}_x$  islands with water. We find that water adsorbs at the edges of the islands where it easily dissociates, forming hydroxyls. Furthermore, these hydroxyls can diffuse from the edges into the island centre, mediated by the presence of water molecules.



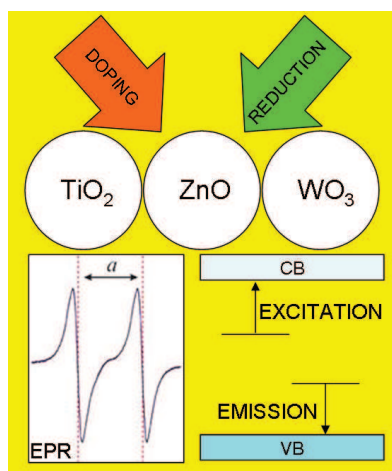
1. Yeo, B. S.; Bell, A. T. *J. Am. Chem. Soc.* **2011**, 133, (14), 5587-5593.
2. Bajdich, M.; García-Mota, M.; Vojvodic, A.; Nørskov, J. K.; Bell, A. T. *J. Am. Chem. Soc.* **2013**, 135, (36), 13521-13530.
3. Friebel, D.; Bajdich, M.; Yeo, B. S.; Louie, M. W.; Miller, D. J.; Sanchez Casalongue, H.; Mbuga, F.; Weng, T.-C.; Nordlund, D.; Sokaras, D.; Alonso-Mori, R.; Bell, A. T.; Nilsson, A. *Phys. Chem. Chem. Phys.* **2013**, 15, (40), 17460-17467.

## TiO<sub>2-x</sub>, ZnO<sub>1-x</sub>, WO<sub>3-x</sub> : a perspective on reducible oxides from hybrid DFT

Cristiana Di Valentin, Gianfranco Pacchioni

Dipartimento di Scienza dei Materiali, Università di Milano-Bicocca, Milano Italy  
cristiana.divalentin@mater.unimib.it

In this talk we will present a comparative theoretical analysis of oxygen deficient TiO<sub>2</sub>, ZnO and WO<sub>3</sub> based on hybrid density functional calculations. Substoichiometric forms of these semiconducting oxides have relevance in many technological applications including photocatalysis, touch screens, electrodes and smart glasses. Most of the interesting chemical, electronic, optical and magnetic properties essentially arise as a consequence of the defectivity introduced or intrinsically present in the lattice. Crucial differences are found in the nature of the oxygen vacancy defect of these three semiconducting oxides which have been studied by means of the same hybrid density functional (B3LYP) for comparison on an equal footing. In some cases, the introduction of a portion of exact exchange in the exchange-correlation functional is found to lead to a completely different picture than that obtained with local or semilocal functionals. Electronic transitions associated to absorption or emission spectroscopies are estimated in terms of optical and adiabatic transition energy levels. The degree of localization/delocalization of the defect is estimated in terms of the spatial distribution of the excess electron charge density. A critical issue is to establish whether the extra electrons deriving from the oxygen depletion cause the reduction of the lattice cations oxidation state or are, instead, simply trapped at the vacancy site through stabilization by the lattice potential. Computational results will be directly compared to experimental spectroscopic data when available.



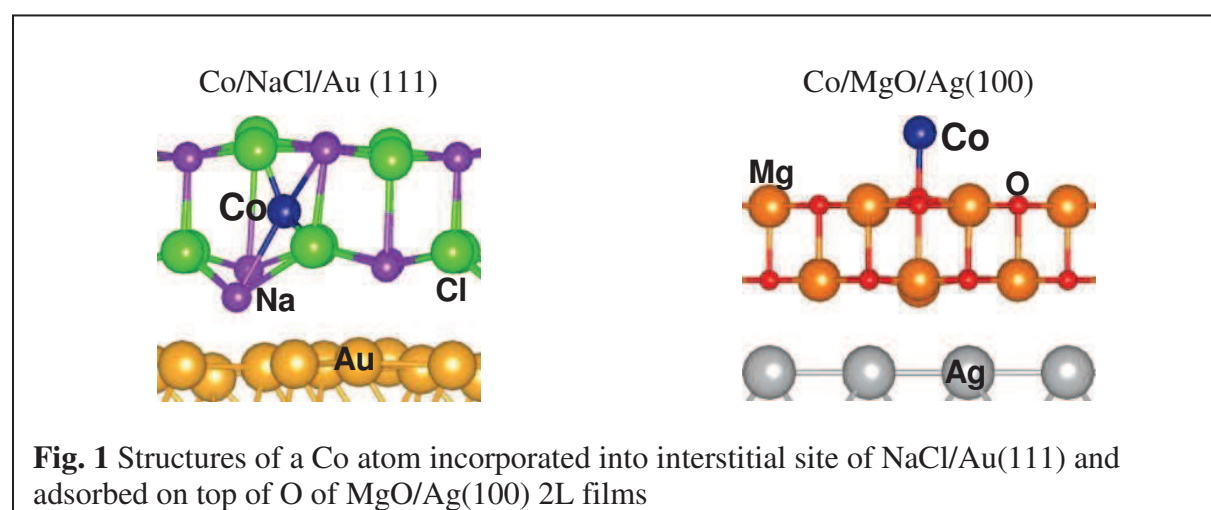
[1] C. Di Valentin, G. Pacchioni, *Acc. Chem. Res.* [dx.doi.org/10.1021/ar4002944](https://doi.org/10.1021/ar4002944) (2014).

# Properties of two-dimensional insulators: a DFT study of Co adsorption on NaCl and MgO ultrathin films

Hsin-Yi Tiffany Chen and Gianfranco Pacchioni

Dipartimento di Scienza dei Materiali, Università di Milano-Bicocca, Milano, Italy  
hsinyi.tiffany.chen@gmail.com

Lately an increasing attention has been dedicated to the properties of two-dimensional crystals. Recent experimental and theoretical results have shown that Co atoms deposited on ultrathin NaCl films grown on Au(111) result in spontaneous substitutional doping of the two-layers insulating material<sup>1,2</sup>. This result opens the general question of the reactivity of transition metal (TM) atoms with ultrathin films consisting of few atomic layers. In this study, density functional theory (DFT) has been applied to compare the adsorption properties of Co atoms on three different supports: (1) models of bulk NaCl and MgO(100) surfaces; (2) free-standing two-layer (2L) NaCl and MgO films; (3) metal supported 2L NaCl/Au(111) and MgO/Ag(100) films. We found that Co interacts strongly with NaCl/Au(111) 2L films, and that Co incorporation in interstitial positions between the first and second NaCl layers is thermodynamically preferred compared to adsorption on the surface sites. Differently from NaCl, Co adsorbs preferentially on top of O in both unsupported and supported MgO 2L films. Co incorporation in the interstitial sites of MgO is highly unfavorable. These results show that the reactivity of TM atoms like Co is completely different on NaCl or MgO ultrathin films, which can be attributed to the smaller lattice constant of MgO than that of NaCl and the stronger Madelung field in the oxide compared to the chloride. Plus, the supported metals make the charge transfer possible, *i.e.*, Co atoms can donate charge to the metal support in the cases of Co adsorbed on hollow site, incorporated into interstitial site of NaCl/Au(111) 2L films and incorporated into interstitial site of MgO/Ag(100) 2L films; this forms  $\text{Co}^{\delta+}$ , reduces the steric repulsion and thus increases the energy gain, compared to the unsupported films.



- [1] Z. Li, H.-Y. T. Chen, K. Schouteden, K. Lauwaet, L. Giordano, M. I. Trioni, E. Janssens, V. Iancu, C. Van Haesendonck, P. Lievens and G. Pacchioni, *Phys. Rev. Lett.* **112**, 026102 (2014).
- [2] H.-Y. T. Chen, L. Giordano, G. Pacchioni, *J. Phys. Chem. C* **118**, 12353 (2014).
- [3] H.-Y. T. Chen and G. Pacchioni, *Phys. Chem. Chem. Phys.*, in press (2014).

## AFM imaging of the Au/CeO<sub>2</sub>(111) system: DFT study

Krzysztof Kośmider<sup>1</sup>, Maria Verónica Ganduglia-Pirovano<sup>2</sup>, Rubén Pérez<sup>1</sup>

<sup>1</sup>Departamento de Física Teórica de la Materia Condensada, UAM, Madrid, 28049, Spain

<sup>2</sup>Instituto de Catálisis y Petroleoquímica, CSIC, 28049 Madrid, Spain

krzysztof.kosmider@uam.es

Ceria-supported gold has recently attracted significant interest [1] as a potential catalyst for the industrially very important water-gas shift (WGS) reaction. However, despite the significant amount of research performed in this topic, there is still a lack of fundamental understanding of the Au-Ceria interaction and the mechanism controlling adsorption at the atomic scale. Theoretical investigations [2] show that charge transfer in this system depends on the Au adsorption site and may even change sign in the presence of vacancies. Furthermore, different exchange-correlation functionals and calculation details seem to provide conflicting results for this charge transfer. Non-contact atomic force microscopy (NC-AFM), which proved to be capable to distinguish between different charge states of Au on NaCl/Cu [3], is a promising method to experimentally determine the Au charge states.

Here, we present a systematic DFT+U study of the NC-AFM imaging of the Au/CeO<sub>2</sub>(111) sample. We exploit the different charge states for Au adsorbed on the clean or reduced surface to address the possible AFM visualization of oppositely charged Au atoms. We simulate AFM force spectroscopy with different tips, including O- and OH-terminated tips [4] and analyze the influence of the tip apex on the contrast. We provide guidelines for prospect AFM measurements.

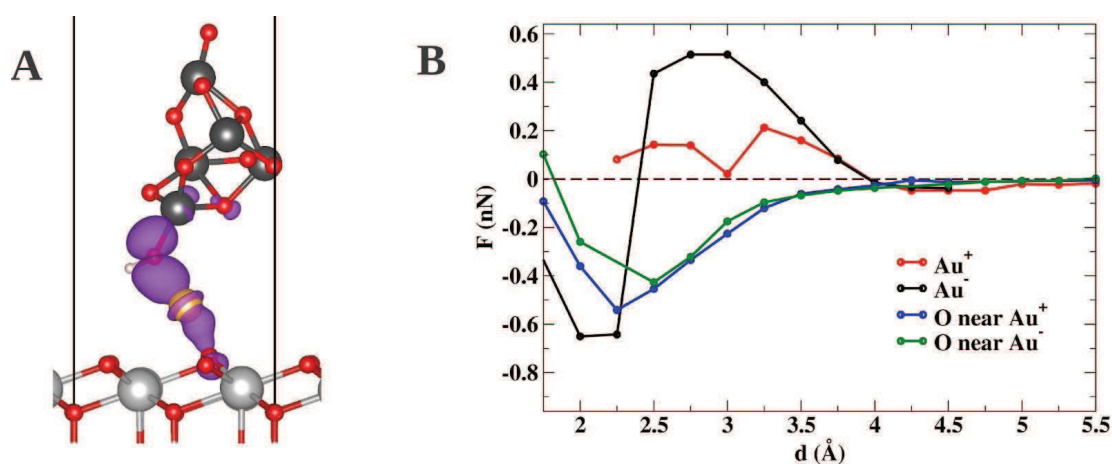


**Figure 1.** A) Structure for an OH-terminated TiO<sub>2</sub> AFM tip making contact with the Au/CeO<sub>2</sub>(111) sample, B) Computed tip-sample forces between this tip and positively /negatively charged Au and nearby O surface atoms.

[1] J. A. Rodriguez et al., *Science*, **318**, 1757, (2007).

[2] C. Zhang, A. Michaelides and S.J. Jenkins, *Phys. Chem. Chem. Phys.* **13**, 22, (2010).

[3] L. Gross et al., *Science* **324**, 1428, (2009).

[4] A. Yurtsever et al., *Phys. Rev. B* **85**, 125416, (2012).

## Study of formate species in the CH<sub>3</sub>OH/CeO<sub>2</sub> reaction: combining IR spectroscopy and statistical thermodynamics techniques

P. G. Lustemberg<sup>1</sup>, A. Bonivardi<sup>2</sup>, M. V. Bosco<sup>2</sup>, H. F. Busnengo<sup>1</sup> and M. V. Ganduglia-Pirovano<sup>3</sup>

<sup>1</sup>Instituto de Física Rosario (IFIR), Santa Fe, Argentina

<sup>2</sup>Instituto de Desarrollo Tecnológico para la Industria Química (INTEC), Santa Fe, Argentina

<sup>3</sup>Instituto de Catálisis y Petroleoquímica (ICP), Madrid, Spain

lustemberg@ifir-conicet.gov.ar

Formate species (HCOO<sup>-</sup>) have been suggested as intermediates or spectators in chemical reactions of industrial relevance, such as the water-gas-shift and the methanol steam reforming reaction [1]. Several catalysts, some of them based on ceria, have been proposed to improve the performance of these reactions. One of the main reasons of choosing ceria has been its intrinsic redox properties, but only few works describe the formate formation under the oxidizing/reducing environment, usually modulated by the reaction itself. In this work, we have studied the stability of formate groups in the CH<sub>3</sub>OH/CeO<sub>2</sub> system. *In situ* transmission infrared spectroscopy was used to study the temperature-programmed surface reaction (TPSR-IR) of adsorbed methanol. Three types of formates were observed based on the OCO stretching frequencies [ $\nu(\text{OCO})$ ] (Figure 1). Type III formate ( $\nu_{\text{as}} = 1550 \text{ cm}^{-1}$ ) was the first one obtained over 450 K, where no Ce<sup>3+</sup> was detected. However, after increasing the temperature, types I and II ( $\nu_{\text{as}} = 1580$  and  $1561 \text{ cm}^{-1}$ ) species emerged accompanied by the appearance of surface Ce<sup>3+</sup> species. The phase diagram of formate structures in contact with a gas environment of O<sub>2</sub> and H<sub>2</sub>, to simulate oxidizing/reducing conditions, was calculated using density-functional theory and statistical calculations. The formate binding structure was found to crucially depend on temperature and partial pressures of the reactants in the gas phase. In the absence of methanol the CeO<sub>2</sub>, CeO<sub>2-x</sub>, O<sub>2</sub>/CeO<sub>2</sub> and several OH-coverages phases coexist. As methanol pressure increases, we found a bridge formate with two next neighbors hydroxyls adsorbed (NN-OH<sub>ads</sub>) and no Ce<sup>3+</sup>, named Brg-A ( $1535 \text{ cm}^{-1}$ ). At higher methanol chemical potential (Figure 2), a monodentate formate with three NN-OH<sub>ads</sub> and a bridge state with one NN-OH<sub>ads</sub>, named Mono-B and Brg-B, respectively, appeared together with the formation of Ce<sup>3+</sup> species ( $1564$  and  $1540 \text{ cm}^{-1}$ , respectively). We conclude that the experimentally observed formate species correspond to those monodentate and bridge types.

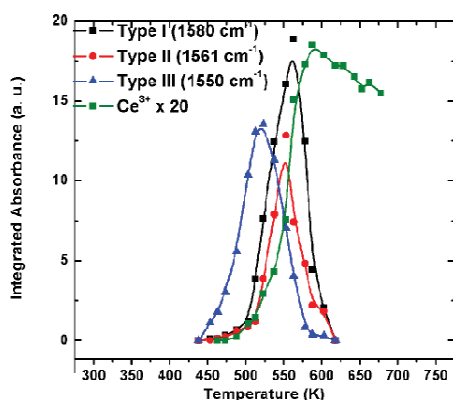


Figure 1. Thermal evolution of IR signals of formate and Ce<sup>3+</sup> species.

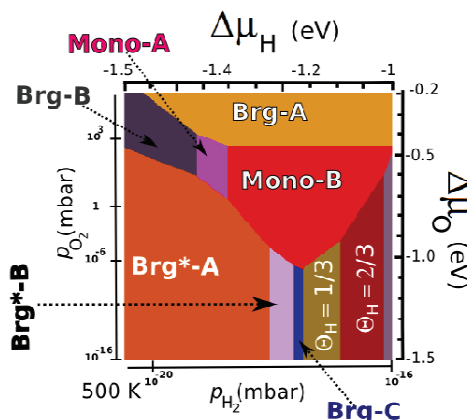


Figure 2. Phase diagram of formate species in oxidized/reduced surfaces.

[1] T. Shido and Y. Iwasawa, J. Catal., **136**, 493 (2003).

## The effect of atomically thin TiO<sub>x</sub> structures on the morphology and reactivity of nano-sized Rh films

L. Deák<sup>1</sup>, I. Szenti<sup>2</sup>, R. Gubó<sup>2</sup>, L. Óvári<sup>1</sup>, A. Berkó<sup>1</sup> and Z. Kónya<sup>1,2</sup>

<sup>1</sup>MTA-SZTE, Reaction Kinetics and Surface Chemistry Research Group, H-6720 Szeged

<sup>2</sup>University of Szeged, Department of Applied and Environmental Chemistry, Hungary  
sir@chem.u-szeged.hu

The impact of atomically thin TiO<sub>x</sub> structures, being on top, beneath or mixed with nano-sized Rh films on the morphology and reactivity of Rh films has been investigated by AES, STM, LEIS, XPS, TPD and work function measurements under UHV conditions. Rh layers were formed on a nearly stoichiometric TiO<sub>2</sub>(110) single crystal by PVD. TiO<sub>x</sub> encapsulation layers were produced on ultrathin Rh films by appropriate heat treatments and their morphology and composition has been determined. The desorption of CO test molecule from the CO-saturated Rh nanoparticles was characterized by a molecular (T<sub>p</sub>=550 K) and a recombinative (T<sub>p</sub>=770 K) desorption state, the amount of latter being proportional to the extent of CO dissociation. The TiO<sub>x</sub> overlayer had twofold effect on both Rh nanoparticles and on highly defective continuous Rh films produced by Ar<sup>+</sup>-ion sputtering. On the one hand, the uptake of molecular CO was suppressed due to blocking of adsorption sites and a linear change with TiO<sub>x</sub> coverage could be established on the Rh films. On the other hand, the amount of recombinative CO desorption state went through maximum at intermediate TiO<sub>x</sub> concentrations on both type of rhodium surfaces, proving that the decomposition of CO is promoted by TiO<sub>x</sub>. This finding is in harmony with previous high pressure studies regarding the maximum methanation rate of CO on rhodium at intermediate TiO<sub>x</sub> coverages [1]. The promotion exerted by TiO<sub>x</sub> species in inverse catalyst systems can be related to oxide-metal boundary effect [2, 3].

The effect of an ultrathin supporting TiO<sub>x</sub> film on the adsorption properties of Rh deposit (0.4 ML) was studied at different temperatures. An Rh-TiO<sub>x</sub>-Rh structure was formed at 230 K by deposition of Rh on a continuous TiO<sub>x</sub> film prepared on a 20 ML thick Rh multilayer. The molecular CO TPD states indicated that this Rh overlayer was nearly intact and exhibited high reactivity, while the enhancement of the deposition temperature to 265 K resulted in a dramatic change in the metal-oxide-metal (MOM) structure. The structural rearrangement is accompanied by the mixing of TiO<sub>x</sub> with the post-deposited Rh as it can be deduced from the appearance of a CO desorption feature with T<sub>p</sub>=360 K, characteristic of the presence of TiO<sub>x</sub> overlayer. Enhancing the deposition temperature to 300 K, the reactivity of the TiO<sub>x</sub>+Rh film towards CO became limited, suggesting a strong interaction between the Rh deposit and the atomically thin TiO<sub>x</sub> film supported by the Rh multilayer. The low temperatures allowing the observation of the mixing between TiO<sub>x</sub> and Rh deposits indicate that this process possesses low activation energy. The driving force of the restructuring is the formation of strong Rh-Rh bond and the lower surface free energy of TiO<sub>x</sub> overlayer related to that of the bare Rh surface. Noticeably, the Rh deposit formed and saturated with CO at 230 K was stable well above 300 K, up to the desorption temperature of molecular CO, suggesting that the stability of nano-sized MOM structures can be influenced considerably by the presence of adsorbates.

[1] K. Hayek, M. Fuchs, B. Klötzer, W. Reichl, G. Rupprechter, *Top. Catal.* **13**, 55, (2000).

[2] J. Schoiswohl, S. Surnev, F.P. Netzer, *Topics in Catalysis* **36**, 91, (2005).

[3] J. A. Rodriguez, S. Ma, P. Liu, J. Hrbek, J. Evans, M. Pérez, *Science* **318**, 1757 (2007).

## Excess electrons in TiO<sub>2</sub> – delocalized solutions in anatase vs. localized polarons in rutile

Martin Setvin,<sup>1</sup> C. Franchini,<sup>2</sup> X. Hao,<sup>1</sup> B. Daniel,<sup>1</sup> M. Schmid,<sup>2</sup> G. Kresse,<sup>1</sup> U. Diebold<sup>1</sup>

<sup>1</sup> Institute of Applied Physics, TU Vienna, Wiedner Hauptstrasse 8-10/134, A-1040 Vienna

<sup>2</sup> Faculty of Physics and Centre for Computational Materials Science, Universität Wien, Sensengasse 8/12, A-1090 Wien, Austria

setvin@iap.tuwien.ac.at

TiO<sub>2</sub> is a prototypical metal oxide used in photocatalysis, photoelectrochemical (Grätzel) solar cells, and transparent conducting oxides. Industrially two forms of TiO<sub>2</sub> are used, rutile and anatase. The behavior of charge carriers is of key importance in virtually all applications of these materials. When excess electrons are added to the conduction band of an oxide, they can either retain a delocalized (band-like) character, or form localized (small) polarons due to the strong electron-phonon coupling [1].

We used a combination of STM, STS and DFT+*U* to investigate the degree of electron localization in TiO<sub>2</sub> rutile and anatase [2]. The excess electrons in rutile can localize at any lattice Ti atom, forming a small polaron. The polarons in rutile can easily hop to neighboring sites. Electrons in a perfect anatase lattice prefer delocalized (band-like) solutions, while electron trapping is only possible at defects. Delocalized electrons were observed in Nb-doped anatase in vicinity of subsurface Nb dopants. The consequences of different electron behavior in these materials are illustrated on several applications [3].

The work was supported by ERC Advanced Research Grant ‘Oxide Surfaces’

[1] I. G. Austin and N. F. Mott, *Adv. Phys.* **50**, 757 (2001)

[2] M. Setvin *et al.*, *Phys. Rev. Lett.* **113**, 086402 (2014)

[3] M. Setvin *et al.*, *Angew. Chem. Int. Ed.* **53**, 4714 (2014)

## TiO<sub>2</sub> anatase (101) - Single crystal growth and surface preparation in UHV

Martin Setvin,<sup>1</sup> V. Mansfeldova,<sup>2</sup> Michael Schmid,<sup>1</sup> L. Kavan,<sup>2</sup> and Ulrike Diebold<sup>1</sup>

<sup>1</sup> Institute of Applied Physics, TU Vienna, Wiedner Hauptstrasse 8-10/134, A-1040 Vienna

<sup>2</sup> J. Heyrovsky Institute of Physical Chemistry of the ASCR, v.v.i., Dolejskova 2155/3, CZ-182 23 Prague 8, Czech Republic

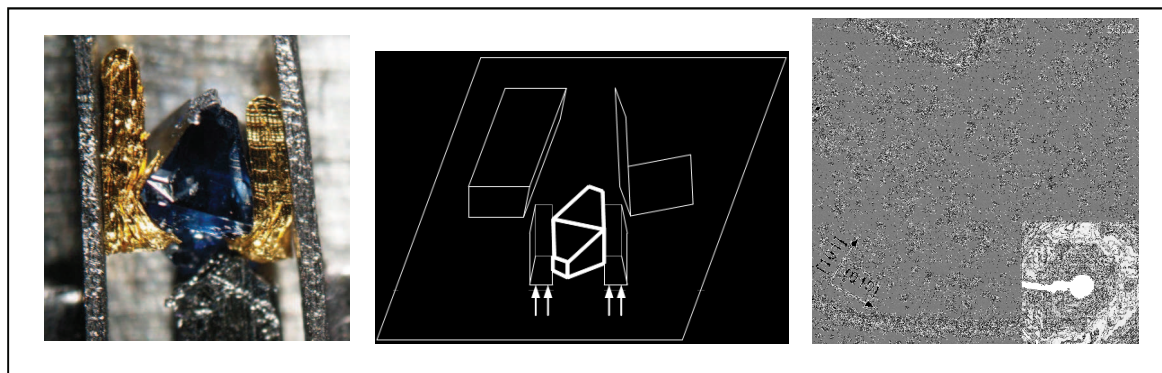
setvin@iap.tuwien.ac.at

Titanium dioxide is a versatile material that is used in a wide range of applications. While the rutile phase of TiO<sub>2</sub> is well-investigated in surface science, it is the metastable anatase that is present in most nanomaterial and often considered the technologically more relevant polymorph.

The key impediment in the fundamental research of anatase is the lack of suitable single-crystals of high purity and sufficient size. While natural anatase crystals can be up to 1 cm large, they suffer from contamination by other elements. Synthetically grown anatase crystals have a well-defined dopant concentration but they are very small (few nm).

We discuss optimal ways of sample mounting and cleaning in UHV, in order to avoid contamination of the surface from the sample mount [1]. We compare the surface quality obtained on polished, cleaved and as-grown anatase (101) planes. We discuss the role of bulk impurities for the surface preparation. Fe is the most troublesome material present in natural anatase single crystals. Fe segregates at the surface upon annealing the crystal in partial O<sub>2</sub> pressure, resulting in overgrowth of iron oxide on the surface.

As an alternative to the natural single crystals, we present our progress in the growth of synthetic anatase crystals by the chemical transport method [2].



[1] M. Setvin *et al.*, Surf. Sci. **626**, 61 (2014)

[2] L. Kavan *et al.*, JACS **118**, 6716 (1996)

**Reaction of (WO<sub>3</sub>)<sub>3</sub> clusters with NiO(100) layers on a Ni(110) surface:  
Formation of epitaxial ternary oxide NiWO<sub>4</sub>(100) films**

N. Doudin, S. Pomp, F.P. Netzer and S. Surnev

*Surface and Interface Physics, Institute of Physics, Karl-Franzens University  
A-8010 Graz, Austria*

R. Resel

*Institute of Solid State Physics, Graz University of Technology, A-8010 Graz, Austria*

Transition metal tungstates MWO<sub>4</sub> (where M is divalent transition metal ion) have recently attracted significant scientific and technological interest due to their application in humidity sensors, photocatalysts, photo- and electrochromic devices. In particular, NiWO<sub>4</sub> has important electrochromic and (photo)catalytic properties, which are superior to those of the binary NiO and WO<sub>3</sub> constituents. Nickel tungstate compounds have been synthesized mostly in bulk form, but with the advance of nanotechnologies there is a growing interest in preparing NiWO<sub>4</sub> structures at the nanoscale, whose physical and chemical properties are unexplored as yet. Recently, we have fabricated a two-dimensional (2-D) ternary oxide CuWO<sub>4</sub> nanolayer on a Cu(110) surface via a UHV surface epitaxial growth route using a solid-state chemical reaction in two dimensions and have characterized the structural, electronic and vibrational properties of this novel ternary oxide material [1]. In this work, we show that this preparation approach can be successfully applied also for the growth of epitaxial NiWO<sub>4</sub> films. Specifically, (WO<sub>3</sub>)<sub>3</sub> clusters have been deposited from the gas phase onto a NiO(100) layer supported on a Ni(110) surface. Oxidation in an oxygen pressure of 5x10<sup>-6</sup> mbar at 700°C initiates a solid-state reaction between the (WO<sub>3</sub>)<sub>3</sub> clusters and the NiO layer, resulting in the formation of nanometer-size crystallites, which coexist with bare NiO patches at low (WO<sub>3</sub>)<sub>3</sub> coverage, as demonstrated on the STM image in Fig. 1a. The crystallites exhibit a well-developed shape, comprising top and side facets (Fig. 1b), with the top facet being imaged with atomic resolution and revealing a good structural order (Fig. 1c). At higher (WO<sub>3</sub>)<sub>3</sub> coverage the crystallites coalesce and form a NiWO<sub>4</sub> film (Fig. 1d), as unambiguously identified by ex-situ X-ray diffraction (XRD) measurements (Fig. 1e). The XRD results show also that the NiWO<sub>4</sub> film is epitaxially oriented with its (100) crystal planes parallel to the Ni(110) substrate.

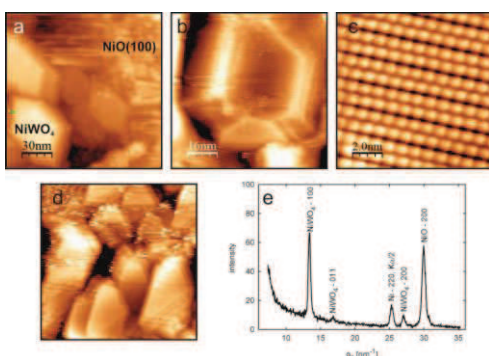


Fig. 1: (a) STM image of 1 ML (WO<sub>3</sub>)<sub>3</sub> clusters deposited onto a NiO(100) film on Ni(110) and post-oxidized in 5x10<sup>-6</sup> mbar O<sub>2</sub> at 700°C leading to the formation of NiWO<sub>4</sub> nanocrystallites and bare NiO areas; (b) STM image of an individual NiWO<sub>4</sub> nanocrystallite; (c) STM image of the top NiWO<sub>4</sub> facet; (d) STM image of 5 ML (WO<sub>3</sub>)<sub>3</sub> clusters leading to the formation of NiWO<sub>4</sub> film; (e) XRD specular diffraction scan of the 5 ML NiWO<sub>4</sub>(100) film.

[1] M. Denk, D. Kuhness, M. Wagner, S. Surnev, F.R. Negreiros, L.Sementa, G. Bacaro, I. Vobornik, A. Fortunelli, and F.P. Netzer, ACS Nano 8 (2014) 3947

Work supported by FWF Project P26633-N20 and the EU COST Action CM1104

## Cobalt Oxide Model Catalyst as Alternative to Noble Metal Catalysts

**Christoph Rameshan**<sup>1</sup>, Kresimir Anic<sup>1</sup>, Andrey Bukhtiyarov<sup>1</sup>, Günther Rupprechter<sup>1</sup>  
Institute of Materials Chemistry, Vienna University of Technology, Getreidemarkt 9,  
1060 Vienna, Austria  
christoph.rameshan@tuwien.ac.at

Cobalt oxide has recently turned out to be a novel, highly active heterogeneous catalyst for many industrial important reactions. Most important, cobalt oxide-based catalysts hold an unique potential for replacing or reducing the demand for critical materials (noble metals and rare earth oxides) for oxidations. However the origin of the high cobalt oxide activity in catalysis is still not well explained.

We have chosen a thin cobalt oxide film with a well-defined structure as model catalysts for low temperature CO oxidation. The cobalt oxide film was grown on the surface of an Ir(100) single crystal by physical vapor deposition (PVD) in O<sub>2</sub> background with subsequent post-oxidation [1-3]. With this routine a 8 ML thick Co<sub>3</sub>O<sub>4</sub>(111) or CoO(111) film were prepared. The characterization of the films has been performed by low energy electron diffraction (LEED) and X-ray photoelectron spectroscopy (XPS).

Furthermore, we investigated the state of the active component and the interaction of CO, CO<sub>2</sub> and gas mixture (CO+O<sub>2</sub>) with different surfaces of cobalt oxide by XPS, polarization modulation infrared reflection absorption spectroscopy (PM-IRAS) and temperature programmed desorption (TPD) in the temperature range 200 K – 470 K and in the pressure from UHV to 100 mbar.

It has been shown that CO does not adsorb on Co<sub>3</sub>O<sub>4</sub> films at the studied temperatures and pressures. Using XPS and PM-IRAS it has been shown that for both Co<sub>3</sub>O<sub>4</sub>(111) and CoO(111), depending on the conditions of CO adsorption, we obtained appearance of two different carbon-containing species which could be identified as carbonates and elementary carbon. Furthermore, in case of Co<sub>3</sub>O<sub>4</sub>(111) film CO adsorption leads to partial reduction of cobalt oxide, for higher gas pressures even at room temperature (“pressure gap”). The thermal stability of carbonates and elementary carbon formed during CO adsorption on Co<sub>3</sub>O<sub>4</sub>(111) film was investigated by TPD. It has been shown that both desorbed from the surface at 520 K -700 K as CO<sub>2</sub>, at the same time the Co<sub>3</sub>O<sub>4</sub>(111) film has been reduced to CoO(111). It could be shown by IRAS, that CO adsorbs in an on top geometry on CoO and upon subsequent reduction to Co(0) no adsorption was observed any more.

Experiments showed that it is possible to recover the film (initial state of composition and structure) after CO adsorption and desorption experiments by an oxidation treatment at 550 K and subsequent annealing in UHV to 670 K.

- [1] K. Biedermann, M. Gubo, L. Hammer, K. Heinz, *J. Phys.: Condens. Matter*, **21**, 185003, (2009).
- [2] M. Gubo, C. Ebensperger, W. Meyer, L. Hammer, K. Heinz, *J. Phys.: Condens. Matter*, **21**, 0474111, (2009).
- [3] W. Meyer, D. Hock, K. Biedermann, M. Gubo, S. Müller, L. Hammer, K. Heinz, *Phys. Rev. Lett.*, **101**, 016103, (2008).

Support by the Austrian Science Fund (FWF DACH I 1041-N28) is gratefully acknowledged.

## Theoretical and experimental study of the interaction of NO with ceria

Mihail Y. Mihaylov,<sup>1</sup> Elena Z. Ivanova,<sup>1</sup> Hristiyan A. Aleksandrov,<sup>2</sup> Georgi N. Vayssilov,<sup>2\*</sup>  
and Konstantin I. Hadjiivanov<sup>1\*</sup>

<sup>1</sup> Institute of General and Inorganic Chemistry, Bulgarian Academy of Sciences, Sofia 1113, Bulgaria, e-mail: kih@svr.igic.bas.bg

<sup>2</sup> Faculty of Chemistry and Pharmacy, University of Sofia, 1126 Sofia, Bulgaria, e-mail: gnv@chem.uni-sofia.bg

Interaction of NO with ceria has been studied by density functional modeling and FTIR spectroscopy. The spectral studies using isotope labeled nitrogen monoxide revealed various bands corresponding to different types of nitrogen-containing species on ceria - nitrite species, hyponitrite species and nitrate species. The conversion of the species with the temperature and the amount of NO was studied in order to estimate their stability. In order to clarify the structure of those species we modelled computationally such species on different positions on the facets and edges of a ceria nanoparticle. The calculations were performed with DFT+U approach using periodic code VASP. Ceria was modelled as Ce<sub>21</sub>O<sub>42</sub> nanoparticle, used in previous studies [1,2]. For all nitrogen-containing species the vibrational frequencies were calculated and compared to the experimentally measured value. Similar to previous work on surface carbonates [2], this approach allowed assignment of the IR bands to specific structures of the surface species.

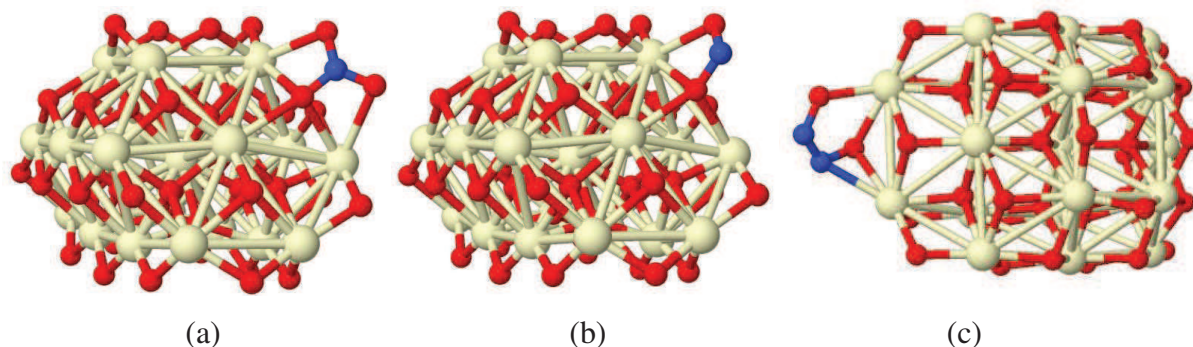


**Fig. 1.** Selected model structures of nitrate (a), nitrite (b), and hyponitrite (c) species on ceria nanoparticle.

*Acknowledgments:* The authors are grateful for the support from the European Commission (FP7 project BeyondEverest), COST Action CM1104, Bulgarian National Science Fund (project DCVP 02/02) and the Bulgarian Supercomputer Center for provided resources.

1. Migani, A.; Vayssilov, G. N.; Bromley, S. T.; Illas, F.; Neyman K. *M.J. Mater. Chem.* **2010**, *20*, 10535.

2. Vayssilov, G. N.; Mihaylov, M.; Petkov, P. St.; Hadjiivanov, K. I.; Neyman, K. M. *J. Phys. Chem. C* **2011**, *115*, 23435.

# Hybrid DFT study of the Fe:NiOOH O<sub>2</sub> electroevolution catalyst

José C. Conesa

Inst. de Catálisis y Petroleoquímica, CSIC, Campus de Cantoblanco, 28049 Madrid, Spain.

e-mail: jcconesa@icp.csic.es

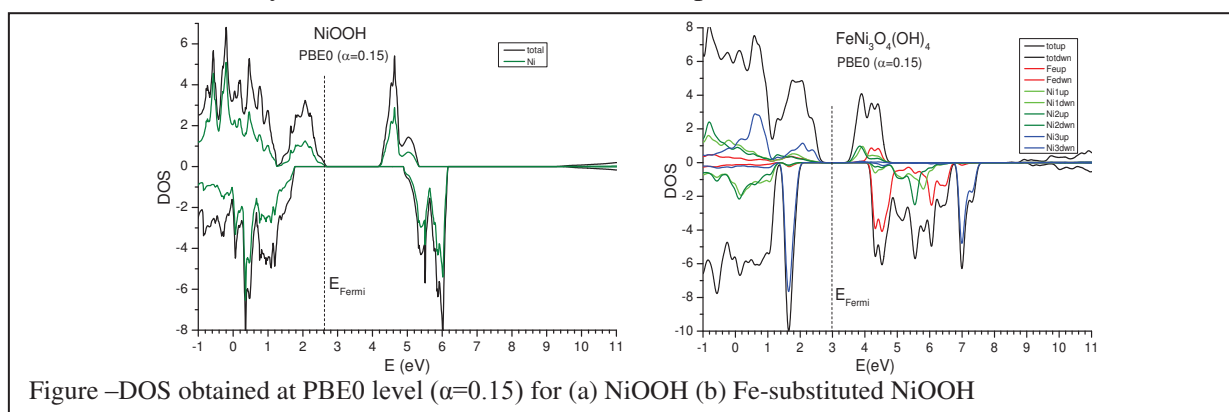
The layered compound NiOOH, especially when Fe-doped, is one of the best catalysts for evolution of O<sub>2</sub> in photo/ electrocatalytic water splitting, the mechanism involving probably Fe<sup>4+</sup> or Ni<sup>4+</sup> species [1]. That compound is however not well understood, as the protons in it are disordered and its electronic structure is not well clarified. The only DFT studies made, at the GGA+U level [2], assume that all OH groups are at the same side in each layer and propose a location of Fe for the most active site.

Here the bulk system, doped or Fe-free, is modelled with hybrid functional method PBE0 where the fraction  $\alpha$  of Fock exchange is taken, on the basis of GW theory concepts, as the inverse of the optical dielectric constant  $\epsilon_{\infty}$ , determined if needed self-consistently by the same method. This gives accurate bandgap values for very different semiconductors [3]. Calculations use periodic code VASP on a model having 50% of protons at each layer side, to avoid unphysical effects on the  $\epsilon_{\infty}$  result.

The NiOOH structure was relaxed with a GGA+U+vdW functional, giving for Ni a distorted octahedral coordination with 2 longer Ni-O bonds in *trans* situation. Ni<sup>3+</sup> ions (low spin) show ferro-magnetic order, the antiferromagnetic one having slightly higher energy.  $\alpha=0.15$  and an indirect bandgap of 1.45 eV, agreeing with the absorption edge measured at 850 nm [4], are computed for the ground state. The resulting DOS is given in Fig. (a).

From this structure a Fe-substituted model was built and relaxed at the GGA+U+vdW level, and calculations with same DFT method and  $\alpha$  value were made. Ni<sup>3+</sup> is found to oxidize the iron substituent to Fe<sup>4+</sup> (in agreement with XAFS data [5]), with ejection of two protons from the OH ligands bound to the latter ion and formation of one Ni<sup>2+</sup>; the gap decreases to 0.95 eV (Fig. (b) ), which may help to increase (hole) conductivity as observed experimentally [1].

The same systems (Fe-doped or not) computed at GGA+U level give much lower gap values (below 0.3 eV), they are even metallic for some OH positions GGA+U is not suitable here.



- [1] L. Trotochaud et al., *J. Am. Chem. Soc.* **136**, 6744 (2014).
- [2] Y.F. Li, A. Selloni, *ACS Catalysis* **4**, 1148 (2014).
- [3] E. Menéndez-Proupin et al., *Phys. Rev. B* **90**, 045207 (2014) and references therein.
- [4] A.J. Varkey, A.F. Fort, *Thin Solid Films* **235**, 47 (1993).
- [5] M. Balasubramanian et al., *J Phys. Chem. B* **104**, 4300 (2000).

## Cu/ZnO charge transfer depends on Cu size, Cu shape, and H<sub>2</sub>O pressure

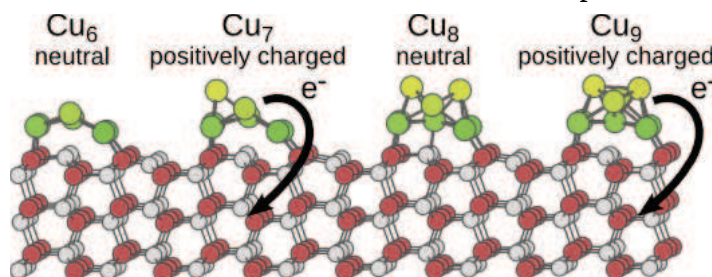
Matti Hellström, Daniel Spångberg, Peter Broqvist, and Kersti Hermansson  
Department of Chemistry - Ångström Laboratory, Uppsala University, Uppsala, Sweden  
matti.hellstrom@kemi.uu.se

Catalysts composed of Cu/ZnO nanoparticles are widely used in industry for the catalysis of, for example, methanol synthesis ( $\text{CO}/\text{CO}_2 + \text{H}_2 \rightarrow \text{CH}_3\text{OH}$ ) and the water-gas shift reaction ( $\text{H}_2\text{O} + \text{CO} \rightarrow \text{H}_2 + \text{CO}_2$ ). Several totally different catalytic active sites have been proposed, such as a Cu-Zn alloy, metallic Cu, or adsorbed  $\text{Cu}^+$  species.

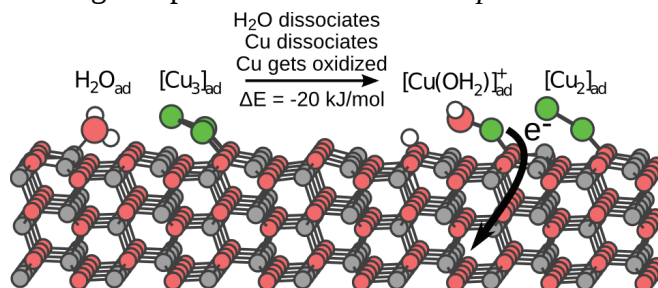
In this work, we investigate the fundamental Cu-ZnO interactions during the early stages of Cu particle growth on ZnO [1]. Using hybrid density functional theory, we adsorbed successively larger  $\text{Cu}_n$  clusters ( $n=1,\dots,9$  atoms) of many different shapes on the most stable ZnO surface, ZnO(10 $\bar{1}$ 0), and also investigated water adsorption characteristics for some of the smaller clusters ( $n=1,\dots,4$  atoms) [2].

Small *gas-phase* Cu clusters show even-odd alternations in their ionization energies as a function of the number of atoms. Remarkably, we find that this fundamental property affects the *adsorption* of Cu clusters on ZnO in several ways.

- Odd-numbered clusters can become positively charged (oxidized) by donating electrons into the ZnO conduction band. Even-numbered clusters are always neutral.
- Polyhedral Cu clusters more easily become oxidized than planar Cu clusters.
- For odd Cu sizes  $\geq 5$  atoms, this redox reaction occurs spontaneously.



- A *single* water molecule can oxidize the Cu atom and the Cu trimer (odd-numbered clusters). In contrast, *two* water molecules are needed to oxidize the Cu dimer and tetramer (even-numbered clusters) - but second water adsorption is endothermic.
- The Cu trimer undergoes spontaneous *water adsorption-induced dissociation*.



Finally, we note that care is required when modelling the oxidized Cu clusters with DFT [1,3].

- [1] M. Hellström et al., J. Phys. Chem. C **118**, 6480-6490 (2014)  
[2] M. Hellström et al., in preparation  
[3] M. Hellström et al., J. Chem. Theory Comput. **9**, 4673-4678 (2013)

## Comparison of vdW-functionals for improved description of water-ionic surface interactions - NaCl(100) and MgO(100) as prototype substrates

**Getachew Kebede**, Daniel Spångberg, Peter Broqvist, Pavlin M. Mitev and Kersti Hermansson  
Dept. of Chemistry – Ångström, Uppsala University, Box 538, SE-751 21 Uppsala, Sweden  
e-mail: kersti@kemi.uu.se

The interaction of water with ionic surfaces is of fundamental interest across many scientific areas, such as atmospheric chemistry and heterogeneous catalysis. The MgO(001) and NaCl(001) surfaces have been extensively used as prototype substrates in the literature. From a theoretical point view, the density functional theory (DFT) with semi-local GGA approximations has been most frequently used to describe water-surface interactions. However, in the GGA-formalism, the important dispersion interactions are not explicitly taken into account. Recently, several new density functionals have been proposed which account for the missing non-local correlation in DFT, collectively known as vdW-functionals [1-4]. To the best of our knowledge, a comparative study of the performance of such different vdW-functionals for the water–ionic surface systems has not yet been published.

Here we present a systematic comparison of various vdW-functionals (vdW-DF, vdW-DF2, cx-vdW-DF, optPBE-vdW-DF, optB88-vdW-DF, optB86b-vdW-DF) for the adsorption of a water monomer, small water clusters and a water monolayer on NaCl(001) and MgO(001). The resulting adsorption energies ( $E_{\text{ads}}$ ) and structures are compared with published experimental values and reference calculations made at the CCSD(T) and MP2 level of theory.

We observe that all vdW-functionals perform better than PBE with respect to the reference experimental and high-level theoretical results. In all cases, the dispersion contributions to the water-surface interactions are much larger than for the water–water interactions. All the functionals (vdW as well as PBE) display similar trends as the water coverage is increased from monomer to monolayer.

The optPBE-vdW-DF, optB88-vdW-DF, and optB86b-vdW-DF functionals [3] give the largest  $E_{\text{ads}}$  (and are similar among each other). The vdW-DF2 [2] and the very recent cx-vdW-DF functional [4] give quite similar  $E_{\text{ads}}$  for NaCl(001) but not for MgO(001). All the functionals predict similar water configurations on NaCl(001). However, for water on MgO(001), some of the functionals favor dissociation of water while others favor molecular adsorption.

- [1] M. Dion, H. Rydberg, E. Schröder, D.C. Langreth and B.I. Lundqvist, Phys.Rev. Lett.**92**,246401 (2004).
- [2] K. Lee, E.D. Murray, L. Kong, B.I. Lundqvist, D.C.Langreth, Phys. Rev. **B82**, 081101 (2010).
- [3] J. Klimeš, D.R. Bowler, A. Michaelides, Phys.: Cond. Matt. **22**, 022201 (2010); Phys.Rev. **B83**, 195131 (2011)
- [4] K.Berland, P.Hyldgaard, Phys. Rev. **B89**, 035412 (2014).

## Supercharged oxygen storage in nanoceria revisited using hybrid functionals

Dou Du, Kersti Hermansson and Peter Broqvist

Dept. of Chemistry – Ångström, Uppsala University, Box 538, SE-751 21, Uppsala, Sweden

e-mail: dou.du@kemi.uu.se

Ceria is a reducible oxide material used in oxidation catalysis as an oxygen storage material owing to its remarkable oxygen chemistry. Recent experiments have shown that the oxygen storage capacity (OSC) of nanoceria is size- [1] and shape-dependent [2], and a dramatically increased OSC has been measured for very small nanoparticles ( $d < 5$  nm) [1]. Based on theoretical calculations this effect has been suggested to originate from the stabilization of superoxo-ions at corner and edges of partially reduced ceria nanoparticles [3]. But, within the theoretical prediction, the superoxo-ions were found to bind too weakly to fit with experimental TPR-data [1].

Having in mind that the binding energies calculated in Ref. [3] suffer from limitations in the used density functional (PBE+U), we here set out to refine those predictions using a better, but at the same time more computationally costly, theory. Hybrid density functionals are known to overcome many of the known limitations of the semi-local ones. In this study, we have the screened Coulomb hybrid density functional HSE06, and also a modified HSE06 density functional where we have tuned the amount of exact exchange from the standard 25%. The modified HSE06 functional performs well for the electronic properties of bulk ceria but leads to a small overestimation of the O<sub>2</sub> binding energy. Thus, no single hybrid functional is yet capable of describing our system satisfactorily. However, by combining results using both functionals, we will be able to estimate binding energies for direct comparisons to experimental data.

The nanoparticles used in Ref. [3] are too large to be treated within the current computational setup. Instead, we use a series of small stoichiometric, reduced and supercharged clusters ( $n_{\text{Ce}} = 4-10$ ) which have in a previous study been showed to serve as good model structures for the larger ceria nanoparticles [4], i.e. showing similar oxygen chemistry. Our calculations show that while stability trends between the stoichiometric, reduced and supercharged clusters are similar using the hybrid and the PBE+U functionals, absolute numbers differ. The reduced clusters are significantly destabilized using the hybrid functional whereas the stoichiometric and supercharged clusters are merely unaffected. This effect results in a stronger O<sub>2</sub> adsorption energy for the supercharged clusters, stronger than in the corresponding PBE+U calculations. These results provide support for the interpretation that the superoxo-ions are responsible for the dramatically increased OSC seen in experiments [1].

[1] J. Xu et al., *Chem. Commun.*, 2010, **46**, 1887-1889.

[2] Z. Wu et al., *Langmuir*, 2010, **26**, 16595-16606.

[3] J. Kullgren, K. Hermansson, P. Broqvist, *J. Phys. Chem. Lett.*, 2013, **4**, 604-608.

[4] J. Kullgren, K. Hermansson, P. Broqvist, *Proc. of SPIE.*, 2013, **8822**, 88220D1-8.

## Half hydroxylation of the Ceria(111) surface at monolayer-water adsorption

Seif Alwan, Kersti Hermansson and Peter Broqvist

Dept. of Chemistry – Ångström, Uppsala University, Box 538, SE-751 21 Uppsala, Sweden.

Seif.Alwan@kemi.uu.se

The nature of the water-solid interface is an important factor governing the chemical reactivity of metal-oxides. For example, the degree of surface hydroxylation can strongly affect the adsorption of reactants in a catalytic process. In this study, we investigate the monolayer-water/CeO<sub>2</sub>(111) interface using density functional theory calculations. To accurately account for the important non-local correlation effects (vdW-interactions) present in water systems, we have tested a new branch of GGA density functionals which treats the non-local correlation self-consistently, collectively referred to as vdW-functionals [1].

We have studied monolayer water adsorption, which implies the adsorption of one H<sub>2</sub>O molecule over each Ce-ion on the CeO<sub>2</sub>(111) surface. A H<sub>2</sub>O molecule can either adsorb molecularly, or dissociatively (hydroxylating the surface). The most stable “water and hydroxylation” structural pattern, and the accompanying adsorption energy ( $E_{\text{ads}}$ ), has been determined for each degree of dissociation ( $Q$ ). In Fig.1, we give the results calculated with the optPBE-vdW density functional [2].

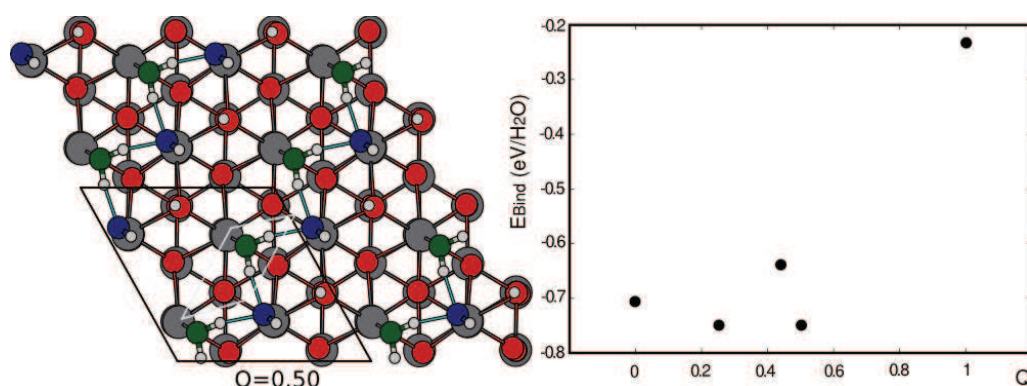


Figure 1: (Left) ball-and-stick models of the H<sub>2</sub>O monolayer structures with adsorption energies presented to the right. The  $Q$  values represent the degree of hydroxylation (=degree of dissociation). Grey balls are Ce, red, green and blue balls are oxygen in the ceria slab, adsorbed water molecule and dissociated water molecule, respectively. Small white balls are hydrogen.

Our results show that the different vdW-functionals tested all give the same trends (structure and stability vs.  $Q$ ), but differ in absolute adsorption energies. The repulsion between adjacent OH-groups on the surface limits the degree of hydroxylation of the ceria surface. As seen in the figure, it is therefore not favourable for the system to have hydroxylation degrees larger than 50%. We find that the structural pattern of the adsorbed water molecules and OH-groups determines the adsorption energy where the governing factor is the number of hydrogen bonds. In the most stable configurations, the adsorbed molecules are found in a row-wise pattern with alternating water molecules and OH-groups along the short diagonal of the cell, which maximises the number of hydrogen bonds and minimises the repulsion. In conclusion, water monolayer adsorption will never fully hydroxylate the CeO<sub>2</sub>(111) surface, instead, half hydroxylation is preferred.

[1] Dion M. *et al.* *Phys. Rev. Lett.* **92**, 246401 (2004)

[2] J. Klimeš, D. R. Bowler, and A. Michaelides, *J. Phys.: Cond. Matt.* **22**, 022201 (2010)

## A first-principles microkinetic model for CH<sub>4</sub> oxidation over PdO(101)

Maxime Van den Bossche<sup>1</sup>, Henrik Grönbeck<sup>1</sup>

<sup>1</sup>Competence Centre for Catalysis, Chalmers University of Technology, Sweden

E-mail: maxime.vandenbossche@chalmers.se

Transition metals for catalytic oxidation reactions often form oxides under environmental reaction conditions. One example is palladium, where the PdO(101) facet recently has been suggested to be the active phase for methane oxidation [1]. In this study, we have explored the mechanism for oxidation of methane to carbon dioxide and water over the PdO(101) surface. This was done using a first-principles kinetics approach, where the kinetic parameters are obtained by applying density functional and transition state theory.

The results of the kinetic modelling confirm the common assumption that the first dissociation reaction is the rate limiting step, where both energetic and entropic contributions create a large free energy barrier for this reaction (see Figure 1). The resulting CH<sub>3</sub> species is converted to CO<sub>2</sub> through a series of surface intermediates such as CH<sub>2</sub>, CH<sub>2</sub>O, CHO and CO. Incorporation of oxygen into the molecule occurs via a Mars – van Krevelen mechanism. The reduced oxide is then reoxidized by O<sub>2</sub> adsorption and dissociation. Additionally, adsorbed OH was found to be required to break down the CH<sub>3</sub> species on the surface, as this species reacts too slowly with the oxygen atoms of the oxide lattice (see Figure 1). Another finding is that, at low temperatures and in the presence of water vapour, the process is hindered by adsorbed H<sub>2</sub>O. This is in agreement with the negative reaction order in water pressure observed experimentally under those conditions. Lastly, comparison with the metallic Pd(100) surface shows that the reaction proceeds faster on the oxide surface, due to a lower electronic energy barrier for the initial dissociation.

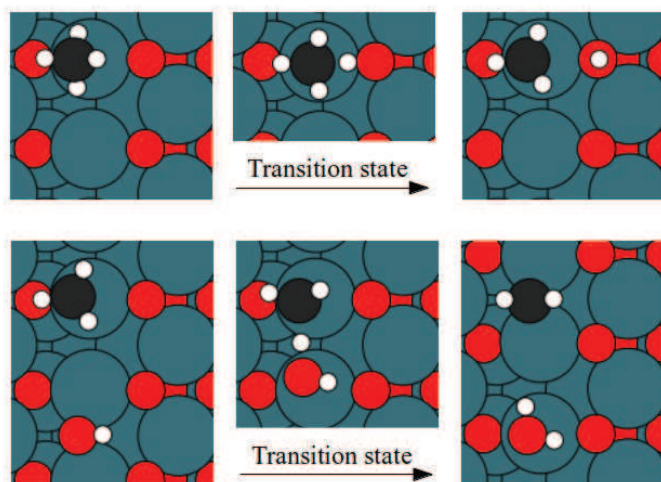


**Figure 1.** Illustrations of the first two steps in the oxidation of methane over the PdO(101) surface: the first (*top*) and second (*bottom*) C-H dissociation by reaction with an undercoordinated surface oxygen atom and adsorbed OH, respectively. Atomic color codes: Pd (blue), O (red), C (black), H (white).

[1] A. Hellman et al., J. Phys. Chem. Lett., **3**, 678 (2012).

## Metal-oxide sites for facile methane dissociation

Adriana Trincherro, Anders Hellman, Henrik Grönbeck  
Competence Centre for Catalysis, Chalmers University of Technology, Sweden  
E-mail: adriana.trincherro@chalmers.se

Experimental and theoretical studies have lately revealed that under-coordinated Pd-sites in the PdO(101) surface act as efficient centers for methane dissociation [1]. Here, the density functional theory is used to explore the underlying reason for the low activation energy by systematically investigating a range of hypothetical metal-oxides in the PdO structure [2].

The investigated metals are chosen to probe how the filling of the d-shell affects the methane dissociation energy. The adsorption ( $E_i$ ), final state ( $E_f$ ) and activation energies ( $E_a$ ) over the considered metal oxide surfaces are reported in Fig. 1. The present calculations suggest low activation energy for oxides with metals having open d-shells.

To further investigate the methane dissociation process, the one-dimensional potential energy surface (PES) of methane approaching PdO(101) and AgO(101) are shown in Fig. 2. The favorable catalytic property is traced to reduced Pauli repulsion between methane and the surface in the case of PdO(101). The results suggest that the ability to dissociate methane is a local atomic property and provide handles for rational design of new catalytic formulations.

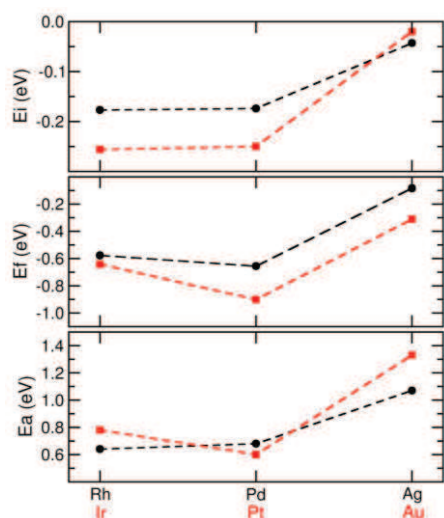


**Fig. 1.** Energetic properties of methane adsorption and dissociation over different metal oxides.  $E_i$  is adsorption energy of molecular methane,  $E_f$  is adsorption energy of dissociated methane, and  $E_a$  is activation energy.

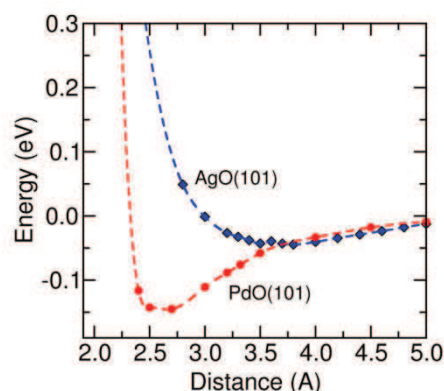


**Fig. 2.** Potential energy surface for methane approaching PdO(101) and AgO(101).

[1] A. Hellman et al., J. Phys. Chem. Lett., **3**, 678, (2012).

[2] A. Trincherro, A. Hellman and H. Grönbeck, Phys. Status Solidi RRL **8**, 605 (2014).

## Ethylene hydrogenation over transition metal surfaces: What governs the reactivity?

Christopher Heard, Samira Siahrostami and Henrik Grönbeck

Department of Applied Physics and Competence Centre for Catalysis, Chalmers University of Technology, Göteborg, Sweden

[christopher.heard@chalmers.se](mailto:christopher.heard@chalmers.se)

Selective hydrogenation of unsaturated hydrocarbons is an important catalytic process to improve the stability of biologically derived fuel feedstocks. To isolate and, ultimately to manipulate the governing parameters in such reactions, a detailed atomistic understanding is required of important reaction steps together with their sensitivity to reaction conditions, such as temperature, partial pressures and catalyst identity. However, before treating complex unsaturated aldehydes, we consider hydrogenation of alkenes by investigating archetypal ethylene hydrogenation over transition metal surfaces.

We apply plane wave density functional theory methods[1-3] to the elucidation of relevant energetics, in order to correlate the important parameters for activity. Accurate activation energies, Arrhenius prefactors and adsorption energies are calculated, which when coupled to a microkinetic model, allow us to explore the equilibrium properties of the system as a function of temperature and reactant coverage.

To this end, we have explored the relevant elementary steps for a large set of late transition metal (Fe, Co, Ni, Cu, Ru, Rh, Pd, Ag, Os, Ir, Pt and Au) surfaces. Ethylene and hydrogen adsorption has been investigated at different coverages so as to systematically determine the role of hydrogen loading, ethylene coverage and catalyst identity for the two-step hydrogenation of ethylene to ethane.

The preference of binding mode for ethylene is found to vary significantly between metals, which impacts upon the activation barrier to hydrogenation, while the coverage of ethylene does not exhibit a noticeable effect. Hydrogen loading appears to control ethylene binding, both energetically and by structurally distorting the substrate, promoting the hydrogenation reaction. The partial pressures of reactants are predicted to play a significant role for the reactivity. Overall, the hydrogenation of ethylene is found to be a complex process, subtly affected by various reaction conditions.

[1] G. Kresse and J. Hafner. *Phys. Rev. B*, **47**:558, (1993).

[2] G. Kresse, and J. Joubert, *Phys. Rev. B* **59**, 1758 (1999).

[3] P.E. Blöchl, *Phys. Rev. B* **50**, 17953 (1994).

## Oxygen-Isotopes Labeled Titanium Dioxide

**Ladislav Kavan**, Svatopluk Civis, Martin Ferus, Barbora Laskova, Marketa Zukalova  
J. Heyrovsky Institute of Physical Chemistry, Dolejskova 3, CZ-18223 Prague 8  
kavan@jh-inst.cas.cz

Titania samples labeled by oxygen isotopes 16, 17, 18 were synthesized, each in anatase and rutile forms, and characterized by Raman spectroscopy[1,2] and by Raman spectroelectrochemistry of Li-insertion.[3,4] The experimental and theoretical (DFT) Raman frequencies allowed addressing the open questions about the second-order Raman scattering in rutile, and the analysis of overlapping features in the anatase spectrum.[2] The  $^{17}\text{O}$  atoms in the anatase crystal lattice caused the EPR line broadening, which was interpreted as a superposition of signals attributed to Ti(III) with axial symmetry arising from an interaction with an  $^{17}\text{O}$  nucleus[5]. The reactions at the interface of titania and gaseous reactants were investigated by high-resolution FTIR spectroscopy in dark and upon UV-excitation[6-9]. The vacuum-annealed  $\text{Ti}^{18}\text{O}_2$  exhibited high oxygen-exchange activity with  $\text{C}^{16}\text{O}_2$ . The product of oxygen isotope exchange at the  $\text{Ti}^{18}\text{O}_2(\text{s})/\text{C}^{16}\text{O}_2(\text{g})$  interface was  $\text{C}^{18}\text{O}_2$  with small amount of  $\text{C}^{16}\text{O}^{18}\text{O}$ . The  $^{18}\text{O}-\text{C}-^{16}\text{O}$  acts as an intermediate in the mixture and its concentration remains almost constant. The UV photocatalytic formation of methane, acetylene and  $\text{C}^{16}\text{O}$  was studied at the  $\text{Ti}^{18}\text{O}_2$  surface. The production of ‘solar fuels’ such as methane and acetylene is promoted by the co-adsorption of HCl.[6] Compatible data were acquired for photocatalytic and catalytic processes of formic acid[7] and COS[8] at the  $\text{Ti}^{18}\text{O}_2$  surface. The disproportion of OCS to  $\text{CO}_2$  and  $\text{CS}_2$  is catalyzed by  $\text{Ti}^{3+}$  centers on the partly doped titania.[8] Formic acid  $\text{HC}^{16}\text{O}^{16}\text{OH}$  did not exchange oxygen with titania during adsorption and decomposition processes towards  $\text{CO}_2$ ,  $\text{CO}$ , and  $\text{H}_2\text{O}$ , but blocked active sites and thereby inhibited the exchange between  $\text{CO}_2$  and  $\text{Ti}^{18}\text{O}_2$ .

Acknowledgement: This work was supported by the Grant Agency of the Czech Republic (contract No. 13-07724S) by the COST Action CM1104

- [1] L. Kavan, M. Zukalova, M. Ferus, J. Kürti, J. Koltai and S. Civis, *Phys. Chem. Chem. Phys.*, **13**, 11583 (2011).
- [2] O. Frank, M. Zukalova, B. Laskova, J. Kürti, J. Koltai and L. Kavan, *Phys. Chem. Chem. Phys.*, **14**, 14567 (2012).
- [3] L. Kavan, *J. Solid State Electrochem.*, **18**, 2297 (2014).
- [4] B. Laskova, O. Frank, M. Zukalova, M. Bousa, M. Dracinsky and L. Kavan, *Chem. Mater.*, **25**, 3710 (2013).
- [5] V. Brezova, Z. Barbierikova, M. Zukalova, D. Dvoranova and L. Kavan, *Catal. Today*, **230**, 112 (2014).
- [6] S. Civis, M. Ferus, P. Kubat, M. Zukalova and L. Kavan, *J. Phys. Chem. C*, **115**, 11156 (2011).
- [7] S. Civis, M. Ferus, M. Zukalova, P. Kubat and L. Kavan, *J. Phys. Chem. C*, **116**, 11200 (2012).
- [8] S. Civis, M. Ferus, J. E. Sponer, J. Sponer, L. Kavan and M. Zukalova, *Chem. Commun.*, **50**, 7712 (2014).
- [9] S. Civis, M. Ferus, M. Zukalova, L. Kavan and Z. Zelinger, *Opt. Mater.*, **36**, 159 (2014).

## Magnetic interactions, polarity effects and phase transitions in low dimensional covalent systems: Transition Metal Dichalcogenides' nanoribbons.

Francisco Guller<sup>1,2</sup>, Verónica Vildosola<sup>1,2</sup>, Ana María Llois<sup>1,2,3</sup>, Jacek Goniakowski<sup>4,5</sup> and Claudine Noguera<sup>4,5</sup>

<sup>1</sup>Condensed Matter Department, GAIyAN-CNEA, Buenos Aires

<sup>2</sup>Laboratorio Internacional Franco-Argentino en Nanociencias (LIFAN)

<sup>3</sup>Department of Physics JJ Giambiag, FCEyN, University of Buenos Aires.

<sup>4</sup> CNRS, Institut des Nanosciences de Paris, UMR 7588, 4 place Jussieu, 75252 Paris cedex 05, France

<sup>5</sup> Sorbonne Universit'es, UPMC Univ Paris 06, UMR 7588, INSP, F-75005 Paris, France

**E-mail: llois@cnea.gov.ar**

In the year 2004, Novoselov *et al* successfully isolated not only graphene but also layers of some transition metal dichalcogenides (TMDs) [1].

TMDs are well known for their laminar structure. They consist, in the bulk, of three atoms thick monolayers (trilayers) held together through weak Van der Waals interactions. Each monolayer consists of a plane of transition metal atoms sandwiched by two planes of chalcogen ones. There is a strong molecular bonding between metal and chalcogen atoms within the monolayers, which present an ionic as well as covalent character. Many TMDs have been thoroughly studied in the last 30 years due to their many potential applications. In this talk I am going to address interesting effects switched on by low dimensionality and edge effects in both, semiconducting as well as metallic TMD's nanoribbons.

Starting with semiconducting TMD's nanostructures we focus in particular on MoS<sub>2</sub> and WS<sub>2</sub>, which have gained increasing importance in a number of recent technological applications. Relying on first principles simulations, we predict a metal-to-semiconductor transition for zigzag ribbons of small width and monolayer thickness due to the structural and electronic flexibility associated to polarity effects. This finding opens the possibility for controlling the ribbon type during synthesis in compounds of major technological importance.

We finish by focusing on NbS<sub>2</sub>, a metallic dichalcogenide, whose monolayers belong to the 1H polytype. Bulk NbS<sub>2</sub> is non magnetic. It presents neither charge nor spin density waves, at variance with other related dichalcogenides, such as bulk NbSe<sub>2</sub>, which develops charge density waves below 40 K due to 2D Fermi surface instability (nesting).

We have shown that zigzag nanoribbons cut out from the 1H NbS<sub>2</sub> monolayers present a magnetic ground state triggered by the zigzag edges and that this ground state is actually a spin density wave. In this presentation, the origin and features of this ground state are going to be traced back, analysed and compared with the cases of NbSe<sub>2</sub>, TaS<sub>2</sub> and the semiconducting MoS<sub>2</sub>.

[1] K.S. Novoselov et al, PNAS 102(2005), 10451

# Ordering of oxygen vacancies and charge localization in reduced bulk ceria

G. E. Murgida, M. V. Ganduglia-Pirovano<sup>1</sup>, V. Ferrari and A.M. Llois

Centro Atómico Constituyentes, GHyANN, CNEA, and CONICET, Buenos Aires, Argentina

<sup>1</sup>Instituto de Catálisis y Petroleoquímica - CSIC, Madrid, Spain

murgida@tandar.cnea.gov.ar

The importance of ceria ( $\text{CeO}_2$ ) in many applications originates from the ease of oxygen vacancy formation and healing. The ordering of vacancies and the whereabouts of the excess charge in bulk  $\text{CeO}_2$  are of no less significance than at ceria surfaces, but they have not received the same attention. In this work, the formation of neutral oxygen vacancies in bulk  $\text{CeO}_2$  is investigated using density-functional theory (DFT) in the DFT+ $U$  ( $U$  is an effective onsite Coulomb interaction parameter) approach for a broad range of vacancy concentrations ( $1/64 \leq \Theta \leq 1/4$ ). We find that the excess charge prefers to be localized in cation sites such that the mean  $\text{Ce}^{3+}$  coordination number is maximized, and if nearest-neighbor cation sites are reduced, they rather be nonuniformly distributed [1]. Furthermore, we show that a vacancy repels other vacancies from its nearest-neighbor shell and that the [110] and [111] directions are possible directions for clustering of second- and third-neighbor vacancies, respectively. Vacancies prefer not to share cations. The results are discussed in a simple physical picture which enables the separation of the different contributions to the averaged vacancy formation energy. We also consider cells with fluorite structure and same stoichiometries as in existing bulk phases, i.e.,  $\text{Ce}_{11}\text{O}_{20}$  ( $\Theta = 1/11$ ),  $\text{Ce}_7\text{O}_{12}$  ( $\Theta = 1/7$ ), and  $\text{Ce}_2\text{O}_3$  ( $\Theta = 1/4$ ), as well as the corresponding real structures. We find that the vacancy ordering and the location of the excess electrons are consistent with the results for single-phase reduced  $\text{CeO}_2$ , but the  $\text{Ce}_{11}\text{O}_{20}$ ,  $\text{Ce}_7\text{O}_{12}$ , and  $\text{Ce}_2\text{O}_3$  structures are substantially more stable. The stability of these phases as a function of pressure and temperature is discussed. Vacancy-induced lattice relaxation effects are crucial for the interpretation of the results.

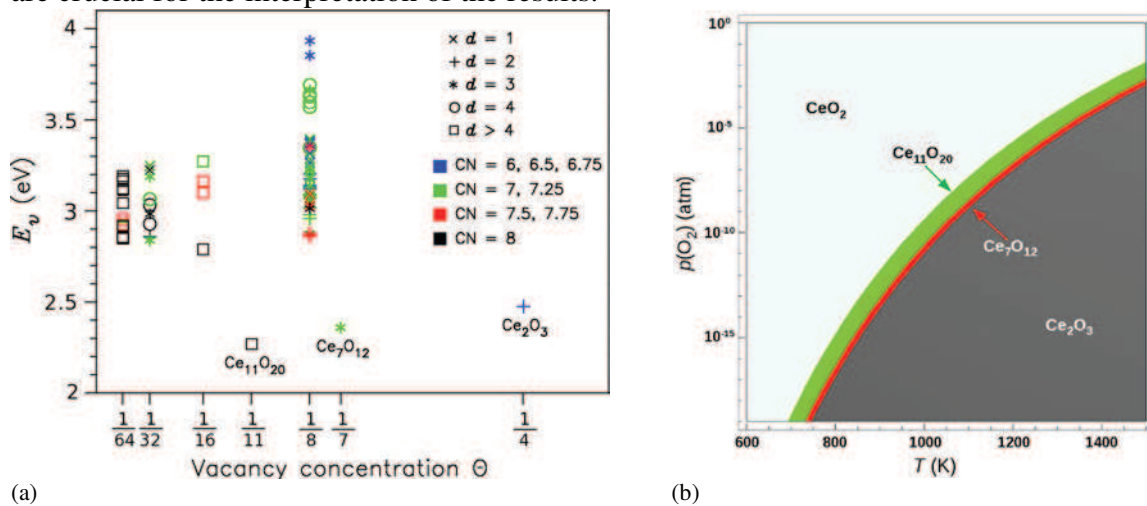


Fig. 1(a) Averaged vacancy formation energies as a function of vacancy concentration for all structures with fluorite unit cell considered. The mean coordination number (CN) of  $\text{Ce}^{3+}$  ions and the closest distance between vacancies ( $d$ ) are indicated using color and symbols, respectively. (b) Phase diagram showing the stability regions for bulk  $\text{CeO}_2$  and the reduced  $\text{Ce}_{11}\text{O}_{20}$ ,  $\text{Ce}_7\text{O}_{12}$ , and (C-type)  $\text{Ce}_2\text{O}_3$  true bulk phases.

[1] G. E. Murgida, M. V. Ganduglia Pirovano, V. Ferrari, and A. M. Llois, Phys. Rev. B (2014); in press

## SERS effect of dopamine adsorbed on TiO<sub>2</sub> nanoparticles

I. Urdaneta<sup>1,2</sup>, E. Luppi<sup>1</sup>, D. Finkelstein-Shapiro<sup>1,3</sup>, A. Keller<sup>2</sup>, V. Mujica<sup>3</sup>, M. Calatayud<sup>1</sup>

<sup>1</sup> Université Pierre et Marie Curie and CNRS, Paris, France

<sup>2</sup> ISMO Univ. Paris Sud, France

<sup>3</sup> Arizona State University, USA

calatayu@lct.jussieu.fr

Recently it has been observed an important increase of the emitted Raman signal upon adsorption of dopamine on titania nanoparticles with respect to the bare molecule [1]. This phenomenon known as Surface Enhanced Raman Scattering (SERS) is quite common for metallic supports, but is by far less characterized for semiconducting materials. The mechanism explaining the enhancement of the Raman signal in the dopamine-TiO<sub>2</sub> system has been postulated as a charge transfer one, involving an electron charge transfer from the molecule to the nanoparticle. The goal of the present work is to investigate the interface dopamine-TiO<sub>2</sub> on an atomic level by means of Density Functional Theory (DFT) periodic calculations in order to elucidate the features connecting geometrical and electronic structures.

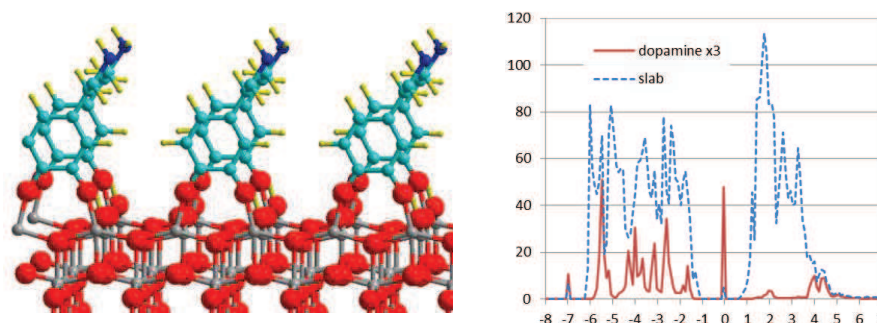


Fig. 1: left, periodic model for dopamine adsorbed on a (001) TiO<sub>2</sub> anatase slab; right, density of states projected on the molecule and on the slab (arbitrary units vs eV) E<sub>F</sub>=0 eV.

Dopamine adsorbs by an acid/base mechanism with the surface, transferring the two H<sup>+</sup> to surface oxygen sites, and forming two Ti-O bonds [2]. The calculated adsorption energy is exothermic by more than 1 eV and depends on the anatase surface exposed. The corresponding electronic structure presents the HOMO states located at the dopamine and the LUMO states at the surface Ti sites. This picture is coherent with a charge transfer from the molecule to the nanoparticle and would support the CT transfer mechanism proposed in the literature to explain the SERS effect [3].

[1] A. Musumeci et al. J. Am. Chem. Soc, 131 6040 (2009)

[2] I. Urdaneta et al. J. Phys. Chem. C 118 20688 (2014)

[3] I. Urdaneta et al. J. Phys. Chem. A 118 1196 (2014)

## **Metal oxide catalysed selective oxidations**

**N. Raveendran Shiju**

Van 't Hoff Institute for Molecular Sciences, University of Amsterdam, The Netherlands  
E-mail: n.r.shiju@uva.nl

Transition metal oxides are used as catalysts in many commercially important reactions. Structural features strongly influence the catalytic performance. In this talk, I will present our results on selective oxidation of lower alkanes such as propane and ethane and oxidation of biomass derivatives. In the former, we observed strong influence of basal planes of mixed oxides in determining the selectivity of oxidation products. In the latter, we tested various solid catalysts for catalytic oxidative dehydrogenation of ethyl lactate and found that simple and inexpensive  $\text{TiO}_2$  efficiently catalyses this reaction under mild conditions. Furthermore, molecular oxygen was used as the terminal oxidant. This reaction runs well also using inexpensive commercial solvent mixtures. Both the desired reaction and the by-products formation follow a free-radical mechanism. Addition of activated carbon, a solid radical scavenger, enhanced the product selectivity without affecting activity.

## Aspects of morphology, molecular structure, O-lattice order and defect-induced vibrational properties of CeO<sub>2</sub>/ZrO<sub>2</sub> based materials probed by *in situ* Raman spectroscopy.

Antonios Tribalis and Soghomon Boghosian

Department of Chemical Engineering, University of Patras and FORTH/ICE-HT,  
Patras, Greece

[bogosian@chemeng.upatras.gr](mailto:bogosian@chemeng.upatras.gr)

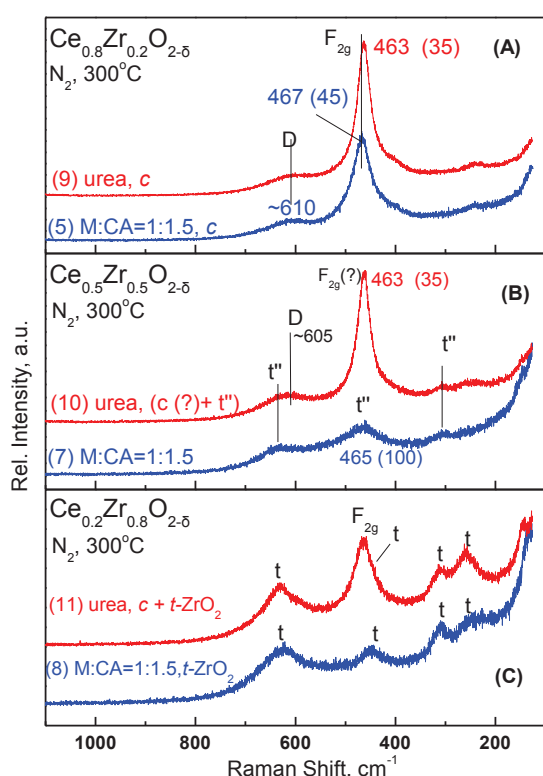


**Figure .** *In situ* Raman spectra of Ce<sub>1-x</sub>Zr<sub>x</sub>O<sub>2-δ</sub> materials synthesized by the citrate sol-gel and urea methods at 300°C under flowing N<sub>2</sub>(g). D: defect band; t: band due to *t*-ZrO<sub>2</sub>; t'': mixed (Ce,Zr)O<sub>2</sub> phase. Laser wavelength, 491.5 nm; laser power, 40 mW.

The citrate sol-gel and urea-precipitation based methods have been used to prepare Ce<sub>1-x</sub>Zr<sub>x</sub>O<sub>2-δ</sub> (x=0.2, 0.35, 0.5 and 0.8) materials and *in situ* Raman spectroscopy has been applied in the temperature range 300-450°C under inert [N<sub>2</sub>(g)] and reducing [4.5%H<sub>2</sub>/N<sub>2</sub>(g)] atmospheres with a view to: a) identify the (micro)phases present; b) assess the extent of structural defects and O vacancies in the O-sublattice; and c) examine the response of the materials under H<sub>2</sub>(g) atmosphere at 450°C. The effect of the calcination temperature (1000°C vs 800°C) as well as the effect of 5 atom% doping with rare earth oxides (RE<sub>2</sub>O<sub>3</sub>, RE= La, Pr, Y, Nd) at fixed material composition, (Ce<sub>0.8</sub>Zr<sub>0.15</sub>RE<sub>0.05</sub>O<sub>2-δ</sub>, *i.e.*: x = 0.2) is also examined.

As shown in Fig. 2A, one single distorted cubic (*c*) phase is evidenced for Ce<sub>0.8</sub>Zr<sub>0.2</sub>O<sub>2-δ</sub> (M:CA, urea), suggesting the incorporation of Zr<sup>4+</sup> ions in the CeO<sub>2</sub> lattice with some structural perturbations. In Fig. 2B (x = 0.5, Ce<sub>0.8</sub>Zr<sub>0.2</sub>O<sub>2-δ</sub>) the characteristics of the t'' phase are evidenced for the material prepared by the citrate sol-gel method, whereas the mixed oxide prepared by the urea-precipitation method exhibits features

suggesting the co-occurrence of both a tetragonal (*t*-ZrO<sub>2</sub>?) and a cubic (*c*) φάση. Doping with rare earth oxides creates additional O vacancies (to compensate for the effective negative charge induced by the Ce<sup>4+</sup> ↔ RE<sup>3+</sup> substitution). Treatment with hydrogen containing gas is shown to result in changes that are interpreted to indicate an increase in the O vacancies. A procedure based on reduction of normalized spectra that disentangles the inherent structural vibrational effects/properties from thermal (temperature induced/non-structural) effects is deployed for studying the temperature dependence of the vibrational properties.

**Acknowledgment.** Research supported by the RPF/THEPIS program (TECHNOLOGIA/THEPIS/0311(BE)/33).

# Polaronic trapping of positrons and holes on acceptor sites in ZnO and GaN

Ilja Makkonen and Filip Tuomisto

Department of Applied Physics, Aalto University School of Science, Espoo, Finland

Positron annihilation spectroscopy is a very powerful technique for the detection, identification and quantification of vacancy-type defects in semiconductors and oxides [1]. Recently we have also identified the substitutional Li on Zn site ( $\text{Li}_{\text{Zn}}$ ) in ZnO, a defect involving only very little open volume compared to a Zn vacancy, using positron techniques [2]. The characteristic lifetime of  $\text{Li}_{\text{Zn}}$  is only a few picoseconds above the lifetime of positrons in the perfect bulk, which makes the component difficult to resolve. On the other hand, Be on Ga site in GaN appears to be a similar positron trap [3]. These very same defects have been suggested to trap holes in polaronic states on anion sites surrounding the dopant atoms [4]. We model these trapped positrons and holes, compare them to one another, and discuss the physical origins of their trapping. As an example, Fig. 1 displays isosurfaces of localized positron and hole densities around a negative  $\text{Li}_{\text{Zn}}$  in ZnO. Comparison is made with existing experimental positron data.

[1] F. Tuomisto and I. Makkonen, *Rev. Mod. Phys.* **85**, 1583 (2013).

[2] K. M. Johansen, A. Zubiaga, I. Makkonen, F. Tuomisto, P. T. Neuvonen, K. E. Knutsen, E. V. Monakhov, A. Yu. Kuznetsov, and B. G. Svensson, *Phys. Rev. B* **83**, 245208 (2011).

[3] F. Tuomisto, I. Makkonen et al, unpublished.

[4] S. Lany and A. Zunger, *Phys. Rev. B* **80**, 085202 (2009); *Appl. Phys. Lett.* **96**, 142114 (2010).

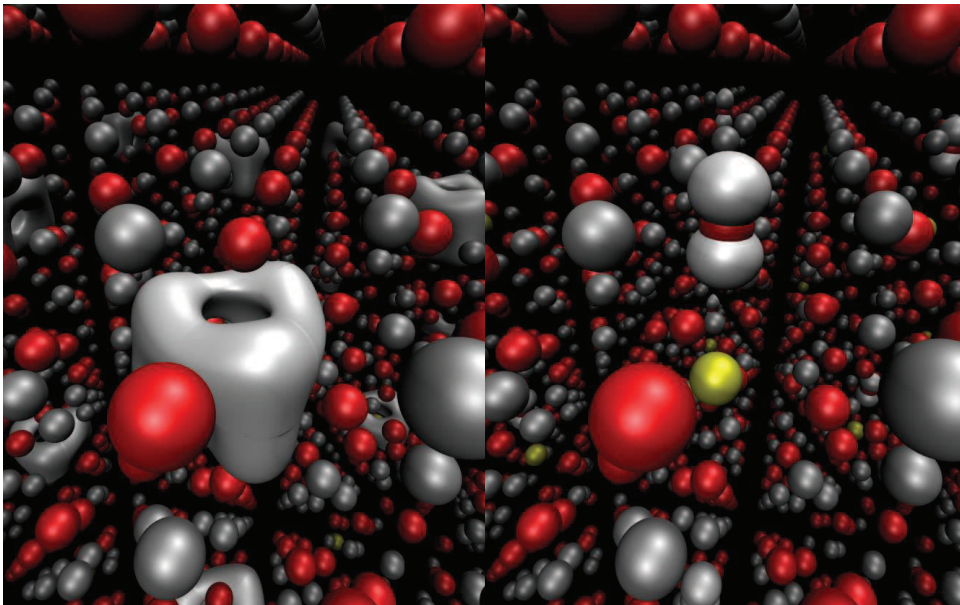


Fig. 1: A positron density isosurface for a positron trapped around a negative  $\text{Li}_{\text{Zn}}$  in ZnO (left), and a spin density isosurface of a hole trapped on a  $p$  orbital of a neighboring O site (right).

## MWCNT@Pd/TiO<sub>2</sub> hybrids as efficient catalysts for ethanol and glycerol photoreforming

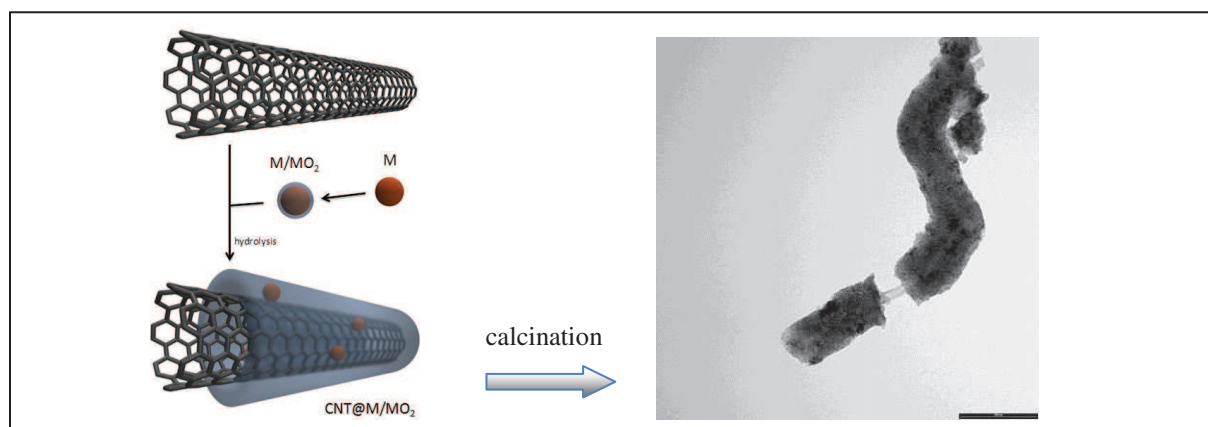
Michele Melchionna, Alessandro Beltram, Maurizio Prato, Paolo Fornasiero

Dept Chemical and Pharmaceutical Sciences, INSTM, ICCOM-CNR, University of Trieste  
[pfornasiero@units.it](mailto:pfornasiero@units.it)

Clean and efficient hydrogen production is of interest because hydrogen is envisioned as the fuel of the future. In particular, hydrogen production from biomass-derived alcohols has attracted great interest because of the potential application in fuel cells.

A hierarchical synthetic approach has been used to prepare nano hybrids in which appropriately functionalized multiwalled carbon nanotubes (MWCNTs) were embedded inside mesoporous layers of TiO<sub>2</sub>, which in turn contained dispersed metal nanoparticles (Pd) [1].

The synthesis can be modulated in order to vary the composition and microscopy characterization displays that by fine-tuning the reaction conditions, it is possible to obtain uniform coverage of the MWCNTs with layers of the inorganic core-shell Pd@TiO<sub>2</sub> system. After calcination, the presence of nanotubes induces a specific anatase crystal phase of the TiO<sub>2</sub> and we show that the as-assembled catalysts possess a pronounced activity for photocatalytic hydrogen evolution from biomass-derived products such as ethanol and glycerol.



- [1] M. Cargnello, M. Grzelczak, B. Rodríguez-González, Z. Syrgiannis, K. Bakhmutsky, V. La Parola, L. M. Liz-Marzán, R. J. Gorte, M. Prato and P. Fornasiero, *J. Am. Chem. Soc.*, **134**, 11760 (2012).

## Methanol partial oxidation over $\text{PtO}_x$ , $\text{Pt/CeO}_2$ , and $\text{CeO}_2/\text{Pt}$ catalysts

Andrii Rednyk, **Anna Ostroverkh**<sup>1</sup>, Viktor Johánek, Vladimír Matolín, Peter Kúš

Department of Surface and Plasma Science, Charles University in Prague

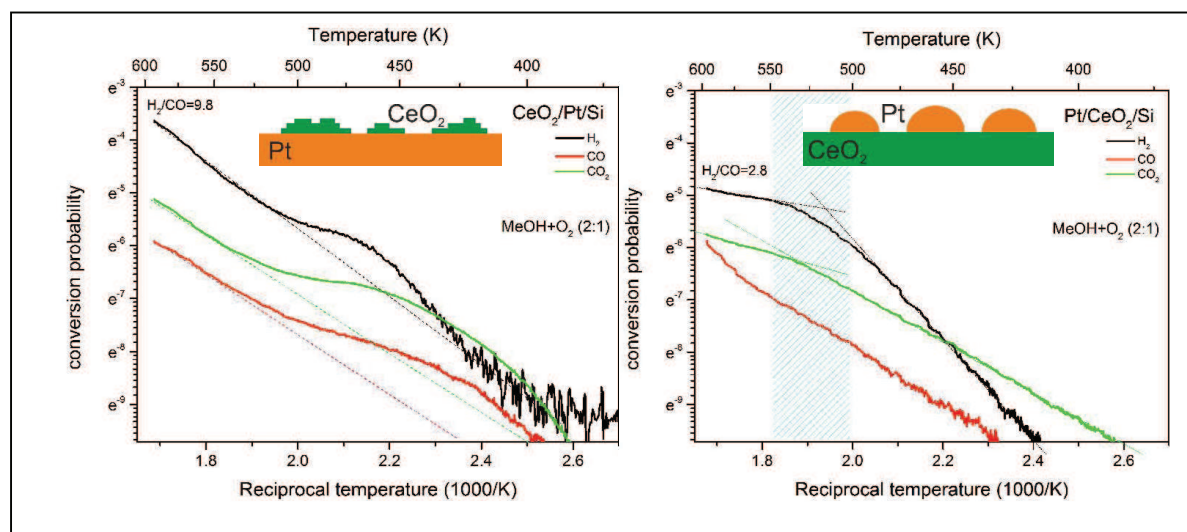
<sup>1</sup> Department of adsorption phenomena Institute of Physics of NAS of Ukraine

e-mail: ostroverkh84@gmail.com

Production of hydrogen by partial oxidation of methanol (POM), has been studied in a microreactor system over a series of  $\text{PtO}_x$ ,  $\text{Pt/CeO}_2$ , and inverse  $\text{CeO}_2/\text{Pt}$  model catalysts. All the catalysts were prepared by reactive rf-magnetron sputtering in oxygen as the most efficient method for the fabrication of nanostructured materials due to its accurate control over the thin film chemistry, thickness, and morphology of deposited layers. [1]. Catalysis by platinum oxide is related to Pt-ceria via the the supreme redox capability of ceria which can lead to co-existence of metallic and cationic platinum phases.

Temperature programmed reaction (TPR) was used to measure absolute reactivity and selectivity of hydrogen and carbon monoxide/dioxide production on a reference  $\text{PtO}_x$  catalysts at different ratios of  $\text{O}_2$  and methanol. The observation of significant amounts of water and increase of selectivity for carbon monoxide at  $\text{O}_2/\text{MeOH}$  more than 0.3 indicates that parallel or consecutive reactions other than POM are involved.

It was found, that ceria actively participates in surface reactions via spill-over of surface species between Pt and ceria [2]. In Fig. 2a TPR of POM (stoichiometric ratio of reactants  $\text{O}_2/\text{MeOH}=0.5$ ) on Pt nanoparticles (1 nm average thickness) supported on 10 nm thin film of  $\text{CeO}_2$  is presented. We found the loss of hydrogen production capability above ca. 500 K which reveals instability of the catalyst, probably due to encapsulation of Pt by ceria. In Fig. 2b the TPR of methanol oxidation was performed under identical conditions on an "inverse catalyst" comprising 10 nm thin film of Pt covered by ceria nanoparticles (0.5 nm average thickness). It exhibits not only very stable reactivity (with arrhenian character) at temperatures up to at least 600K but also higher absolute methanol to hydrogen turnover frequency in both low and high temperatures compared to the  $\text{Pt/CeO}_2$  system and, perhaps even more importantly, lower ratio of undesired CO to  $\text{H}_2$ .



[1] M. Dubau et al., ACS Appl. Mater. Interfaces **6**, 1213 (2014).

[2] Y. Lykhach et al., Phys. Chem., **13**, 253 (2011).

## Cation vacancies and electrical compensation in Sb-doped thin-film SnO<sub>2</sub> and ZnO

V. Prozheeva, E. Korhonen, F. Tuomisto, O. Bierwagen<sup>1,4</sup>, J. S. Speck<sup>1</sup>, M. E. White<sup>1</sup>, Z. Galazka<sup>2</sup>, H. Liu<sup>3</sup>, N. Izyumskaya<sup>3</sup>, V. Avrutin<sup>3</sup>, Ü. Özgür<sup>3</sup> and H. Morkoç<sup>3</sup>

Department of Applied Physics, Aalto University, 00076 Aalto, Finland

<sup>1</sup> Materials department, University of California, Santa Barbara, 93106 California, USA

<sup>2</sup> Leibniz Institute for Crystal Growth, 12489 Berlin, Germany

<sup>3</sup> Department of Electrical and Computer Engineering, Virginia Commonwealth University, Richmond, Virginia 23284, USA

<sup>4</sup> Paul-Drude-Institut, Hausvogteiplatz 5-7, 10117 Berlin, Germany

vera.prozheeva@aalto.fi

SnO<sub>2</sub> and ZnO are promising transparent semiconducting oxides (TCOs) sharing the lack of reliable *p*-doping. Direct wide bandgap (3.3 eV for ZnO and 3.6 eV for SnO<sub>2</sub>) and optical properties draw special interest as these TCOs find their application in photovoltaics and optoelectronics [1]. Both materials tend to favour *n*-type conduction both intrinsically and extrinsically. Sb-doping is supposed to lead to both *p*- and *n*-type conductivity in ZnO [2], and in SnO<sub>2</sub> it acts as efficient shallow donor [3].

The samples include series of both SnO<sub>2</sub> and ZnO thin-film Sb-doped layers grown by PAMBE on sapphire substrates [2, 3]. In order to investigate the effectiveness of doping and also its effect on the growth quality, the Sb-doping concentration was varied between samples. Vacancy type defects were identified using positron annihilation spectroscopy (PAS) in conventional Doppler mode.

In SnO<sub>2</sub>, the effect on the defect concentration is surprising, as low ( $< 10^{19} \text{ cm}^{-3}$ ) Sb-doping leads to a higher defect density than higher concentrations, which is contradictory to typical thermodynamic trends. In ZnO, the samples with the highest Sb concentrations are dominated by  $V_{\text{Zn}}$  and have the lowest electron concentrations. In samples with lower [Sb], a varying amount of vacancy clusters are detected in addition to  $V_{\text{Zn}}$ , indicating competition between the two types of defects. In both materials, Sb-doping seems to improve to some extent the quality of epitaxial growth. The mechanisms of electrical compensation in these two materials are discussed in the light of vacancy identities and concentrations.

[1] M. Batzill, U. Diebold, Prog. Surf. Sci., **79**, 47 (2005).

[2] H. Y. Liu et al., J. Appl. Phys., **112**, 103713 (2012).

[3] M. E. White et al., J. Appl. Phys., **106**, 093704 (2009).

## Comparing the Quasiparticle Level Alignment for the TiO<sub>2</sub>(110)–H<sub>2</sub>O and TiO<sub>2</sub>(110) – CH<sub>3</sub>OH Photocatalytic Interfaces

Anna Paola Migani

ICN2—Institut Català de Nanociència i Nanotecnologia and CSIC—Consejo Superior de Investigaciones Científicas, ICN2 Building, Campus UAB, E-08193 Bellaterra (Barcelona), Spain

Heterogeneous photocatalysis has emerged as a research area that can offer feasible solutions to energy and environmental issues. Two of the most important applications of photocatalysis are water splitting, and the purification of air and water. In this context, TiO<sub>2</sub> has emerged as the most commonly studied material due to its long-term photostability. This allows it to be used in many different applications outside the laboratory.

The electronic energy level alignment between the rutile TiO<sub>2</sub>(110) surface and an adsorbed molecular (H<sub>2</sub>O or CH<sub>3</sub>OH) layer prior to irradiation is a fundamental quantity. It is required to achieve a complete description of the photocatalysis of the molecular layer assisted by the rutile TiO<sub>2</sub>(110) surface.

Standard density functional theory (DFT)-based methods have proven unable to provide a quantitative description of this interfacial level alignment. This requires a proper treatment of the anisotropic screening, necessitating the use of quasiparticle (QP) techniques.<sup>1</sup>

I will provide results on the QP electronic energy level alignment prior to irradiation at the TiO<sub>2</sub>(110)–H<sub>2</sub>O<sup>2</sup> and the TiO<sub>2</sub>(110) –CH<sub>3</sub>OH<sup>3,4</sup> interfaces obtained with G<sub>0</sub>W<sub>0</sub> calculations. The accurate QP level alignment is directly compared to the interfacial level alignment probed by metastable impact electron spectroscopy (MIES), ultraviolet photoelectron spectroscopy (UPS), and two-photon photoemission (2PP) spectroscopy. In particular, a comparison between the QP level alignment between the highest occupied and lowest unoccupied molecular levels of H<sub>2</sub>O and those of CH<sub>3</sub>OH adsorbed on the TiO<sub>2</sub>(110) surface will be provided.

---

<sup>1</sup> **Quasiparticle level alignment for photocatalytic interfaces**, Migani, A.; Mowbray, D.J.; Zhao, J.; Petek, H.; Rubio, A., *Journal of Chemical Theory and Computation*, **10** (5), 2103–2113 (2014)

<sup>2</sup> **Quasiparticle interfacial level alignment of highly hybridized frontier levels: H<sub>2</sub>O on TiO<sub>2</sub>(110)**, Migani, A.; Mowbray, D.J.; Zhao, J.; Petek, H.; Rubio, A., *submitted*.

<sup>3</sup> **Level alignment of a prototypical photocatalytic system: Methanol on TiO<sub>2</sub>(110)**, Migani, A.; Mowbray, D.J.; Iacomino, A.; Zhao, J.; Petek, H.; Rubio, A., *Journal of the American Chemical Society*, **135**, 11429–11432 (2013)

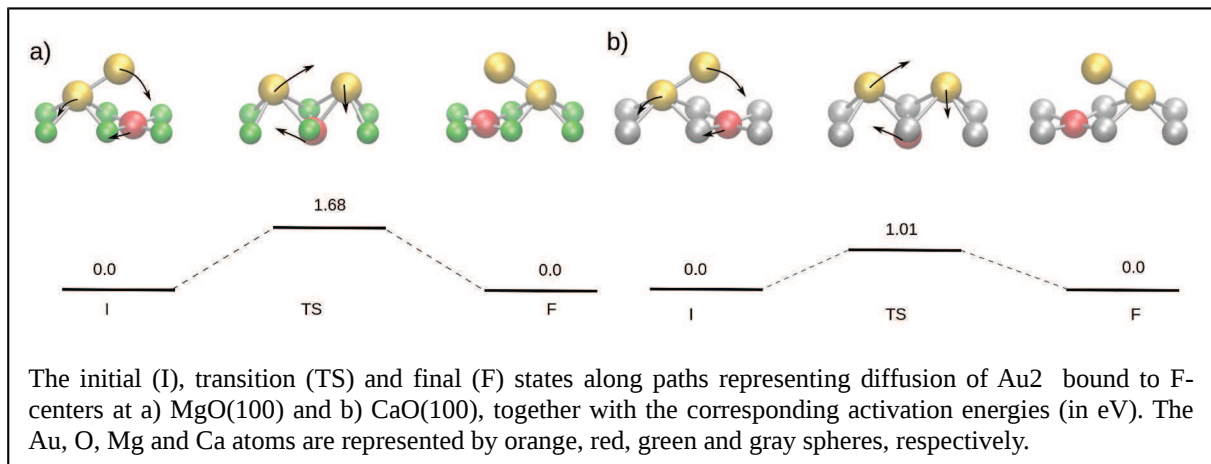
<sup>4</sup> **Coverage dependence of the level alignment for methanol on TiO<sub>2</sub>(110)**, Migani, A.; Mowbray, D.J., *Computational and Theoretical Chemistry*, **1040–1041**, 259–265 (2014)

## Diffusion of gold clusters trapped at F-centers of MgO(100) and CaO(100) surfaces

Željko Šljivančanin

Vinča Institute of Nuclear Sciences, P.O.Box 522, 11001 Belgrade, Serbia  
zeljko@vinca.rs

Few-atom gold clusters get trapped at the F-centers of MgO(100) and CaO(100) surfaces quickly upon deposition due to much stronger binding at the defects compared to the  $O_{5c}$  sites of the ideal terraces. Yet, our density functional theory (DFT) calculations reveal that their mobility is not fully suppressed since the Au dimers and trimers can diffuse at CaO(100) surface together with the F-centers they are bound to, along paths with activation energies not higher than 1.0 eV. The low energy paths are enabled by combined effects of high electron affinity of Au, the modest strength of the bonds within Au clusters and a favorable topology of the point-defect electronic states along the paths. For other metals the same diffusion mechanism is less effective than for gold.



## Engineering Polarons at a Metal Oxide Surface

Chi Ming Yim<sup>1</sup>, Matthew B. Watkins<sup>2</sup>, Chi Lun Pang<sup>1</sup>, Matthew J. Wolf<sup>2,3</sup>, Kersti Hermannson<sup>3</sup>, Alex L. Shluger<sup>2</sup>, Geoff Thornton<sup>1</sup>

<sup>1</sup>Department of Chemistry/London Centre for Nanotechnology, University College London

<sup>2</sup>Department of Physics/London Centre for Nanotechnology, University College London

<sup>3</sup>Department of Chemistry, Ångström Laboratory, Uppsala University

[chi.pang@ucl.ac.uk](mailto:chi.pang@ucl.ac.uk)

Polarons play a pivotal role in the physics and chemistry of metal oxides. Although it is difficult to access polarons in the bulk of a material, in principle they can be probed and manipulated at the surface, allowing their formation, properties and interactions to be investigated.

It is known that oxygen vacancies on TiO<sub>2</sub>(110) introduce electronic states that lie within the band-gap (so-called band-gap states or BGS). Here, we probe these BGS using simultaneously recorded empty- and filled-states scanning tunnelling microscopy (STM) as well as theoretical calculations. At low temperature, the BGS electron distribution is asymmetric (Figure 1d) and our calculations indicate this is due to the polaronic character of the band-gap state electrons. Consistent with earlier work [1], at 78 K (Fig. 1c), we observe a symmetric BGS electron distribution due to thermally-assisted hopping.

By applying electrical pulses (+4 V sample bias) from the STM tip, we manipulated the positions of O<sub>b</sub>-vac and show that the BGS electrons follow the O<sub>b</sub>-vac. These pulses were also used to drive O<sub>b</sub>-vac together, forming dimer, trimer, and tetramer complexes, each of which are associated with a modified BGS distribution.

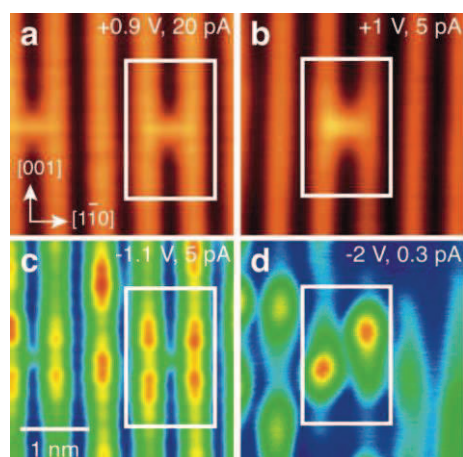


**Figure 1** STM images of oxygen vacancies on TiO<sub>2</sub>(110). **a,c** Simultaneously recorded empty-states and filled-states, respectively, at 78 K. **b,d** Simultaneously recorded empty-states and filled-states, respectively, at 7 K.

[1] T. Minato et al., J. Chem. Phys. **130**, 124502 (2009).

## A Model Catalyst System for the Water-Gas-Shift Reaction

Bobbie-Jean Shaw, **David C. Grinter**, Chi L. Pang, Geoff Thornton

Department of Chemistry & London Centre for Nanotechnology, University College London, London, UK

Ceria-based materials have been the focus of intense study due their wide range of applications across many fields. The suitability of ceria as a heterogeneous catalyst support due to its excellent oxygen storage and release characteristics is well-known. One particular system, that of gold nanoparticles supported on ceria, has displayed high catalytic activity towards the low temperature water-gas-shift reaction.[1] In this work we describe the preparation and characterisation of model systems employed to study such catalysts. To overcome charging problems inherent in the use of electron-based spectroscopy and microscopy to probe insulating materials such as ceria, we have prepared ultrathin epitaxial films of  $\text{CeO}_{2-x}(111)$  on a number of conducting substrates including Pt(111),[2,3] Rh(111),[4] and Re(0001).[5]

A key aim of this work is to thoroughly characterise the atomic scale structure and reactivity of the  $\text{CeO}_{2-x}(111)$  surface and its associated defect structures. The key technique to probe objects at this scale is STM, which we have used to examine oxygen vacancy structures, adsorbed water, and individual gold atoms along with small (<5 nm) gold nanoparticles. We also report on some of the contrast mechanisms that are observed in the course of making atomically resolved STM measurements.

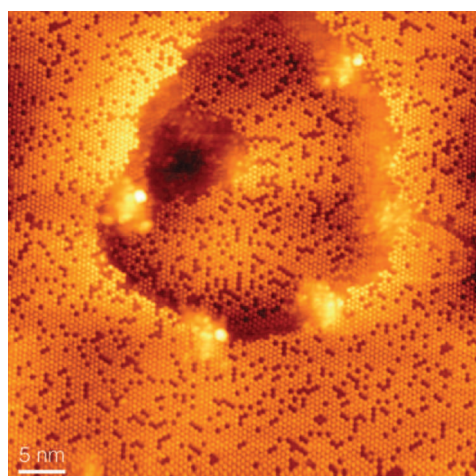


**Figure 1.** Filled-states STM image of a  $\text{CeO}_2(111)$  film on Pt(111). Surface oxygen vacancies appear as dark spots located at the sites of top layer oxygen ions.  
[50 x 50 nm<sup>2</sup>,  $V_s = -3.2$  V,  $I_t = 0.05$  nA]

### References:

- [1] Fu, Q. et al. *Science* **301**, 935 (2003).
- [2] Grinter, D.C. et al. *J. Phys. Chem. C* **114**, 17036 (2010).
- [3] Grinter, D.C. et al. *J. Elec. Spec. Rel. Phenom.* **195**, 13 (2014).
- [4] Grinter, D.C. et al. *J. Phys. Chem. C* **118**, 19194 (2014).
- [5] Grinter, D.C. et al. *J. Phys. Chem. C* **117**, 16509 (2013).

## Oxygen Vacancies versus Fluorine Impurities at CeO<sub>2</sub>(111): A Case of Mistaken Identity?

J. Kullgren<sup>1</sup>, M. J. Wolf<sup>1,2</sup>, C. W. M. Castleton<sup>3</sup>, P. Mitev<sup>1</sup>, W. Briels<sup>4</sup>, K. Hermansson<sup>1</sup>

<sup>1</sup>Uppsala University, Department of Chemistry-Ångström, Uppsala, Sweden

<sup>2</sup>University College London, Department of Physics & Astronomy, London, UK

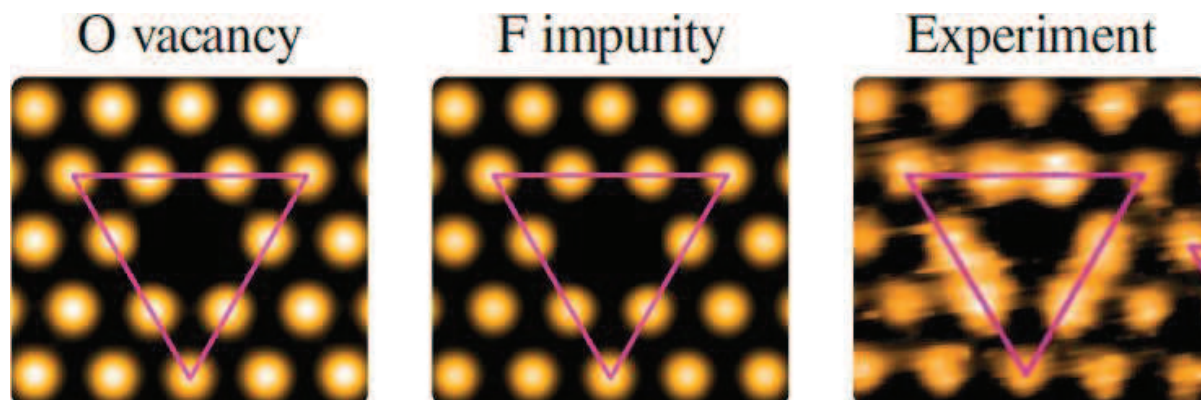
<sup>3</sup>Nottingham Trent University, School of Science and Technology, Nottingham, UK

<sup>4</sup>Twente University, Computational Biophysics, Enschede, The Netherlands

matthew.wolf@kemi.uu.se

Obtaining a detailed knowledge of the properties of oxygen vacancies in the near-surface region of CeO<sub>2</sub>(111) is naturally of fundamental importance for developing an understanding of the chemistry of this prototypical reducible oxide, and much research effort has been expended to this end in recent years. In principle, Scanning Tunnelling Microscopy (STM) can provide direct atomically resolved information on both the geometric and electronic structure of such defects, but the interpretation of STM images is not always straightforward and appearances can sometimes be deceiving.

Recently, a large fluorine contamination was found in CeO<sub>2</sub> single crystals from the source used in most, if not all, studies utilising such samples in the literature, with enrichment close to the surface [1]. Based on this report, we consider the possibility that the apparent depressions that are visible in atomically resolved STM images of the (111) surface facet of CeO<sub>2</sub> single crystals [2] were surface fluorine impurities, as opposed to surface oxygen vacancies to which they were previously attributed. In particular, from the results of our DFT+U calculations, we predict that surface F impurities and O vacancies should be essentially indistinguishable based on their STM appearances alone. However, while the most stable location (surface vs. subsurface), the mobility, and the propensity to cluster of F impurities is in agreement with the behaviour of the depressions observed in [2], the same properties of O vacancies are not. Based on these results, we propose that the depressions were indeed F impurities, not O vacancies [3].



[1] H. H. Pieper *et al.*, Phys. Chem. Chem. Phys. **14**, 15361 (2012).

[2] F. Esch *et al.*, Science **309**, 752 (2005).

[3] J. Kullgren *et al.*, Phys. Rev. Lett. **112**, 156102 (2014).

## Characterizing Metal Adsorption at the Fe<sub>3</sub>O<sub>4</sub>(001) Surface

Roland Bliem<sup>1</sup>, Oscar Gamba<sup>1</sup>, Zbynek Novotny<sup>1</sup>, Michael Schmid<sup>1</sup>, Ulrike Diebold<sup>1</sup>,  
and Gareth S Parkinson<sup>1</sup>

<sup>1</sup>Institute of Applied Physics, Vienna University of Technology, 1040 Vienna, Austria  
Parkinson@iap.tuwien.ac.at

The Fe<sub>3</sub>O<sub>4</sub>(001) surface has been shown to stabilize ordered arrays of single metal adatoms up to temperatures as high as 700 K [1], providing an ideal model system to study cluster nucleation and growth as well as single atom catalysis.

My poster will present systematic STM studies of several metals at different coverages and temperatures. The experiments reveal two classes of behaviour; elements, which cannot exist in solid solution with Fe<sub>3</sub>O<sub>4</sub> (e.g. Au [1], Pd [2], Ag [3]) form adatom arrays until the coverage or the temperature is high enough to initiate cluster nucleation. Elements that do form ferrites (MFe<sub>2</sub>O<sub>4</sub>, M = Ni, Co, Fe [4]) populate the surface as stable adatoms at room temperature, but the adatoms are incorporated into the surface layer with mild annealing. Incorporation of a full monolayer of Ni or Co into the surface results in the lifting of the ( $\sqrt{2} \times \sqrt{2}$ )R45° surface reconstruction, resulting in a surface that can be viewed as an ultrathin film of ferrite supported on Fe<sub>3</sub>O<sub>4</sub>. The incorporation of adatoms into the surface agrees well with a new surface model comprising ordered Fe vacancies in the subsurface [5].

- [1] Z. Novotný...G.S.Parkinson, *Physical Review Letters* **108**, 216103 (2012).
- [2] G. S. Parkinson *et al.*, *Nature Materials* **12**, 724 (2013).
- [3] R. Bliem ... G.S. Parkinson, *ACS Nano* **8**, 7531 (2014).
- [4] R. Bliem ... G.S. Parkinson, *in preparation*
- [5] R. Bliem...G.S. Parkinson, *submitted* (2014)

## Surface Contact Engineering in Photoactive ZnO Nanostructures

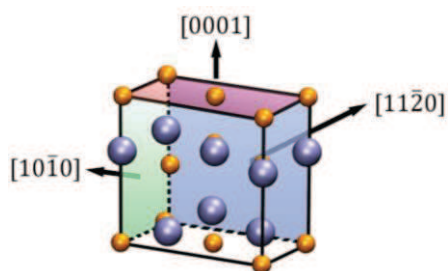
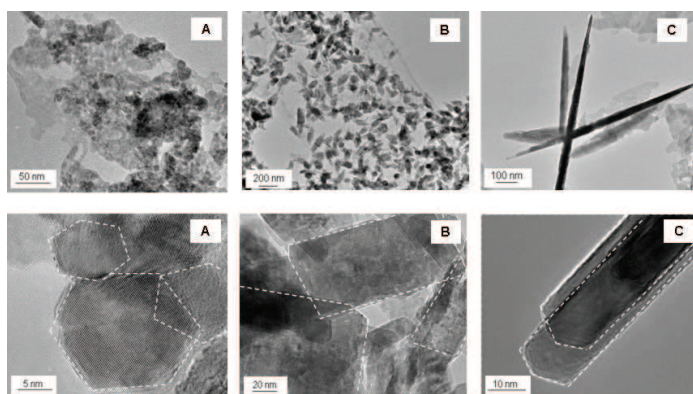
Ana Iglesias-Juez,<sup>1,\*</sup> Francesc Viñes,<sup>2</sup> Oriol Lamiel-García,<sup>2</sup> Marcos Fernández-García,<sup>1</sup> and Francesc Illas,<sup>2,\*</sup>

<sup>1</sup> *Instituto de Catálisis y Petroleoquímica, CSIC, c/Marie Curie 2, Cantoblanco, 28049 Madrid, Spain.*

<sup>2</sup> *Departament de Química Física & Institut de Química Teòrica i Computacional (IQTCUB), Universitat de Barcelona, c/Martí i Franquès 1, 08028 Barcelona, Spain.*

\*corresponding authors: ana.iglesias@icp.csic.es, francesc.illas@ub.edu

A series of ZnO nanostructures with variable morphology were prepared by a microemulsion method and their structural, morphological, and electronic properties were investigated by a combined experimental and theoretical approach using microscopy (high resolution transmission electron microscopy) and spectroscopic (X-ray diffraction, Raman and UV-visible) tools, together with density functional theory calculations. The present experimental and computational study provides a detailed insight into the relationship between surface related physicochemical properties and the photochemical response of ZnO nanostructures. Specifically, the present results provide conclusive evidence that light-triggered photochemical activity of ZnO nanostructures is intimately governed by a synergistic effect between polar and nonpolar surfaces rather than by the predominance of highly-active (polar) surfaces, bandgap sizes, carrier mobilities and other variables usually mentioned in the literature.



## Atomically dispersed M species (M = Pd, Ni, Cu) in ceria nanoparticles: Stability and red-ox processes

Alberto Figueroba,<sup>1</sup> Konstantin M. Neyman<sup>1,2</sup>

<sup>1</sup>Departament de Química Física and IQTC, Universitat de Barcelona, Barcelona, Spain

<sup>2</sup>Institució Catalana de Recerca i Estudis Avançats (ICREA), Barcelona, Spain

afigure89@gmail.com

Pt is one of the most versatile elements in catalysis. However, the high price of this precious metal often hinders his applications in catalytic materials. One of the alternatives is replacement of Pt by other less expensive metals.

By means of density functional calculations, we have studied the adsorption and doping effects of single atoms of three different metals M (M = Pd, Ni, Cu) on CeO<sub>2</sub> nanoparticles. Binding sites for adsorption of all three metals have been identified on {100} facets leading to cationic M<sup>2+</sup> species. These species are stable enough to resist diffusion inside ceria nanoparticles and sintering processes that may occur in real catalysts. The same anchoring sites have been recently found in Pt-CeO<sub>2</sub> nanocomposites featuring high efficiency as fuel cell anode catalysts [1]. Furthermore, the effect of reductive environments on the M-CeO<sub>2</sub> systems has been studied considering two possible mechanisms: formation of oxygen vacancies (see Figure) and hydrogen adsorption. These processes lead to the formation of M species in different charge states, which may give rise to high efficiency fuel cell catalysts.

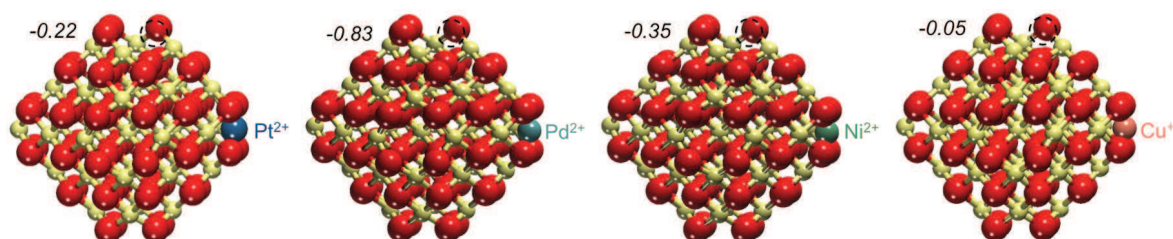


**Figure.** Model M-doped (M = Pt, Pd, Ni, Cu) M Ce<sub>39</sub>O<sub>79</sub> nanoparticles with a charge-compensating oxygen vacancy. Yellow, red and different colour balls correspond to Ce, O and dopant M atoms, respectively. The atom M substitutes a Ce atom in a corner position. Position of the oxygen vacancy O<sub>vac</sub> is shown by a dashed circle. Formation energy of the O<sub>vac</sub> (eV) calculated with respect to 1/2 O<sub>2</sub> is also given. Negative energy values indicate the exothermic processes.

- [1] A. Bruix, Y. Lykhach, I. Matolínová, A. Neitzel, T. Skála, N. Tsud, M. Vorokhta, V. Stetsovych, K. Ševčíková, J. Mysliveček, R. Fiala, M. Václavů, K.C. Prince, S. Bruyère, V. Potin, F. Illas, V. Matóin, J. Libuda, K.M. Neyman, *Angew. Chem. Int. Ed.* **53**, 10525 (2014)

## Charge Trapping in TiO<sub>2</sub> Polymorphs as Studied by Means of EPR and HR-TEM Techniques

**Mario Chiesa**, Maria Cristina Paganini, Stefano Livraghi, Elio Giamello, Zbigniew Sojka<sup>2</sup>,  
Dipartimento di Chimica, Università di Torino. Via Giuria, 7 10125- Torino, Italy

<sup>1</sup> Faculty of Chemistry, Jagiellonian University, ul. Ingardena 3 30-060 Krakow, Poland  
mario.chiesa@unito.it

Photoinduced charge separation and formation of trapped electrons and trapped holes in semiconducting oxides are phenomena of paramount importance in the fields of photochemistry, photocatalysis and artificial photosynthesis. In all these fields titanium dioxide (TiO<sub>2</sub>) plays a strategic role.

Electron Paramagnetic Resonance techniques have been employed to investigate charge carriers trapping in the three polymorphs of titanium dioxide, namely anatase, rutile and brookite, with particular attention to the features of electron trapping sites (formally Ti<sup>3+</sup> ions). The classic CW-EPR technique in this case provides signals based on the g tensor only. Nevertheless a systematic analysis of the signals obtained in the various cases (anatase, rutile, brookite, surface and bulk centers, regular and defective sites) has been performed providing useful guidelines in a field affected by some confusion. The problem of the localization of the unpaired electron spin density have been tackled by means of Pulse-EPR hyperfine techniques on samples appositely enriched with <sup>17</sup>O. This approach highlighted a substantial difference, in terms of wave function localization between anatase (electrons trapped in regular lattice sites exhibiting delocalized unpaired electron density) and rutile (interstitial sites showing localized electron density). The spectroscopic results are compared with high resolution TEM microscopies with the aim of linking the topological features of polycrystalline TiO<sub>2</sub> polymorphs with the observed charge separated states.

- [1] M. Chiesa, M.C. Paganini, S. Livraghi, E. Giamello, *Phys. Chem. Chem. Phys.*, 15, (2013), 9435.
- [2] S. Livraghi, M. Chiesa, M.C. Paganini, E. Giamello, *J. Phys. Chem. C*, 115, (2011), 25413.

## ***Synthesis and characterization of NiO: Au nanoparticles by laser ablation of Ni bulk in Au colloidal solution***

<sup>1</sup>Suzana Petrović, <sup>2</sup>B. Salatić, <sup>1</sup>D. Milovanović and <sup>2</sup>B. Jelenković

<sup>1</sup>Institute of Nuclear Science—Vinča, University of Belgrade, POB 522, 11001 Belgrade, Serbia

<sup>2</sup>Institute of Physics Belgrade, University of Belgrade, Pregrevica 118, 11080 Belgrade, Serbia

Nickel oxide is a binary transition non-toxic metal oxide with excellent chemical stability and ease of fabrication. Pure NiO with a wide band gap (3.6-3.8 eV) as a p-type semiconductor has attracted considerable interest as a candidate for many applications such as a gas sensors, catalysis, solar cells and magnetic materials. Nanostructured NiO shows interesting optical, magnetic and electronic properties due to quantum confinement. Hydrogen sensors based on NiO are able to detect concentrations as low as 500 ppm, operate in 300-650 °C temperature range. Recently, NiO film with embedded Au nanoparticles achieved sensing of hydrogen concentration below of 5 ppm in 100-160 °C temperature intervals. Pulsed laser ablation technique for the synthesis of nanoparticles (NPs) metal oxides in liquid media using solid target has simple and clean method, which does not require costly chambers and high vacuum pumping systems. Changing available parameters involved in the laser ablation in the liquids, regarding both the laser source (wavelength, pulse duration, laser energy, repetition rate, ablation time) and the liquid (composition, dipole moment, dielectric constant, absorption constant), one can control size, shape, and morphology of generated NPs which could lead in change of the physical and chemical properties of synthesized materials.

Metal oxide NiO and bimetallic oxide NiO: Au nanoparticles (NPs) are generated by ablation of nickel bulk target in water and aqueous Au colloidal solution, respectively. The experiments were performed using nanosecond and picosecond Nd: YAG laser operating at 1064 nm with similar energy per pulses. Composition and structure of the generated NPs are characterized by UV–VIS absorption spectroscopy, X-ray diffraction (XRD), X-ray photoelectron spectroscopy (XPS) and transmission electron microscopy (TEM). Synthesized pure metal oxide NiO NPs were used for comparison with results obtained for NiO: Au NPs produced by the laser interaction with Ni sample in previously prepared Au colloidal solution. From UV-vis analysis of the appropriate colloidal of NiO: Au NPs it was determined that the predominant absorption arises from Au component, in the absence of Ni. The Au NPs are mainly spherical, and it has been found that their average diameters are about 5 nm. Composition analysis obtained with XPS and XRD techniques were shown that oxide phases of NiO and Ni<sub>2</sub>O<sub>3</sub> were dominant in colloidal solutions after laser ablation with both types of pulses. Important result was the formation of NiO: Au NPs with specific core-shell structure (NiO shell around Au core) with size about 8 nm, which agreed very well with the predicted mechanism for generation of NPs by picosecond laser ablation in liquids. However, after laser ablation with nanosecond pulses, Au nanoparticles are fairly homogeneously distributed in the NiO amorphous phase, without changing their size and shape.

## ***Synthesis of ultra-thin bimetallic AlFe-oxide layer on 3x(Al/Fe)/Si multilayer structure by laser processing***

**B. Jelenković<sup>1</sup>, A. Kovačević<sup>1</sup>, B. Salatić<sup>1</sup>, S. Petrović<sup>2</sup>, D. Pantelić<sup>1</sup> and M. Trtica<sup>2</sup>**

<sup>1</sup>University of Belgrade, Institute of Physics Belgrade, Pregrevica 118, 11080 Belgrade, Serbia

<sup>2</sup>University of Belgrade, Institute of Nuclear Science-Vinča, POB 522, 11001 Belgrade, Serbia

Preparation of a new anion-selective catalyst, especially using metal oxides or surfactants, has attracted attention in recent years since it combines a good catalytic activity with a high stability against leaching. Metal-oxide Al<sub>2</sub>O<sub>3</sub>-Fe<sub>2</sub>O<sub>3</sub> based catalyst has been developed for the elimination of volatile organic compounds at lower temperatures (200 – 600 °C). Mixtures of iron and aluminum oxides are the most spread, excellent candidates as heterogeneous catalysts for the removal of organic water pollutants, especially phenol and phenol derivatives, homolytic decomposition of peroxide and arsenic adsorption in aqueous solution. It is a presumption that the physic-chemical properties of bimetal AlFe-oxide differ from those of their single components, making it as a promising material for phosphate removal by adsorption reaction from contaminated water in engineering systems [1,2].

In this work, the conditions of the formation of ultra-thin oxide films in the Al/Fe multilayer structures, after the surface treatment with the femtosecond laser radiation were studied. Thin films composed of three (Al/Fe) bilayers were deposited by DC ion sputtering on (100) Si wafers, to the total thickness of 410 nm. Laser irradiations were performed using 40 fs pulses of a Ti:Sapphire laser operating at 800 nm, at fluences slightly higher than the ablation threshold. The samples were characterized by Auger electron spectroscopy (AES), X-ray photoelectron spectroscopy (XPS), and scanning electron microscopy (SEM). For lower fluence at about 0.43 J cm<sup>-2</sup>, the interaction results in intermixing between Al and Fe layers, with formation of intermetallic phases, starting from the top through the interior of the multilayer structure down to the substrate. At the same time, oxygen molecules adsorbed on the surface were dissociated, and oxygen atoms penetrate into the sample with preferential formation of metal-oxides [3]. Oxygen reacts with the target material during the laser irradiation in air, and triggers the iron surface segregation and deep penetration of aluminium. An ultra-thin oxide layer, thickness of 20 nm, was formed at the surface, with the specific combination of the oxide phases, Al<sub>2</sub>O<sub>3</sub> and Fe<sub>2</sub>O<sub>3</sub>, depending on the applied fluences. Laser-induced modification was accompanied with the ablation of the material and the creation of parallel periodic structures. These effects of laser-induced morphological features are increased with increasing laser fluences, caused by the pronounced mobility of the materials. The special morphology of the laser-assisted synthesis of mixture Al<sub>2</sub>O<sub>3</sub> and Fe<sub>2</sub>O<sub>3</sub> in form of ultra-thin oxide layer can improve characteristics of composite multilayer structure for functional applications, as catalysts and sensors.

[1] Y. Yang, D. Yan, Y. Dong, X. Chen, L. Wang, Z. Chu, J. Zhang, J. He, J. Alloys Comp. 579 (2013) 1-6 [2] P. Brankovic, A. Milutinovic-Nikolic, Z. Mojovic, N. Jovic-Jovicic, M. Perovic, V. Spasojevic, D. Jovanovic, Microporous and Mesoporous Mater. 165 (2013) 247-256 [3] N.K. Das, T. Shoji, International Jour. of Hydrogen Energ. 38 (2013) 1644-1656

# Influence of post-treatment of bimetallic Au-Pd catalysts supported on ceria-zirconia for selective oxidation of benzyl alcohol

Carol M. Olmos<sup>1</sup>, Alberto Villa<sup>2</sup>, Lidia E. Chinchilla<sup>1</sup>, Juan J. Delgado<sup>1</sup>, Ana B. Hungría<sup>1</sup>, José J. Calvino<sup>1</sup>, Laura Prati<sup>2</sup>, Xiaowei Chen<sup>\*,1</sup>

1. Facultad de Ciencias, Universidad de Cádiz, 11510, Puerto Real (Spain)

2. Dipartimento di Chimica, Università di Milano, 20133 Milan (Italy)

(\*) corresponding author: xiaowei.chen@uca.es

It has been found that the addition of a second metal to Au catalyst improves the activity and selectivity for selective oxidation of alcohol [1]. Metal-support interaction, metal particle size, post-treatments, oxidation state of the metals and the method of preparation [2] are important factors that can affect the catalytic behavior of bimetallic Au-Pd catalysts. In this work, bimetallic Au-Pd supported on ceria zirconia catalyst was prepared by sol-immobilization using PVP as stabilizers. The influence of post-treatment conditions on the removal of PVP from the active site and on the morphology of the catalyst has been studied.

Bimetallic Au-Pd/Ce<sub>0.62</sub>Zr<sub>0.38</sub>O<sub>2</sub> catalyst was synthesized by two steps: firstly a monometallic Au/Ce<sub>0.62</sub>Zr<sub>0.38</sub>O<sub>2</sub> catalyst was prepared. The second step was dispersion of the Au/Ce<sub>0.62</sub>Zr<sub>0.38</sub>O<sub>2</sub> sample in water followed by the addition of Na<sub>2</sub>PdCl<sub>4</sub> and PVP. H<sub>2</sub> was then bubbled through the solution at atmospheric pressure and room temperature for 1 h. Finally the sample was washed and dried at 80 °C for 2 h (AuPdCZ-F). Subsequently the AuPdCZ-F catalyst was treated under oxygen for 1 h at 250 °C (AuPdCZ-O). One part of the AuPdCZ-O sample was reduced bubbling H<sub>2</sub> at room temperature during 2 h (AuPdCZ-H).

The real Au and Pd loadings of AuPdCZ-F sample are 0.55 and 0.21 wt% according to ICP analysis, suggesting that the Au/Pd ratio is 1.4:1, not the theoretical value 1.5:1. This might be due to a loss of Au and Pd during the preparation or leaching during the washing process. The HAADF-STEM images of fresh bimetallic Au-Pd catalyst and bimetallic catalyst treated by O<sub>2</sub> and H<sub>2</sub> show that the metal particles are very homogeneous and the metal particle size is in the range of 2 and 5 nm. This result indicates that the post-treatment of bimetallic catalyst does not lead to any aggregation of metals.

After oxidation of the AuPd catalyst with O<sub>2</sub> at 250 °C, the catalytic activity increased (TOF of 805 h<sup>-1</sup> and 2260 h<sup>-1</sup> for AuPdCZ-F and AuPdCZ-O, respectively). The treatment in O<sub>2</sub> was able to remove the excess of protective agent from the active site without changing the oxidation state of the metal. Surprisingly the successive treatment with H<sub>2</sub> results in a decrease of the activity. To fully understand the observed phenomena, further characterization of these catalysts using XPS, TEM and other techniques is currently under way.

**Table 1.** Catalytic activity of the AuPd catalysts in the benzyl alcohol oxidation

Catalyst	TO F (h <sup>-1</sup> ) <sup>a</sup>	Conversion (%)				Selectivity at 50% conversion	
		0.25 h	0.5 h	1 h	2 h	Benzaldehyde	Toluene
AuPdCZ-F	805	3.7	10.1	24.5	77	99	0
AuPdCZ-O	2260	8.1	28.4	82.4	98.5	98	0.7
AuPdCZ-H	1036	7.1	13.1	32.2	90.3	98	0.3

<sup>a</sup> TOF was calculated after 30 min of reaction. Reaction conditions: benzyl alcohol/cyclohexane= 50/50 (vol/vol), T=80 ° C, P<sub>O<sub>2</sub></sub>=200 kPa, benzyl alcohol/total metal = 3000 mol/mol.

## References

- [1] D.I. Enache, J.K. Edwards, P. Landon, B. Solsona-Espriu, A.F. Carley, A.A. Herzing, M. Watanabe, C.J. Kiely, D.W. Knight, G.J. Hutchings, *Science* **311**, 362-365, (2006).
- [2] J. Campelo, D. Luna, R. Luque, J. Marinas, A. Romero, *Chemsuschem.* **2**, 18, (2009).

## Theoretical study of the CO interaction with mononuclear platinum species supported on nanoparticulate ceria

Hristiyan A. Aleksandrov<sup>1,2</sup>, Konstantin M. Neyman<sup>2,3</sup>, Georgi N. Vayssilov<sup>1</sup>

<sup>1</sup> Faculty of Chemistry and Pharmacy, University of Sofia, 1126 Sofia, Bulgaria.

<sup>2</sup> IQTCUB, Universitat de Barcelona, C/Martí i Franquès 1, 08028 Barcelona, Spain.

<sup>3</sup> Institució Catalana de Recerca i Estudis Avançats (ICREA), 08010 Barcelona, Spain.

e-mails: haa@chem.uni-sofia.bg, konstantin.neyman@icrea.cat, gnv@chem.uni-sofia.bg

Mononuclear platinum species in different (0, 2+ and 4+) oxidation states were modelled on various positions on (111) and (100) facets of a ceria nanoparticle. The calculations were performed with DFT+U approach using periodic code VASP. The relative stability of atomic Pt species was estimated for ceria at various conditions: stoichiometric as well as O poor and O rich conditions. It was found that the Pt species are most stable at small (100) facets. In addition, we found that the presence of mononuclear Pt species on Ce<sub>21</sub>O<sub>42</sub> hinders the O vacancy formation.

The reactivity of different mononuclear platinum species was tested with respect to adsorption of CO (Fig. 1). As a general trend, we found that the binding energy of CO decreases with increasing the oxidation state of Pt.

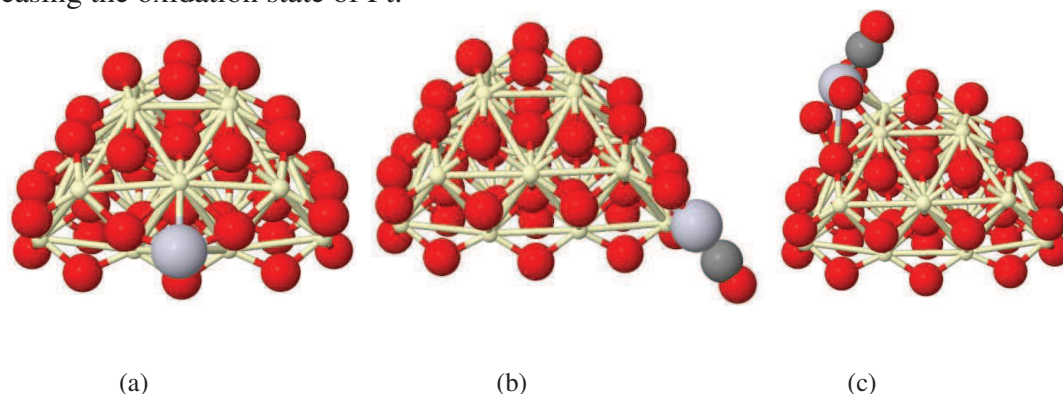


**Figure 1.** Selected model structures of mononuclear platinum species on ceria nanoparticle before (a) and after CO adsorption (b) and (c). Color coding: yellow – Ce, red – O, light blue – Pt, carbon – C.

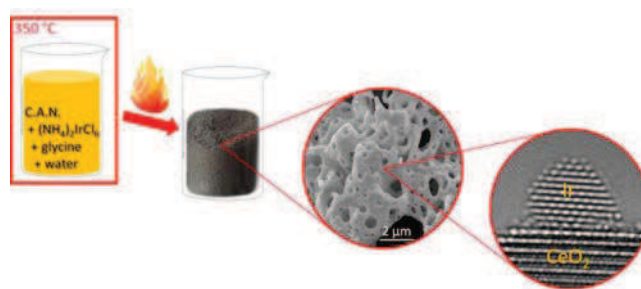
Acknowledgments: The authors are grateful for the support from the European Commission (FP7 projects BeyondEverest and ChipCAT 310191), Spanish MINECO (grant CTQ2012-34969), COST Action CM1104, and the Bulgarian Supercomputer Center for provided computational resources and assistance.

## Solution combustion synthesis of noble metal-loaded ceria catalysts and application to hydrogen production and purification for fuel cells

T.S. Nguyen, G. Postole, F. Morfin, L. Piccolo

IRCELYON, CNRS & Univ. Lyon 1, 2 Avenue Albert Einstein, 69626 Villeurbanne, France  
laurent.piccolo@ircelyon.univ-lyon1.fr

Mesoporous ceria powders doped with up to 2 wt% platinum-group metals (Pt, Pd, Ir, Rh, Ru) were synthesized in one step by the ambient air combustion of an aqueous solution of ceric ammonium nitrate (CAN), chloride or nitrate metal precursor, and glycine or oxalyl dihydrazide used as fuels [1, 2]. The structural properties of the powders, and the influence of such parameters as metal loading and thermochemical post-treatments, were investigated combining aberration-corrected HRTEM, SEM, *in situ* XRD, XPS, DRIFTS, and Raman spectroscopy. The materials, whose texture appeared spongy at the micrometer scale and depended on the fuel nature, exhibited *ca.* 30 nm-sized ceria crystallites with a layered structure at the nanoscale. Comparisons with pure ceria showed that the presence of the metal inhibited ceria grain coarsening.



The powders were successfully employed as catalysts for the production of hydrogen from the steam reforming of methane (SRM) in water-deficient conditions, and for the purification of hydrogen through the preferential oxidation of CO (PROX).

For SRM, 0.1 wt% Ir-CeO<sub>2</sub> exhibited the best performances. Due to its higher Ir dispersion and stronger Ir-CeO<sub>2</sub> interaction, the combustion-synthesized material was more active and stable than its conventionally prepared counterpart. Moreover, it was not permanently deactivated by the introduction of H<sub>2</sub>S in the reactant feed. After reducing treatments, Ir nanoparticles anchored at the surface of ceria grains were imaged, and their size (*ca.* 2 nm) and morphology did not evolve upon further heating at up to 900 °C. A complete picture of the Ir-CeO<sub>2</sub> interface could be established, with the presence of Ir<sup>x+</sup>-O<sup>2-</sup>-Ce<sup>3+</sup> entities along with oxygen vacancies.

For CO oxidation and PROX, systematic comparisons between the samples, which exhibited similar metal nanoparticle sizes, allowed us to rank the Pt-group metals. Rh-CeO<sub>2</sub> appeared as the most active system in H<sub>2</sub>-free CO oxidation. The presence of H<sub>2</sub> boosted the CO oxidation activity of all catalysts, except that of Rh-CeO<sub>2</sub>, which promoted the decomposition of CO and the subsequent formation of methane. Pt-CeO<sub>2</sub>, which was the most active and selective PROX catalyst, was further investigated by changing the nature of the fuel and the metal precursor. Although the catalyst activities were influenced by such parameters, the selectivities were strikingly unaffected.

[1] V. M. Gonzalez-Delacruz, F. Ternero, R. Pereniguez, A. Caballero, and J. P. Holgado, *Appl. Catal. A* **384**, 1 (2010).

[2] M. S. Hegde, G. Madras, and K. C. Patil, *Acc. Chem. Res.* **42**, 704 (2009).

# Electrochemical In-situ IR Spectroscopy on Pt Electrodes: Single Crystals, Metallic Thin -Films, Pt nanoparticles, and Pt-Doped CeO<sub>2</sub>

O. Brummel, R. Fiala<sup>1</sup>, M. Vorokhta<sup>1</sup>, I. Khalakhan<sup>1</sup>, V. Matolín<sup>1</sup>, **J. Libuda**

Friedrich-Alexander-Universität Erlangen-Nürnberg, Erlangen, Germany.

<sup>1</sup>Charles University Prague, Prague, Czech Republic

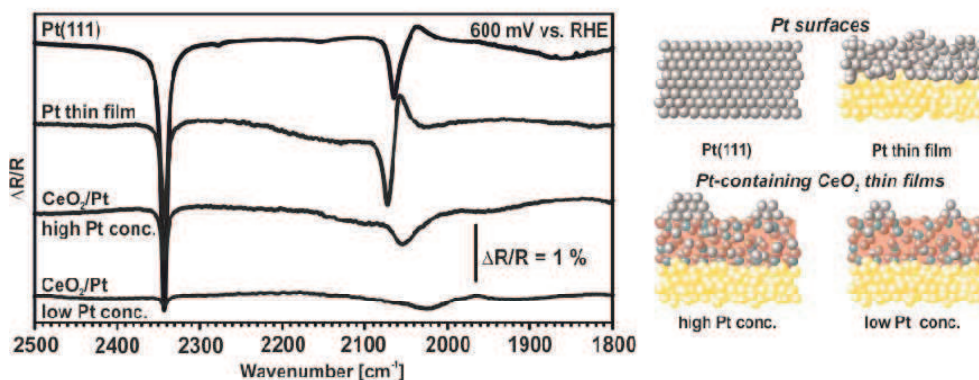
joerg.libuda@fau.de

Pt-doped CeO<sub>2</sub> has been identified as a potential novel anode material in proton exchange membrane fuel cells (PEMFC). Providing very high noble metal efficiency, the material may help to decrease the demand for Pt, while simultaneously increasing the tolerance against CO poisoning.[1]

To explore the chemical state of the Pt species in the ceria matrix under reaction conditions we apply in-situ electrochemical IR spectroscopy. Towards this aim we have set up a new IR spectro-electrochemistry system, that includes a state-of-the-art vacuum FTIR spectrometer and an optimized external reflection cell. We demonstrate that the system is functional and provides an excellent signal/noise ratio.

Using this setup, we have investigated methanol oxidation in acidic solution on different Pt catalysts by Linear Potential Scan Infrared Spectroscopy (LPSIRS). Using the CO that is formed during the reaction as a probe for the Pt surface sites, we compare Pt(111) electrodes, Pt thin-film electrodes, and Pt-containing CeO<sub>2</sub> thin-film electrodes with different Pt concentration. All thin-film samples were prepared by magnetron sputtering and characterized by SEM, EDS and cyclic voltammetry. Before measurement we cleaned the surfaces by potential cycling.

On all samples, the IR spectra in the CO stretching frequency region are dominated by the on-top CO band between 2000 and 2100 cm<sup>-1</sup>. A slight blue shift to 2074 cm<sup>-1</sup> is observed for the Pt thin film sample in comparison to Pt(111), where the signal appears at 2064 cm<sup>-1</sup>. Possible explanations involve the co-adsorption of electron withdrawing species and/or an increased CO density. Most importantly, the rougher surface of the thin film induces higher reactivity and leads to earlier CO formation, which is also reflected by the more pronounced s-shape of the CO band (Stark shift). In contrast, the Pt-doped CeO<sub>2</sub> electrodes show a strong red shift and a broadening of the signal, which depend on the Pt concentration. Whereas the corresponding band is observed at 2056 cm<sup>-1</sup> at high Pt concentration, the band shows a very strong red shift down to 2023 cm<sup>-1</sup> with decreasing Pt concentration. This observation suggests that, even for low Pt concentration, a fraction of the Pt<sup>2+</sup> is reduced to Pt<sup>0</sup> and stabilized in form of very small nanoparticles.



[1] A. Bruix, Y. Lykhach, I. Matolinová, A. Neitzel, T. Skála, N. Tsud, M. Vorokhta, V. Stetsovych, K. Ševčíková, J. Mysliveček, R. Fiala, M. Václavů, K.C. Prince, S. Bruyère, V. Potin, F. Illas, V. Matolín, J. Libuda, K. M. Neyman., *Angew. Chem. Int. Ed.* (2014), **10.1002/anie.201406634**.

# Relative stability of CeO<sub>2</sub> species on the surfaces and in the cavities of $\gamma$ -Al<sub>2</sub>O<sub>3</sub>: A periodic DFT study

Iskra Koleva,<sup>1</sup> Hristiyan A. Aleksandrov,<sup>1</sup> Georgi N. Vayssilov,<sup>1</sup> Jeroen A. van Bokhoven<sup>2,3</sup>

<sup>1</sup> Faculty of Chemistry and Pharmacy, University of Sofia, 1126 Sofia, Bulgaria; e-mail: gnv@chem.uni-sofia.bg.

<sup>2</sup> Laboratory for Catalysis and Sustainable Chemistry, the Swiss Light Source, Paul Scherrer Institute, Switzerland.

<sup>3</sup> Institute for Chemical and Bioengineering, ETH Zürich, Switzerland.

An important feature of ceria, CeO<sub>2</sub>, is its ability to store and realise oxygen by changing oxidation state of cerium ions between +4 and +3. As a support of CeO<sub>2</sub> species usually is used  $\gamma$ -Al<sub>2</sub>O<sub>3</sub>, as it was recently reported for Rh/CeO<sub>2</sub>/ $\gamma$ -Al<sub>2</sub>O<sub>3</sub> system [1]. In this connection we modelled deposited CeO<sub>2</sub> species and small nanoparticles, Ce<sub>13</sub>O<sub>26</sub>, on two surfaces of  $\gamma$ -Al<sub>2</sub>O<sub>3</sub> - (100) and (001), and compared the energies of the optimized structures with the energies of the structures in which CeO<sub>2</sub> units are incorporated in subsurface or in internal cavities of  $\gamma$ -alumina. Formation of reduced ceria species and exchange of cerium ions by aluminium ions was also considered.

The periodic DFT+U calculations were performed with the program VASP. The valence wave functions were expanded to a plane wave basis with a kinetic energy cut-off of 415 eV, using the projector augmented wave (PAW) method. The U was set to 4.0 eV, as in previous model studies of ceria systems [2].

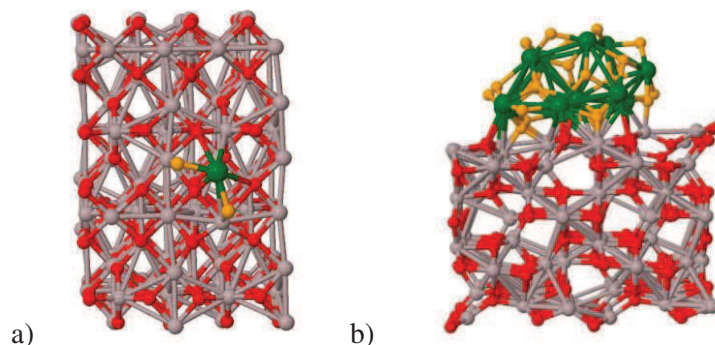


**Figure 1.** Selected optimized structures of: a) one deposited CeO<sub>2</sub> unit on  $\gamma$ -Al<sub>2</sub>O<sub>3</sub>(001) (top view); b) Ce<sub>13</sub>O<sub>26</sub> nanoparticle on  $\gamma$ -Al<sub>2</sub>O<sub>3</sub>(100) (side view). Ce<sup>4+</sup> cations are colored in green and oxygen atoms from ceria are orange.

**Acknowledgments:** The authors are grateful for the support from the European Commission (FP7 projects BeyondEverest and COST Action CM1104) and the Bulgarian Supercomputer Center for provided computational resources and assistance.

## References

- [1] R. B. Duarte, O. V. Safonova, F. Krumeich, M. Makosh, J. A. van Bokhoven, *ASC Catal.* **3**, 1956 (2013).
- [2] A. Migani, G. N. Vayssilov, S. T. Bromley, F. Illas, K. M. Neyman, *J. Mater. Chem.* **20**, 10535 (2010).

# Bi- and trimetallic Ni-based catalysts for methane dry reforming: TEM and DRIFTS investigations of the metals effect

F. Puleo<sup>1</sup>, G. Pantaleo<sup>1</sup>, V. La Parola<sup>1</sup>, Xavier Collard<sup>2</sup>, Carmela Aprile<sup>2</sup>, A. Martinez-Arias<sup>3</sup>  
**L.F. Liotta<sup>1</sup>**

<sup>1</sup>Institute for Study of Nanostructured Materials (ISMN)-CNR, Palermo, Via Ugo La Malfa, 90146, Palermo, Italy.

<sup>2</sup>Department of Chemistry, University of Namur (UNAMUR), 61 rue de Bruxelles, B-5000 Namur, Belgium.

<sup>3</sup>Institute of Catalysis and Petrochemical, CSIC, C/Marie Curie 2, Cantoblanco, 28049, Madrid, Spain.

E-mail: [leonarda.liotta@ismn.cnr.it](mailto:leonarda.liotta@ismn.cnr.it)

Nickel catalysts are the most frequently used materials in the reforming of CH<sub>4</sub> with CO<sub>2</sub>, known also as dry reforming (DRM), because of good catalytic activity and cost-effectiveness as compared with Pt, Ru or Rh-based systems [1]. However, the poisoning by carbon, formed by side reactions, and the sintering of metallic Ni, at the high temperatures used, limit its applications. To overcome these problems, the addition of second noble metals, such as Au, Pt, have been investigated [2,3]. We have recently demonstrated that small amounts of Au and Pt in bi-/trimetallic Ni/Al<sub>2</sub>O<sub>3</sub> catalysts strongly influence the structural and reduction properties and enhance catalytic activity [3]. Moreover, a direct relation between catalytic activity and typology of carbon was found. The best performing catalyst, Ni-Au-Pt/Al<sub>2</sub>O<sub>3</sub>, formed a nice bamboo-like structure not detected for other bimetallic systems of the same series. In the present work, in order to get more insight into the electronic/geometrical effects of the addition of Au/Pt/Pd, DRIFTS investigation of CO adsorption have been carried out over three bimetallic Ni-based catalysts. In Fig.1 (a) the DRIFTS difference spectra after CO adsorption at room temperature followed by flushing under He at 313 K are displayed.

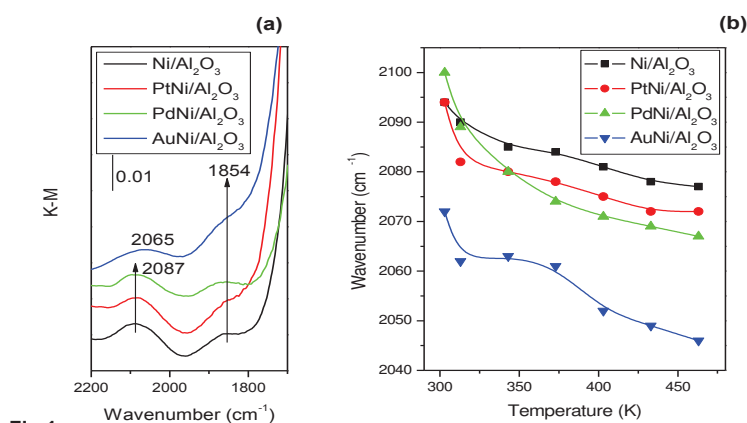


Fig.1

Fig. 1 (b) shows the evolution of the frequency of the linear carbonyl or subcarbonyl species as a function of the temperature of the flushing treatment. TEM observations carried out on the catalysts after catalytic tests performed at different temperatures revealed a clear difference in terms of nature or amount of carbonaceous species as a function of the active sites (Ni, Ni-Au/Pt, Pd) and reaction temperature.

## Acknowledgements

F. Puleo thanks COST Action CM 1104 for supporting his STSM (COST-STSM-CM1104-16226).

- [1] C. Raab, J. A. Lercher, J. G. Goodwin, J. Z. Shyu, *J. Catal.* **122**, 406 (1990).
- [2] A. Horváth, L. Guzzi, A. Kocsonya, G. Sáfrán, V. La Parola, L. F. Liotta, G. Pantaleo, A. M. Venezia, *Appl. Catal. A* **468**, 250 (2013).
- [3] H. Wu, G. Pantaleo, V. La Parola, A. M. Venezia, X. Collard, C. Aprile, L. F. Liotta, *Appl. Catal. B* **156–157**, 350 (2014).

## Characterization of ceria for SOFC anodes applications

Mihaela Florea<sup>1</sup>, Georgeta Postole<sup>2</sup>, Codruța G. Rotaru<sup>1</sup>, Florina Matei<sup>2</sup>, Patrick Gelin<sup>2</sup>

<sup>1</sup>University of Bucharest, Faculty of Chemistry, 050107, Bucharest, Romania

<sup>2</sup>Université Lyon 1, CNRS, UMR 5256, IRCELYON, F-69626 Villeurbanne, France

mihaela.florea@g.unibuc.ro

The high activity of CeO<sub>2</sub> in redox reactions has been attributed to some unique properties, such as high oxygen storage capacity, high oxygen mobility and cerium ability to switch easily between the oxidized and reduced states (Ce<sup>3+</sup> ↔ Ce<sup>4+</sup>). Recently, this material has generated great interest in the solid oxide fuel cells (SOFCs) as an electrode for an intermediate temperature operation [1]. To understand the behaviour of pure ceria it is imperative to deeply understand its redox surface chemistry. Therefore, this study aims firstly to develop a simple methodology, using additives, in order to obtain ceria based materials with relevant properties for being used as anode component in IT-SOFC devices, and secondly to realize advanced studies for the redox properties of these materials by performing successive cycles of TPR - CH<sub>4</sub> - TPO.

Ceria powders were synthesized via a modified route by adding additives such as H<sub>2</sub>O<sub>2</sub> in the precipitation step. The structural features and physical-chemical properties of the powders were determined in depth by XRD, SEM, BET, TG-DTA, Raman, TPR-H<sub>2</sub>, TPR-CH<sub>4</sub> and TPO. The XRD analysis of ceria samples shows cubic fluorite structure with lower crystallites size for the samples treated with H<sub>2</sub>O<sub>2</sub>. TPR-H<sub>2</sub> analysis revealed a better surface reducibility for samples treated with H<sub>2</sub>O<sub>2</sub> in which the reduction of Ce<sup>4+</sup> bulk occurs at lower temperatures. The Raman spectra of ceria prepared by adding H<sub>2</sub>O<sub>2</sub>, proved the existence of adsorbed peroxide (O<sub>2</sub><sup>2-</sup>) and superoxide (O<sub>2</sub><sup>-</sup>) species generated by the hydrogen peroxide in the preparation step, but also the presence of some oxygen vacancies. In Figure 1 are presented the TPO profiles after TPR-CH<sub>4</sub> for CeO<sub>2</sub> samples prepared with and without addition of H<sub>2</sub>O<sub>2</sub>. Taking into account the CO<sub>2</sub> and CO formation during TPO, two peaks can

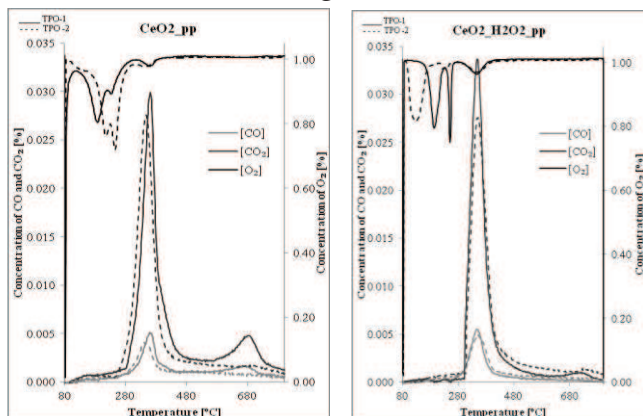


Figure 1. Evolution of O<sub>2</sub>, CO, CO<sub>2</sub> concentration with temperature during the TPO tests

be observed, for both TPO cycles, corresponding to the oxidation of C or coke deposits: a low temperature peak (360-380°C) due to reactive C or coke and a high temperature peak (around 700°C) attributed to graphitic carbon, responsible for deactivation in CH<sub>4</sub> reforming reactions. For the first TPO cycle, it is worthy to note that the preparation by H<sub>2</sub>O<sub>2</sub> addition strongly inhibits the formation of the undesired graphitic carbon, which is expected to lead to better resistance against deactivation during the catalytic reaction.

The results of this study showed that a simple and efficient precipitation methodology, using additives, led to improvement of suited properties of cerium oxide for applications as anode in intermediate temperature Solid Oxide Fuel Cell (IT-SOFC) devices.

The authors kindly acknowledge the UEFISCDI and ANR for the financial support (grant POLCA, 13/2013).

[1] L. Fan, C. Wang, M. Chen, B. Zhu, Journal of Power Sources 234, 154 (2013).

# Gold catalysts on Y doped-ceria for CO-free hydrogen production via PROX

L. Ilieva<sup>1</sup>, P. Petrova<sup>1</sup>, T. Tabakova<sup>1</sup>, G. Pantaleo<sup>2</sup>, L.F. Liotta<sup>2</sup>, R. Zanella<sup>3</sup>, Z. Kaszkar<sup>4</sup>, A.M. Venezia<sup>2</sup>

<sup>1</sup>Institute of Catalysis, Bulgarian Academy of Sciences, 1113 Sofia, Bulgaria

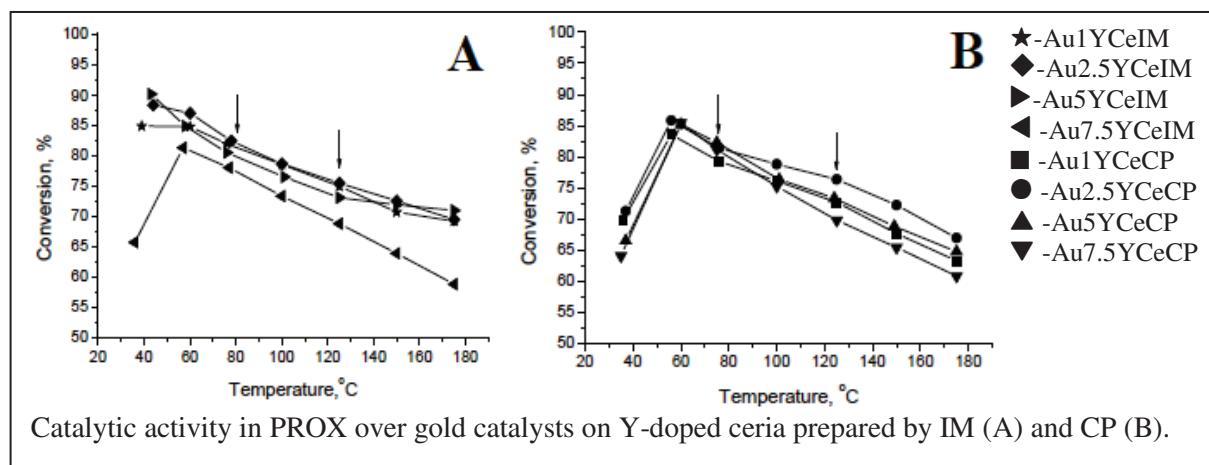
<sup>2</sup>Istituto per lo Studio di Materiali Nanostrutturati, CNR, I- 90146 Palermo, Italy

<sup>3</sup>Universidad Nacional Autónoma de México, P. 04510 México D.F., Mexico

<sup>4</sup>Institute of Physical Chemistry, PAS, Kasprzaka 44/52, 01-224 Warsaw,

e-mail address of corresponding author: luilieva@ic.bas.bg

The catalytic selective oxidation of CO in H<sub>2</sub>-rich gas stream (PROX) is the simplest and most cost effective method for H<sub>2</sub>-purification aiming application in PEM fuel cells. Gold on ceria-based supports are promising candidates for PROX catalysts. The use of different dopants can influence the properties of ceria supports. In the present work Y was chosen as a dopant. The aim is to study the effect of preparation method and Y amount on the catalytic performance in PROX. Two series of Y-modified ceria supports (1, 2.5, 5 and 7.5 wt.% Y<sub>2</sub>O<sub>3</sub>) were synthesized by co-precipitation (CP) and by impregnation (IM). The gold catalysts (3 wt.% Au) were prepared by deposition-precipitation method. The catalysts were characterized by means of XRD, HRTEM and TPR measurements. The activity in PROX was evaluated using 60 vol.% H<sub>2</sub>+1 vol.% CO+1 vol.% O<sub>2</sub> (He as balance), total gas inlet of 50 mL min<sup>-1</sup>. The obtained catalytic activity results are illustrated in the figure. It makes an impression a very high room temperature activity of the gold catalysts on IM supports (except the sample with the highest dopant amount of 7.5 wt.%) as compared to that using CP preparation, which correlates with the TPR data. The values of CO conversion in the interval 80-120 °C (of



interest for fuel cells application) as well as the selectivity toward CO<sub>2</sub> (not shown) are relatively high and they did not differ substantially independent on the differences in the synthesis procedure and Y-amount. Slightly higher activity exhibited Au<sub>2.5</sub>YCeIM (relatively very high selectivity of 45% at 80 °C and 41% at 120 °C, respectively). The activity of Au<sub>7.5</sub>YCeIM is the lowest one. The observed drop in activity and selectivity at realistic conditions (CO<sub>2</sub> and water addition to the feed) over Au<sub>2.5</sub>YCeIM was not very significant. The XRD data have shown that the size of Au particles does not seem to depend strongly on the preparation method. The explanation of the observed catalytic behaviour was search on the basis of the oxidation state of gold (ionic/metallic) and the supports features.

## Acknowledgements:

The study was performed in the frame of COST action CM1104 (STSM-CM1104-040514-042239 of P. Petrova).

# Structure-WGS activity relationship study of gold catalysts supported on Y<sub>2</sub>O<sub>3</sub>- doped ceria

T. Tabakova<sup>1</sup>, L. Ilieva<sup>1</sup>, I. Ivanov<sup>1</sup>, P. Petrova<sup>1</sup>, R. Zanella<sup>2</sup>, Z. Kaszukur<sup>3</sup>, J.W. Sobczak<sup>3</sup>, W. Lisowski<sup>3</sup>, L.F. Liotta<sup>4</sup>, A.M. Venezia<sup>4</sup>

<sup>1</sup>Institute of Catalysis, Bulgarian Academy of Sciences, 1113 Sofia, Bulgaria

<sup>2</sup>Universidad Nacional Autónoma de México, P. 04510 México D.F., Mexico

<sup>3</sup>Institute of Physical Chemistry, PAS, Kasprzaka 44/52, 01-224 Warsaw,

<sup>4</sup>Istituto per lo Studio di Materiali Nanostrutturati, CNR, 90146 Palermo, Italy

e-mail address of corresponding author: tabakova@ic.bas.bg

The water-gas shift reaction (WGS) has a long historical application as an industrially important process for hydrogen production. The utilization of pure hydrogen as energy source in proton exchange membrane fuel cells gave rise to renewed interest in development of active and stable WGS catalysts. Gold catalysts have been proven very efficient for WGS at low temperature. The support plays a decisive role for achieving good catalytic performance. Doping of the ceria by metals of lower oxidation state (below 4<sup>+</sup>) causes formation of oxygen vacancies in the ceria structure and thus increases the oxygen capacity of the ceria-based catalysts. The aim of the present study was to compare the effect of different preparation methods and the amount of doping metal, in particular yttrium, on the WGS activity of Au/CeO<sub>2</sub> catalysts.

Two different synthesis routes - impregnation (IM) and co-precipitation (CP) were used for preparation of Y-modified ceria supports ((1, 2.5, 5 and 7.5 wt.% Y<sub>2</sub>O<sub>3</sub>). Gold catalysts (3 wt.% Au) were prepared by deposition-precipitation method. The WGS activity of the samples was evaluated in a flow reactor at atmospheric pressure. The effects of catalysts pretreatment (reduction at 200 °C, oxidation at 200 °C or 350 °C) and the stability of the best performing samples were also studied.

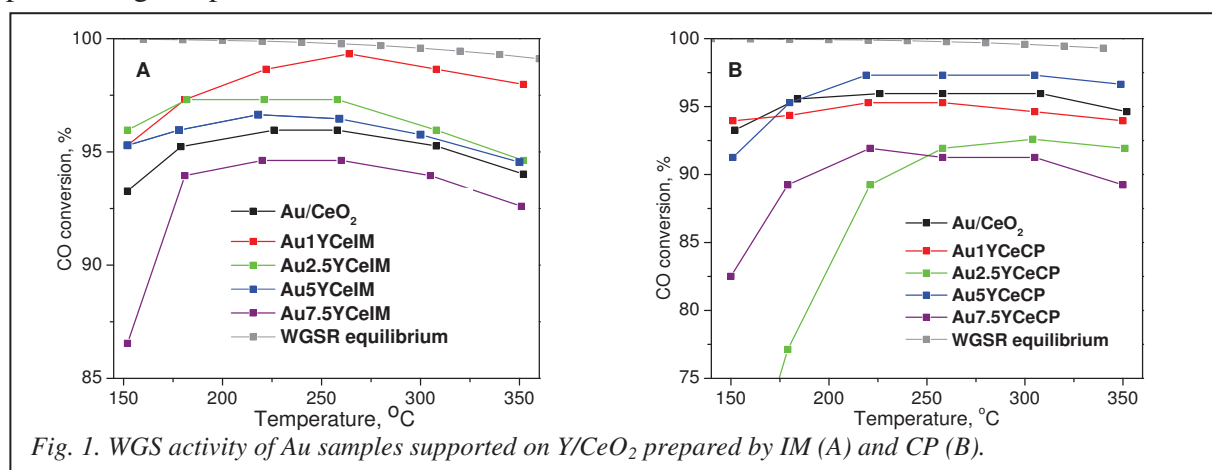


Fig. 1. WGS activity of Au samples supported on Y/CeO<sub>2</sub> prepared by IM (A) and CP (B).

The temperature dependence of CO conversion over gold catalysts supported on IM- and CP-prepared supports after oxidative pretreatment at 350 °C is displayed in Fig. 1. The results reveal very high activity (> 90 % CO conversion) of all catalysts in the range 180-220 °C, specific for low-temperature shift catalysts. Slightly better performance was observed over the samples on IM supports. Regarding the effect of dopant amount, a clear trend of decreased WGS activity was registered for IM samples with increased Y<sub>2</sub>O<sub>3</sub> content. As concerns the CP samples, the behaviour of the sample with 2.5 wt.% Y<sub>2</sub>O<sub>3</sub> differs significantly from that of the other ones. The characterization by means of BET, XRD, HRTEM/HAADF, XPS and TPR will allow to find reliable explanation of the catalytic performance.

**Acknowledgement:** The study was performed in the frame of COST Action CM 1104.

# One pot synthesis of $\text{La}_{0.6}\text{Sr}_{0.4}\text{Co}_{1-x}\text{Fe}_{x-0.03}\text{M}_{0.03}\text{O}_{3-\delta}$ ( $x=0.2/0.8$ ; $\text{M}=\text{Pd}/\text{Ni}$ ) perovskites with tailored oxygen vacancies: structure-properties relationship

S. Guo<sup>1,2</sup>, F. Puleo<sup>1</sup>, A. Longo<sup>1,3</sup>, V. La Parola<sup>1</sup>, G. Pantaleo<sup>1</sup> and L.F. Liotta<sup>1</sup>.

<sup>1</sup>Istituto per lo Studio di Materiali Nanostrutturati (ISMN)-CNR, Via Ugo La Malfa 153, 90146 Palermo, Italy

<sup>2</sup>Northwestern Polytechnical University, Xi'an 710072 PR China.

<sup>3</sup>Dutch-Belgian Beamline (DUBBLE), European Synchrotron Radiation Facility (ESRF), B.P. 220, F-38043 Grenoble, France.

**E-mail:** guoshaoli@mail.nwpu.edu.cn; liotta@pa.ismn.cnr.it

An understanding of the structure and dynamics of catalysts during exposure to gaseous reactants is of paramount importance in predicting their performances. In oxidation reactions catalysed by metal oxides, surface coordinatively unsaturated metal cations and oxygen vacancies are the active sites for hydrocarbons and oxygen activation [1]. Even for oxidation reactions catalysed by noble metals supported on reducible oxides, the role of the support in the activation of oxygen is fundamental [2]. On the other hand, it is widely accepted that the rate-limiting steps of  $\text{O}_2$  reduction process, occurring at the porous cathode of solid oxide fuel cells, are firstly the surface chemical exchange and then the solid state diffusion of oxygen anions through the oxygen vacancies of the cathode lattice.

It appears, therefore, that the synthesis and investigations of metal oxides with tailored oxygen defects are key steps in designing new materials for catalytic and electrochemical applications. LSCF oxides with metal substitution in B-site prepared by different methods, such as solid-state reaction or by impregnation of the perovskite with the metal dopant precursor, have been extensively investigated as new cathodes [3,4]. In the present work, the preparation by one pot citrate method of perovskites with composition  $\text{La}_{0.6}\text{Sr}_{0.4}\text{Co}_{1-x}\text{Fe}_{x-0.03}\text{M}_{0.03}\text{O}_{3-\delta}$  ( $x=0.2/0.8$ ;  $\text{M}=\text{Pd}/\text{Ni}$ ) is reported. Characterizations by several techniques (such as XRD, EXAFS, TPR, XPS, TGA) have been carried out aiming to investigate the effect of the metal (Pd, Ni) insertion on the perovskite structure and oxygen defects. The preliminary results clearly evidence an increase of oxygen vacancies for Pd and Ni doped oxides, confirming recent data by theoretical DFT calculations used as complementary approach [5].

## Acknowledgements

S. Guo thanks COST Action CM 1104 for supporting her STSM (COST-STSM-ECOST-STSM-CM1104-010414-042095).

The CHINA SCHOLARSHIP COUNCIL is also acknowledged for supporting Guo's scholarship.

## References

- [1] L.F. Liotta, H. Wu, G. Pantaleo, A.M. Venezia, *Catal. Sci.&Tech.* **3**, 3085 (2013).
- [2] C. A. Mueller, M. Maciejewski, R. A. Koeppel, R. Tschan, A. Baiker, *J. Phys. Chem.* **100**, 20006 (1996).
- [3] J. M. Porras-Vazquez, P. R. Slater, *Fuel Cells* **12**, 1056 (2012).
- [4] T.J. Huang, X.D. Shen, C.L. Chou, *J. of Power Sources* **187**, 348 (2009).
- [5] Y. Mastrikov, S. Guo, F. Puleo, L.F. Liotta and E. Kotomin, manuscript in preparation.

# Thermodynamics and Spectroscopy of Pt Species at Ceria Surfaces

Fabio Ribeiro, Matteo Farnesi Camellone, and Stefano Fabris

CNR-IOM DEMOCRITOS, % SISSA, Via Bonomea 265, 34136 Trieste ITALY

mfarnesi@democritros.it

Extensive first-principles calculations have been performed to investigate Pt/CeO<sub>2</sub> surfaces in terms of structure optimizations, electronic structure analyses and surface core-level shifts. Ab initio thermodynamics predicts that on the (111) CeO<sub>2</sub> surface under O-rich conditions Pt adsorbed on the stoichiometric surface is thermodynamically favored with a 1+ charge state, whereas lower values of the oxygen chemical potential prefer the same structure provided that subsurface O vacancies are present. When considering the (110) surface it is found that at O-rich, O-moderate and relatively O-poor conditions Pt binds on the stoichiometric surface to a bridge site between two surface Ce leading to the formation of a nearly square-planar arrangement with the central Pt atom bonded to four O atoms, and being in a 2+ oxidation state. Additional calculations suggest that (110) steps on on CeO<sub>2</sub>(111) terrace can accommodate Pt atoms in the usual square-planar coordination suggesting that Pt atoms diffusing in the (111) surface can be easily trapped by a (110)-step, acquiring a 2+ state.

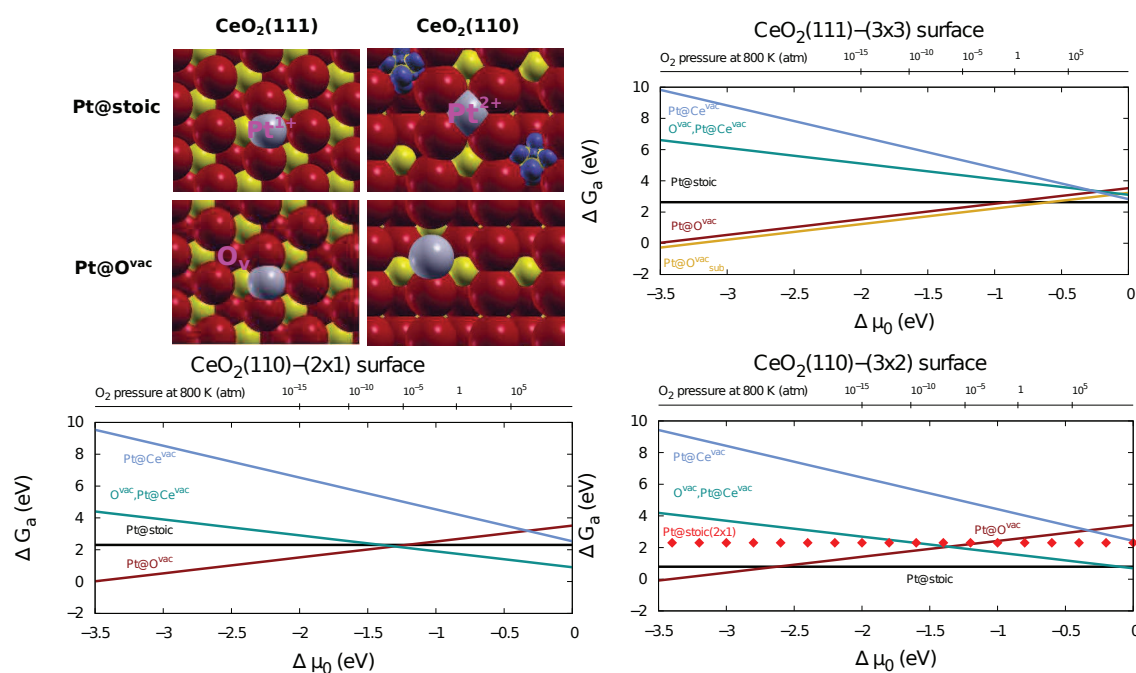


FIG. 1: a) Thermodynamically most stable surface Pt/CeO<sub>2</sub> structures. b) Calculated surrpass phase diagram for Pt adsorption/dispersion on the (111) and (110) CeO<sub>2</sub> surfaces as a function of  $\Delta\mu_{\text{O}}$ .

[1] A. Bruix et al. *Angew. Chem. In. Ed.* DOI: 10.1002/anie.201402342

[2] A. Brux, F. Nazari, K. M. Neyman, and F. Illas, *J. Chem. Phys.* **135**, 244708 (2011).

[3] M. Farnesi Camellone, F. Negreiros Ribeiro, and S. Fabris *Thermodynamics and Spectroscopy of Pt Species at Ceria Surfaces* (submitted)

## Covalency in ceria: A res-ARPES and DFT study

T. Duchoň<sup>1</sup>, M. Aulická<sup>1</sup>, E. F. Schwier<sup>2</sup>, Y. Xu<sup>3</sup>, J. Jiang<sup>2</sup>, H. Iwasawa<sup>2</sup>, K. Veltruská<sup>1</sup>, V. Matolín<sup>1</sup>, K. Shimada<sup>2</sup>, H. Namatame<sup>2</sup>, M. Taniguchi<sup>2,4</sup>

<sup>1</sup>Charles University in Prague, V Holešovičkách 2, 18 000 Prague 8, Czech Republic

<sup>2</sup>HiSOR, Hiroshima University, Hiroshima 739-0046, Japan

<sup>3</sup>Louisiana State University, Baton Rouge, LA 70803, USA

<sup>4</sup>Graduate School of Science, Hiroshima University, Hiroshima 739-0046, Japan

aritentd@gmail.com

beginning of abstract text .....

The interpretation of photoemission spectra of ceria has relied on semiempirical Anderson model calculations for the past 30 years [1]. Recently, calculations using Dirac-Fock and configuration interaction wavefunctions showed that the commonly accepted interpretation may be incorrect due to erroneous description of covalency in the semiempirical calculations [2]. Resolving this discrepancy demands a rigorous experimental study of the nature of f states in ceria.

The admixture of 4f character into the valence p band of ceria has been revealed by resonant photoelectron spectroscopy [3]. In this contribution we present a novel approach to the issue of covalency in ceria by extending resonant photoelectron spectroscopy into angle resolved regime. This allows us to directly reveal the covalent nature of the 4f character admixture into the valence p band in the ground state of ceria. In combination with DFT calculations we interpret our findings in the framework of closed shell screening, supporting the results of the recent DF and CI wavefunction calculations.

end of abstract text .....

- [1] A. Kotani, T. Jo, J. C. Parlebas, *Adv. Phys.*, **37**, 37, (1988).
- [2] C.J. Nelin et al., *Int. J. Quantum Chem.*, **110**, 2752, (2010).
- [3] M. Matsumoto et al., *Phys. Rev. B*, **50**, 11340, (1994).

## Hydrogen activation on ceria-based fuel cell catalysts

Yaroslava Lykhach,<sup>1</sup> Armin Neitzel,<sup>1</sup> Olaf Brummel,<sup>1</sup> Nataliya Tsud,<sup>2</sup> Tomáš Skála,<sup>2</sup> Vitalii Stetsovych,<sup>2</sup> Klára Ševčíková,<sup>2</sup> Mykhailo Vorokhta,<sup>2</sup> Daniel Mazur,<sup>2</sup> Kevin C. Prince,<sup>3</sup> Josef Mysliveček,<sup>2</sup> Vladimír Matolín,<sup>2</sup> Jörg Libuda<sup>1,4</sup>

<sup>1</sup>Lehrstuhl für Physikalische Chemie II, FAU Erlangen-Nürnberg, Erlangen, Germany

<sup>2</sup>Department of Surface and Plasma Science, Charles University, Prague, Czech Republic

<sup>3</sup>Elettra-Sincrotrone Trieste SCpA and IOM, Basovizza-Trieste, Italy

<sup>4</sup>Erlangen Catalysis Resource Center, FAU Erlangen-Nürnberg, Erlangen, Germany

yaroslava.lykhach@fau.de

Superior performance of nanostructured Pt–CeO<sub>2</sub> mixed oxide films as an anode catalyst for hydrogen fuel cells [1] stimulated our interest in the mechanism of hydrogen activation in the presence of ionic Pt. We performed systematic studies on several model systems including nanostructured Pt–CeO<sub>2</sub> mixed oxide films, small metallic nanoparticles of Pt and Pt–Sn alloys supported on CeO<sub>2</sub>, Pt–CeO<sub>2</sub>, and Sn–CeO<sub>2</sub> films. The structure and the composition of the model systems were characterized by the scanning tunneling microscopy (STM) and high-resolution synchrotron radiation photoelectron spectroscopy (SRPES) in combination with resonant photoemission spectroscopy (RPES). The thermal stability of the Pt–CeO<sub>2</sub> films was studied as a function of Pt loading. Using CO molecules as a probe we identified the changes in the composition and morphology of Pt–CeO<sub>2</sub> mixed oxide films caused by annealing in ultrahigh vacuum. We found excellent stability of Pt<sup>2+</sup> for Pt loading less than 12% that results from a specific coordination of Pt<sup>2+</sup> at the (100) nanofacets of the nanostructured CeO<sub>2</sub> film [2]. At higher Pt concentration, a large fraction of the Pt<sup>2+</sup> is converted into metallic Pt particles upon annealing.

We found that hydrogen dissociation occurs exclusively in the presence of metallic Pt<sup>0</sup>. Below 300 K, hydrogen activation involves spillover of hydrogen between Pt (Pt–Sn) nanoparticles and the support resulting in the reversible reduction of Ce<sup>4+</sup> cations. On supported Pt–Sn nanoparticles, we observed significant enhancement of the hydrogen spillover [3]. However, in the presence of oxygen on top of Pt nanoparticles, hydrogen activation yields hydroxyl groups on Pt particles that are associated with the emergence of a new spectral component in the Pt 4f spectra. Simultaneous reduction of Ce<sup>4+</sup> and Pt<sup>2+</sup> (and Sn<sup>2+</sup>) indicates formation of oxygen vacancies upon reaction with hydrogen above 350 K.

In contrast, dissociation of methanol is not affected by the presence of metallic Pt<sup>0</sup>. Interestingly we found that reaction of methanol with Pt–CeO<sub>2</sub> mixed oxide films above 450 K led to appearance of the spectral components in Pt 4f region associated with the hydroxyl groups on top of metallic Pt<sup>0</sup>. This observation suggests that once the dissociation barrier for H<sub>2</sub> dissociation is overcome, the hydrogen can reduce Pt<sup>2+</sup> ions at (100) nanofacets above 450 K.

[1] R. Fiala, M. Vaclavů, M. Vorokhta, I. Khalakhan, J. Lavková, V. Potin, I. Matolínová, V. Matolín, J. Power Sources, accepted, (2014).

[2] A. Bruix, Y. Lykhach, I. Matolínová, A. Neitzel, T. Skála, N. Tsud, M. Vorokhta, V. Stetsovych, K. Ševčíková, J. Mysliveček, R. Fiala, M. Václavů, K.C. Prince, S. Bruyere, V. Potin, F. Illas, V. Matolín, J. Libuda, K.M. Neyman, *Angew. Chem., Int. Ed.*, doi: 10.1002/anie.201402342 (2014).

[3] A. Neitzel, Y. Lykhach, T. Skála, N. Tsud, V. Johánek, M. Vorokhta, K.C. Prince, V. Matolín, J. Libuda, *Phys. Chem. Chem. Phys.*, **16**, 13209 (2014).

## Templated Synthesis of One-Dimensional Nanostructures for Plasmonic Applications

Gilles R. Bourret,<sup>1,3,\*</sup> Tuncay Ozel,<sup>2,3</sup> Martin Blaber,<sup>1,3</sup> Keith A. Brown,<sup>2,3</sup> Abrin L. Schmucker,<sup>1,3</sup> Matthew Rycenga,<sup>1,3</sup> Chad Shade,<sup>1,3</sup> George C. Schatz<sup>1,2,3</sup> and Chad A. Mirkin<sup>1,2,3</sup>

<sup>1</sup>Department of Chemistry, <sup>2</sup>Department of Materials Science and Engineering, and <sup>3</sup>International Institute for Nanotechnology, Northwestern University, 2145 Sheridan Road, Evanston, Illinois 60208, United States

\* Current address: Department of Materials Science and Physics, Hellbrunner Straße 34/III, University of Salzburg, A-5020 Salzburg, Austria

We recently expanded the library of nanostructures that can be made via on-wire lithography (OWL). OWL is based on the templated electrochemical deposition of conducting materials within porous alumina templates.<sup>1</sup> It allows for the generation of one dimensional arrays of metal nanoparticles with a nanometer control over segment lengths and gap distances. The impressive geometrical control afforded by OWL is very well-suited for fundamental studies, as shown by our recent investigation of the emission properties of a polythiophene disk separated by fixed nanoscopic distances from a plasmonic gold nanorod. More functional architectures can also be developed.<sup>2</sup> Indeed, using OWL, we reported the preparation of plasmonic dimers embedded within flexible silica nanosheets for reproducible surface-enhanced Raman scattering (SERS) measurements on surfaces.<sup>3</sup> Control over core-shell nanowire architecture is also possible, as shown by the synthesis of single nanowire photodectors composed of an organic p-type semiconductor core (poly (3-hexylthiophene-2,5-diyl), P3HT) and an inorganic n-type semiconductor shell (CdSe).<sup>4</sup> Electrical characterization supports the formation of a radial p-n junction within the nanowires, which are highly sensitive to visible light. Finally, very recent advances in templated synthesis of core-shell nanowires will be presented.

### References:

- (1) L. Qin, S. Park, C. A. Mirkin *Science* **2005**, 309, 113
- (2) G. R. Bourret, T. Ozel, M. Blaber, C. Shade, G. C. Schatz and C. A. Mirkin *Nano Lett.* **2013**, 13, 2270
- (3) K. D. Osberg, M. Rycenga, G. R. Bourret, K. Brown and C. A. Mirkin *Adv. Mater.* **2012**, 24, 6065
- (4) T. Ozel, G. R. Bourret, A. Schmucker, K. Brown and C. A. Mirkin *Adv. Mater.* **2013**, 25, 4515

## O<sub>2</sub> Adsorption dependent Photoluminescence Emission from Metal Oxide Nanoparticles

Amir R. Gheisi<sup>1</sup>, Chris Neygandhi<sup>1</sup>, Andreas K. Sternig<sup>1</sup>, Esther Carrasco<sup>2</sup>, Hubertus Marbach<sup>2</sup>, Daniel Thomele<sup>3</sup>, Oliver Diwald<sup>3</sup>

<sup>1</sup>Institute of Particle Technology, Universität Erlangen-Nürnberg, Erlangen, (Germany)

<sup>2</sup>Chair for Physical Chemistry II, Universität Erlangen-Nürnberg, Erlangen, (Germany)

<sup>3</sup>Department of Materials Science & Physics, University of Salzburg, Salzburg, (Austria)

oliver.diwald@sbg.ac.at

Optical properties of metal oxide nanoparticles are subject to synthesis related surface defects and impurities.<sup>1</sup> Using photoluminescence spectroscopy and UV diffuse reflectance in conjunction with Auger electron spectroscopic surface analysis we investigated the effect of surface composition and oxygen adsorption on the photoluminescence properties of vapor phase grown ZnO and MgO nanoparticles. On hydroxylated MgO nanoparticles as a reference system, intense photoluminescence features exclusively originate from surface excitons, the radiative deactivation of which undergoes collisional quenching in O<sub>2</sub> atmosphere.<sup>2</sup> Conversely, on as prepared ZnO nanoparticles a broad yellow emission feature centered at  $h\nu_{Em} = 2.1$  eV exhibits an O<sub>2</sub> induced intensity increase. Attributed to oxygen interstitials as recombination centers this effect originates from adsorbate-induced band bending, which is pertinent to the photoluminescence active region of the nanoparticles.<sup>3</sup> Annealing induced trends in the optical properties of the two prototypical metal oxide nanoparticle systems, ZnO and MgO, are explained by changes in the surface composition and underline that particle surface and interface changes that result from handling and processing of nanoparticles critically affect luminescence.

- [1] H. Zhang, A. R. Gheisi, A. Sternig, K. Müller, M. Schowalter, A. Rosenauer, O. Diwald and L. Mädler, *ACS Applied Materials and Interfaces*, 4, 2490–2497 (2012).
- [2] N. Siedl, D. Koller, A. K. Sternig, D. Thomele and O. Diwald, *Phys Chem Chem Phys*, 16, 8339–8345 (2014).
- [3] Z. Zhang and J. T. Yates, *Chem. Rev.*, 112, 5520–5551 (2012).

## Surface structures of ultrathin $\text{TiO}_x$ and $\text{NbO}_x$ films on Au (111)

Xiao Hu, Chen Wu, Matthew S. J. Marshall, and Martin R. Castell

Department of Materials, University of Oxford, Parks Road, Oxford OX1 3PH, UK

[xiao.hu@materials.ox.ac.uk](mailto:xiao.hu@materials.ox.ac.uk); [martin.castell@materials.ox.ac.uk](mailto:martin.castell@materials.ox.ac.uk)

Following the discovery of enhanced catalytic properties of oxide supported nanoparticles of noble metals, especially Au, interactions between the two have become a focus in research [1-3]. The growth of oxides on Au(111) surfaces serves as an inverse model and provides insights into their interactions. Well-ordered  $\text{TiO}_x$  and  $\text{NbO}_x$  layers were grown on  $(22 \times \sqrt{3})$ -reconstructed Au(111) surfaces by Ti and Nb deposition and oxidation.

In the growth of  $\text{TiO}_x$  thin films on Au(111), three different structures were observed with increased amounts of Ti deposited [4]. The first structure occurs for Ti surface coverages of  $<0.5$  monolayer (ML), and exhibits a  $(2 \times 2)$ -reconstructed structure resembling a honeycomb pattern. The second structure arises after depositing 0.5 ML - 1.8 MLs of Ti and exhibits a pinwheel shape. The pinwheel structure forms a  $(\sqrt{67} \times \sqrt{67})R12.2^\circ$  Moiré pattern. The third structure occurs for  $>0.5$  ML Ti depositions and forms triangular shaped islands. Film growth continues via the coalescence of triangular islands with further increased Ti coverage.

For  $\text{NbO}_x$  ultrathin film growth on Au(111), coexistence of a honeycomb  $(2 \times 2)$  and a hollow triangle structure were observed. The  $(2 \times 2)$  honeycomb structure of both  $\text{TiO}_x$  and  $\text{NbO}_x$  illustrated a uniform pattern with different types of domain boundaries. A modelling study of three typical domain boundaries was carried on.

[1] M.S. Chen, and D.W. Goodman, *Science*, **306**, 252, (2004).

[2] S.H. Overbury et al., *Catal. Lett.*, **95**, 99, (2004).

[3] N. Zheng and G.D. Stucky, *J. Am. Chem. Soc.*, **128**, 14278, (2006).

[4] C. Wu, M.S.J. Marshall and M.R. Castell, *J. Phys. Chem. C*, **115**, 8643, (2011).

## **TiO<sub>x</sub>-based linear nanostructures on the SrTiO<sub>3</sub> (001) surface**

M.S.J. Marshall<sup>1</sup>, Y. Gao<sup>1</sup>, A.E. Becerra-Toledo<sup>2</sup>, L.D. Marks<sup>2</sup> and M.R. Castell<sup>1</sup>.

1. Department of Materials, University of Oxford, Parks Road, Oxford, OX1 3PH, U.K.

2. Department of Materials Science and Engineering, Northwestern University,  
Evanston, Illinois 60208, U.S.A.

A class of nanostructure phases have been observed on SrTiO<sub>3</sub> (001) surface by applying atomic resolution scanning tunnelling microscopy (STM). Certain surface treatment on SrTiO<sub>3</sub> (001) including argon ion sputtering (10 minutes, 2-5 μA ion current, 1 keV beam energy) and annealing in the temperature range 875 – 900 °C give rise to the formation of a variety of nanostructures including nanodots and nanolines. 0.5wt% Nb doped SrTiO<sub>3</sub> (001) single crystals were used in this experiment. This surface preparation produced three types of linear nanostructures named as nanolines on the SrTiO<sub>3</sub> (001) surface. According to the different structure arrangement, these three types of nanolines are further named as dilines, trilines and tetralines. All these nanolines consist of parallel rows that assemble into domains that are oriented in the <001> directions. Auger electron spectroscopy (AES) and X-ray photoemission (XPS) show that surfaces decorated with nanolines are TiO<sub>x</sub> rich. XPS spectra obtained from these three types of nanolines reveals significant Ti<sup>2+</sup> peak on trilines compared with a small amount on dilines and no Ti<sup>2+</sup> peak on tetralines.

# Application of mesoporous materials containing ruthenium for hydrogenation of citral

Agnieszka Feliczak-Guzik, Lukasz Szczesniak, **Izabela Nowak**

Adam Mickiewicz University in Poznan, Faculty of Chemistry, Poznan, Poland;  
nowakiza@amu.edu.pl

Mesoporous materials are catalysts containing pores with diameters between 2 and 50 nm (according to IUPAC notation). They play important role in many synthesis of various organic reactions, for example hydrogenation of citral. This compound possess of three unsaturated sites in the molecule, i.e., a carbonyl group, a conjugated and an isolated C=C bond, makes citral an interesting model compound for catalytic tests in the field of selective hydrogenation of  $\alpha,\beta$ -unsaturated carbonyl compounds [1].

In this study heterogeneous catalysts containing ruthenium were applied for the hydrogenation of citral, in the high-pressure reactor by using acetonitrile and ethanol as solvents. As the matrix mesoporous molecular sieves, such as SBA-12, SBA-16, and MCM-41 were used. The reaction products of hydrogenation of citral were identified by GC-Mass spectrometry.

The influence of temperature, pressure, time of the reaction, composition and structural/textural properties of the catalyst on the conversion of citral to the desired products was determined. It was found that the conversion of citral increased with temperature and pressure reaction alterations. The initial reaction rate in terms of TOF was the highest on the mesoporous RuSBA-12 in ethanol used as the reaction medium. The hydrogenation selectivity depends on reaction temperature, i.e., at high temperature the selective hydrogenation of the C=O group was much more difficult in the presence of C=C bond. The product of the first hydrogenation step, citronellal, was isomerized to isopulegol on the acid sites and further hydrogenated to menthol at longer reaction times. The highest selectivity to menthol and isopulegol were observed for mesoporous materials, which are containing ruthenium. The increase in the polarity of the solvent increases the catalytic activity, however the reaction pathway was modified. The hydrogenation of citral over these prepared Ru catalysts indicated that they can be also used as the catalysts for other hydrogenation reactions.

## References

- [1] A. Corma, S. Iborra, A. Velty, *Chem. Rev.*, **107**, 2411 (2007).

## Ordered mesoporous silicas with SBA-16-like structure modified with aminosilanes

Agata Wawrzyńczak, Magdalena Górczyńska and **Izabela Nowak**

Adam Mickiewicz University in Poznan, Faculty of Chemistry, Poznan, Poland

nowakiza@amu.edu.pl

It is well known that the desired physico-chemical properties of silica materials may be obtained by surface functionalization processes. In general, there are two different techniques that may be used to incorporate amino moieties into the structure of silica materials, namely "one-pot" synthesis and post-functionalization (i.e., "grafting"). "One-pot" synthesis involves a co-condensation step that occurs between an aminosilane and inorganic silica precursor (in the presence of the template), whereas post-functionalization process is based on the functionalization of siliceous materials, when the condensation and calcination steps are already completed [1]. Amine-functionalized ordered mesoporous silicas may find a wide range of applications e.g. in catalysis and adsorption [2]. Therefore, during our studies we have focused on the obtaining of amino-modified ordered mesoporous silicas of SBA-16 type, both in the form of powders and films.

SBA-16 materials were prepared in the form of powders and films, according to "one-pot" and "grafting" procedures. Tetraethylortosilicate (TEOS) was used as a silica source and two different aminosilanes, namely: N-( $\beta$ -aminoethyl)- $\gamma$ -aminopropyl-trimethoxysilane and vinylbenzyl-( $\beta$ -aminoethyl)- $\gamma$ -aminopropyl-trimethoxysilane were applied as a source of amino groups. Pluronic F127 (poly(oxyethylene)-poly(oxypropylene)-poly(oxyethylene) triblock copolymer) was a structure directing agent, whereas distilled water or ethanol (96%, pure p.a.) were applied as solvents. Template removal procedure occurred by the calcination or extraction procedures in the case of mesoporous powders and films, respectively.

FT-IR, XRD and TEM/SEM analysis, as well as low temperature nitrogen sorption measurements and elemental analysis were applied in order to characterize obtained samples.

XRD measurements confirmed that the obtained materials, both powders and films, were synthesized with a desired pores ordering. TEM photographs revealed highly ordered pores with a regular cage-like structure characteristic for SBA-16 materials. N<sub>2</sub> sorption measurements revealed type IV isotherms and H2-like hysteresis loops, which are typical for SBA-16 mesoporous materials (according to IUPAC recommendations). Extraction procedures enabled almost complete template removal from SBA-16 films, while calcination was proved to be highly effective in the case of powder samples. It was shown by FT-IR measurements, where declining intensity of bands stemming from the alkyl chain of the template was observed. Elemental analysis confirmed the presence of amino groups in the synthesized silicas.

Catalytic tests in Knoevenagel condensation between benzaldehyde and ethyl acetylacetate revealed that the majority of the synthesized materials may be considered as promising catalysts with selectivity to the desired product (ethyl 2-benzylidene-3-oxobutanoate) as high as 95%.

*National Science Centre is kindly acknowledged for financial support (project no: DEC-2013/10/M/ST5/00652).*

[1] F. Hoffmann, M. Cornelius, J. Moreli, M. Fröba, *Angew. Chem. Int. Ed.*, **45**, 3216 (2006).

[2] F. Zhu, D. Yang, F. Zhang, H. Li, *J. Mol. Catal. A: Chemical*, **363-364**, 387 (2012).

# Structure and electronic states of Au nanodots grown on a curved TiO<sub>2</sub>(110) rutile single crystal

L.A. Miccio<sup>1,\*</sup>, M. Abadía<sup>2</sup>, R. González-Moreno<sup>3</sup>, C. Rogero<sup>4</sup>, J. Lobo-Checa<sup>4</sup>, F. Schiller<sup>4</sup>, and J.E. Ortega<sup>1,2,4</sup>

<sup>1</sup>Donostia International Physics Center DIPC, E-20018 San Sebastian, Spain

<sup>2</sup>Depto. de Física Aplicada I, Universidad del País Vasco UPV/EHU, San Sebastian Spain

<sup>3</sup>Bihurcrystal S.L., San Sebastian, Spain

<sup>4</sup>Centro de Física de Materiales, Centro Mixto CSIC-UPV/EHU, San Sebastian, Spain

\* luisalejandro\_miccio@ehu.es

Surfaces that are vicinal to high symmetry directions have frequently demonstrated their enormous potential for surface science research and applications. Vicinal surfaces exhibit distinct chemical and physical properties due to the high density of atomic steps, and are also useful as templates for nanostructure growth. Both chemical properties and nanostructure growth morphology are of obvious interest in the understanding of the catalytic activity of Au nanoparticles on oxide surfaces, such as TiO<sub>2</sub>.

Using a crystal with a shallow curvature around a high symmetry direction one can smoothly vary, on the same sample, the crystal orientation of the vicinal surface plane, namely the density of surface steps [1]. Such a curved sample appears very convenient for a fast, thorough analysis of step-related phenomena, and hence for a rational optimization of physical-chemical and growth properties that are sensitive to the presence of atomic steps.

Very recently we have successfully prepared a curved TiO<sub>2</sub> rutile surface around the [110] symmetry direction. The Scanning Tunneling Microscopy (STM) and Low Energy Electron Diffraction (LEED) analysis indicates the presence of monatomic step arrays along the  $[1\bar{1}0]$  direction, with a smooth variation of the step density. On top of such surface we have studied the growth of Au nanoparticles by direct sublimation of metallic Au in vacuum. We will discuss, as a function of the step density, the thickness-dependent morphology of the resulting arrays of nanodots, as well as the subsequent changes in electronic states in the TiO<sub>2</sub> rutile band gap region induced by the Au nanodot array, the latter measured by Ultraviolet Photoemission (UPS).

## References

[1] M. Corso, F. Schiller, L. Fernández, J. Cerdón, and J. E. Ortega, *J. Phys.: Cond. Matter* **21**, 353001 (2009).

## Exploring TiO<sub>2</sub> polymorphs with a modified hybrid functional

Kyoung Chul Ko,<sup>1,2</sup> Oriol Lamiel-García,<sup>1</sup> Jin Yong Lee,<sup>2</sup> and Francesc Illas<sup>1</sup>

<sup>1</sup> *Departament de Química Física & Institut de Química Teòrica i Computacional (IQTCUB), Universitat de Barcelona, c/ Martí i Franquès 1, 08028 Barcelona, Spain.*

<sup>2</sup> *Department of Chemistry, Sungkyunkwan University, Suwon 440-746, Korea*

It is nowadays well known that broadly used local-density approximation (LDA) and generalized gradient approximation (GGA) based functionals have problems in describing the band gap of oxides to the point that antiferromagnetic insulators such NiO are described as metals. Bulk TiO<sub>2</sub> is not an exception and the LDA and GGA calculated values for the stable polymorphs are too small. Hybrid functionals such as PBE0 or B3LYP properly describe these materials as insulators but the calculated band gap use to be too large. Here, the overestimation comes from the too large fraction of Fock exchange included in these hybrid functionals. In order to provide a simple yet efficient way to treat these systems, we explored the influence of HF exchange percentage (%) in PBE0 hybrid functional in the calculated properties. A quantitative correlation between HF exchange and band gaps for anatase/rutile TiO<sub>2</sub> at the experimental crystal structure is found suggesting that reducing the amount of HF exchange in PBE0 to 12.5 % can correctly predict the band gap of TiO<sub>2</sub> systems, in agreement with earlier work [1]. Further refinement of crystal structure with this functional leads to values close to experiment indicating that this modified hybrid functional provides a pragmatic approach to describe the electronic structures for various TiO<sub>2</sub> systems. The study of reduced TiO<sub>2-x</sub> systems with this modified hybrid functional is now being carried out in our laboratory.

[1] Y. Zhang, W. Lin, Y. Li, K. Ding, J. Li, J. Phys. Chem. B., **109**, 19270 (2005)

# Self-interaction corrected density functional calculations of localized electron hole at Al dopant in SiO<sub>2</sub>

Hildur Guðmundsdóttir and Hannes Jónsson

Science Institute and Faculty of Physical Sciences, University of Iceland, Reykjavík, Iceland

hj@hi.is

## Abstract:

Theoretical calculations of the localized hole formed near an Al-atom dopant in alpha-SiO<sub>2</sub> are presented. This system has become an important test case for theoretical methodology since generalized gradient approximation energy functionals as well as commonly used hybrid functionals, such as B3LYP, fail to stabilize the localized hole due to the self-interaction error inherent in Kohn-Sham density functional theory [1,2]. The present results show that variational, self-consistent calculations using the Perdew-Zunger self-interaction correction [3,4] involving complex optimal orbitals [5] applied to a 72 atom cell subject to periodic boundary conditions can reproduce well the experimentally deduced lengthening (by 12%) of the Al-O bond to the O-atom where the hole resides as well as the energy of the defect state (calculated to be 1.9 eV above the valence band edge as compared with optical absorption peak at 1.77 eV) and the size of the band gap (9 eV both measured and calculated) [4]. The Perdew-Zunger correction is, however, size-inconsistent so a sufficiently localized initial state needs to be prepared initially. Alternative ways of estimating the self-interaction correction that could make this approach more robust will be discussed.

## References:

- [1] G. Pacchioni, *J. Chem. Phys.* **128**, 182505 (2008).
- [2] G. Pacchioni, F. Frigoli, D. Ricci and J. A. Weil, *Phys. Rev. B* **63**, 054102 (2000).
- [3] J. P. Perdew and A. Zunger, *Phys. Rev. B* **23**, 5048 (1981).
- [4] P. Klüpfel, S. Klüpfel, K. Tsemekhman, and H. Jónsson, *Lect. Notes in Comp. Sci.* **7134**, 23 (2012).
- [5] S. Klüpfel, P. J. Klüpfel and H. Jónsson, *Phys. Rev. A* **84**, 050501 (2011); *J. Chem. Phys.* **137**, 124102 (2012).
- [6] H. Guðmundsdóttir and H. Jónsson (submitted to *Phys. Rev. B*).

# LIST OF PARTICIPANTS

**AFANASIEV, Valeri** (Leuven, Belgium)  
**ALEKSANDROV, Hristiyan** (Sofia, Bulgaria)  
**ALWAN, Seif** (Uppsala, Sweden)  
**BARTH, Clemens** (Marseille, France)  
**BEINIK, Igor** (Aarhus, Denmark)  
**BOGHOSIAN, Soghomon** (Patras, Greece)  
**BONIVARDI, Adrian** (Santa Fe, Argentina)  
**BOUDOIRE Florent** (Dübendorf, Switzerland)  
**BOURRET, Gilles** (Salzburg, Austria)  
**BROMLEY, Stefan** (Barcelona, Spain)  
**BRUIX, Albert** (Aarhus, Denmark)  
**CALATAYUD, Monica** (Paris, France)  
**CAPDEVILA-CORTADA, Marçal** (Tarragona, Spain)  
**CHEN, Hsin-Yi Tiffany** (Milan, Italy)  
**CHEN, Xiaowei** (Cádiz, Spain)  
**CHIESA, Mario** (Torino, Italy)  
**CONESA, José C.** (Madrid, Spain)  
**DE LA FIGUERA, Juan** (Madrid, Spain)  
**DEÁK, László** (Szeged, Hungary)  
**DELGADO, Juan José** (Cádiz, Spain)  
**DI VALENTIN, Cristiana** (Milan, Italy)  
**DIWALD, Oliver** (Salzburg, Austria)  
**DU, Dou** (Uppsala, Sweden)  
**DUCHOŇ, Tomas** (Prague, Czech Republic)  
**FARNESI CAMELLONE, Matteo** (Trieste, Italy)  
**FERNÁNDEZ SANZ, Javier** (Seville, Spain)  
**FIGUEROBA, Alberto** (Barcelona, Spain)  
**FLEGE, Jan Ingo** (Bremen, Germany)  
**FLOREA, Mihaela** (Bucharest, Romania)  
**GANDUGLIA-PIROVANO, María Verónica** (Madrid, Spain)  
**GAO, Yakun** (Oxford, United Kingdom)  
**GIAMELLO, Elio** (Torino, Italy)  
**GONIAKOWSKI, Jacek** (Paris, France)  
**GRACIANI, Jesús** (Seville, Spain)  
**GRINTER, David** (London, United Kingdom)  
**GRÖNBECK, Henrik** (Göteborg, Sweden)  
**GRYBOŚ, Joanna** (Krakow, Poland)  
**GUDMUNSDOTTIR, Hildur** (Reykjavík, Iceland)  
**GUO, Shaoli Guo** (Palermo, Italy)  
**HAMMER, Bjørk** (Aarhus, Denmark)  
**HEARD, Christopher** (Göteborg, Sweden)  
**HELLSTRÖM, Matti** (Uppsala, Sweden)  
**HU, Xiao** (Oxford, United Kingdom)  
**ILIEVA GENCHEVA, Lyuba** (Sofia, Bulgaria)  
**ILLAS, Francesc** (Barcelona, Spain)  
**INDYKA, Paulina** (Krakow, Poland)  
**JELENKOVIĆ Brana** (Belgrade, Serbia)  
**JUPILLE, Jacques** (Paris, France)  
**KAVAN, Ladislav** (Prague, Czech Republic)  
**KEBEDE, Getachew** (Uppsala, Sweden)

**KOLEVA, Iskra** (Sofia, Bulgaria)  
**KORHONEN, Esa** (Aalto, Finland)  
**KOŚMIDER, Krzysztof** (Madrid, Spain)  
**KOTARBA, Andrzej** (Krakow, Poland)  
**LA PAROLA, Valeria** (Palermo, Italy)  
**LAMIEL-GARCÍA, J. Oriol** (Barcelona, Spain)  
**LI, Jun** (Beijing, P. R. China)  
**LIBUDA, Jörg** (Erlangen, Germany)  
**LIOTTA, Leonarda Liotta** (Palermo, Italy)  
**LLOIS, Ana María** (Buenos Aires, Argentina)  
**LLORCA, Jordi** (Barcelona, Spain)  
**LUCHES, Paola** (Modena, Italy)  
**LYKHACH, Yaroslava** (Erlangen, Germany)  
**MADIA, Oreste** (Leuven, Belgium)  
**MAKKONEN, Ilja** (Espoo, Finland)  
**MARTÍNEZ-ARIAS, Arturo** (Madrid, Spain)  
**MASTRIKOV, Yuri** (Riga, Latvia)  
**MATOLÍN, Vladimir** (Prague, Czech Republic)  
**MELCHIONNA, Michele** (Trieste, Italy)  
**MICCIO, Alejandro** (San Sebastián, Spain)  
**MIGANI, Annapaola** (Bellaterra, Spain)  
**MURGIDA, Gustabo Ezequiel** (Buenos Aires, Argentina)  
**NEYMAN, Konstantin** (Barcelona, Spain)  
**NOGUERA, Claudine** (Paris, France)  
**NOTARIO, Almudena** (Barcelona, Spain)  
**NOWAK, Izabela** (Poznan, Poland)  
**ORTEGA, Enrique** (San Sebastián, Spain)  
**OSTROVERKH, Anna** (Kiev, Ukraine)  
**PACCHIONI, Gianfranco** (Milan, Italy)  
**PANG, Chi Lun** (London, United Kingdom)  
**PARKINSON, Gareth** (Vienna, Austria)  
**PÉREZ, Rubén** (Madrid, Spain)  
**PETROVIĆ, Suzana** (Belgrade, Serbia)  
**PICCOLO, Laurent** (Villeurbanne, France)  
**PROZHEEVA, Vera** (Aalto, Finland)  
**PUEYO, Noelia** (Barcelona, Spain)  
**RAMESHAN, Christoph** (Vienna, Austria)  
**RAMOS, Erika** (Barcelona, Spain)  
**RAVEENDRAN, Shiju** (Amsterdam, Netherlands)  
**REICHLING, Michael** (Osnabrück, Germany)  
**RELLÁN, Marcos** (Tarragona, Spain)  
**RÖSCH, Notker** (München, Germany / Singapore)  
**RUPPRECHTER, Günther** (Vienna, Austria)  
**SAUER, Joachim** (Berlin, Germany)  
**SETVIN, Martin** (Vienna, Austria)  
**SHLUGER, Alexander** (London, United Kingdom)  
**ŠLIJVANČANIN, Željko** (Belgrade, Serbia)  
**SOJKA, Zbigniew** (Krakow, Poland)  
**STANKIC, Slavica** (Paris, France)  
**SURNEV, Svetlozar** (Graz, Austria)

**TABAKOVA, Tatyana** (Sofia, Bulgaria)  
**THORNTON, Geoff** (London, United Kingdom)  
**TRINCHERO, Adriana** (Göteborg, Sweden)  
**VALERI, Sergio** (Italy)  
**VAN DEN BOSSCHE, Maxime** (Göteborg, Sweden)  
**VAYSSILOV, Georgi** (Sofia, Bulgaria)  
**VIÑES, Francesc** (Barcelona, Spain)  
**VOGT, Ulrich** (Dübendorf, Switzerland)  
**WALTON, Alexander** (Aarhus, Denmark)  
**WOLF, Matthew** (Uppsala, Sweden)  
**YILDIZ, Huseyin Bekir** (Karaman, Turkey)  
**ZUKALOVA, Marketa** (Prague, Czech Republic)